Daniel Zwick

Simulation and Optimization in Offshore Wind Turbine Structural Analysis

Thesis for the degree of Philosophiae Doctor

Trondheim, April 2015

Norwegian University of Science and Technology
Faculty of Engineering Science and Technology
Department of Civil and Transport Engineering

NTNU – Trondheim
Norwegian University of
Science and Technology

NTNU
Norwegian University of Science and Technology

Thesis for the degree of Philosophiae Doctor

Faculty of Engineering Science and Technology
Department of Civil and Transport Engineering

ISBN 978-82-326-0816-4 (printed ver.)
ISBN 978-82-326-0817-1 (electronic ver.)
ISSN 1503-8181

Doctoral theses at NTNU, 2015:80

Printed by NTNU Grafisk senter

How can you power a planet hungry for electricity without damaging it?

Siemens AG Answers Campaign by Ogilvy & Mather, 2008.

Abstract

The public interest in renewable energy resources is continuously growing as issues of pollution and shortage of limited resources as coal or oil become evident. One promising technical solution for the extraction of renewable energy is to install wind turbines offshore. Stronger and more steady winds as well as the reduced need for land area are substantial advantages compared to onshore wind turbine installations. However, higher costs for offshore installations as well as operation and maintenance issues are by today limiting factors of offshore developments. Therefore, cost reductions in this field are strongly needed in the future.

Investigations in this thesis were focused on simulation and optimization aspects in offshore wind turbine structural analysis. The aim of the work was firstly to contribute to a better understanding of complex time-domain simulations in the research community, and secondly to give insight to several optimization approaches which can be applied to offshore wind turbine structures. Both objectives target at the simplification of simulation tasks, resulting in shorter analysis times and more efficiently designed structures. Analyses performed in this thesis are presented for the example of lattice type sub-structures.

In terms of simulation aspects, a large simulation study was performed to determine the influence of input loading variability to structural responses. The variability was found to be an important source of simulation error as both ultimate and fatigue loads might be estimated with an error of up to 34% and 12%, respectively, when following a simulation setup recommended by international standards. Another aspect in the simulation setup is the number of load cases to be simulated. An approach using statistical regression methods was proposed to estimate the total fatigue damage for a set of load cases, by simulating only a few of them. Interestingly, the number of load cases could be reduced from 21 to 3, by still providing a high accuracy with maximum error of 6%.

Using the definition of structural weight as the main cost criteria, several optimization studies were performed on different lattice type sub-structures. In total

three approaches were developed and/or applied: a local optimization approach, the simultaneous perturbation stochastic approximation, and the genetic algorithm. One result was the identification of fatigue damage as the design driver, another the distribution of loads, resulting in varying member dimensions over the tower height. The local optimization approach was identified as fast and efficient. Stochastic approaches were in comparison more time demanding, but showed some interesting solutions which a human designer would not consider so quickly.

Acknowledgments

The whole story started with a job advertisement in Teknisk Ukeblad with title: *Do you want to work with offshore wind turbines?* - It was Professor Geir Moe who caught my attention by this question, and became my supervisor a few months later when I started my PhD. I would like to thank Geir for giving me the opportunity to work in this interesting research field and for many interesting discussions about offshore wind turbines.

After Geir passed away, Associate Professor Michael Muskulus became my new supervisor for the second half of my work at NTNU. With Michael's help, and two brand-new powerful workstations in place, I got to know new opportunities and challenges in the application of simulations in offshore wind turbine structural analysis. Thanks to Michael for guiding me into this interesting research field, for challenging me to learn more about statistics and for helping me to improve academic writing skills.

Thanks to the faculty of engineering science and technology for granting my scholarship, to the committee members for their efforts and to the staff at the department of civil and transport engineering. It has been a pleasure to contribute in the research community of NOWITECH and to get to know many PhD candidates and researchers across various disciplines working with wind turbines. I also enjoyed being part of the marine civil engineering group in the basement at BAT, thanks to all of you!

Trondheim, March 2015
Daniel Zwick

List of publications

List of publications appended in the thesis

Paper 1 **Zwick D**, Muskulus M. The simulation error caused by input loading variability in offshore wind turbine structural analysis. *Wind Energy* 2014; DOI: 10.1002/we.1767.

Paper 2 **Zwick D**, Muskulus M. Simplified fatigue load assessment in offshore wind turbine structural analysis. *Wind Energy* 2015; DOI: 10.1002/we.1831.

Paper 3 **Zwick D**, Schafhirt S, Brommundt M, Muskulus M, Narasimhan S, Mechineau J, Haugsøen PB. Comparison of different approaches to load calculation for the OWEC Quattropod jacket support structure. *Journal of Physics: Conference Series* 2014; **555**: 012110:1-10.

Paper 4 **Zwick D**, Muskulus M, Moe G. Iterative optimization approach for the design of full-height lattice towers for offshore wind turbines. *Energy Procedia* 2012; **24**: 297-304.

Paper 5 **Zwick D**, Muskulus M. Two-stage local optimization of lattice type support structures for offshore wind turbines. Submitted to *Ocean Engineering* 2014.

Paper 6 Molde H, **Zwick D**, Muskulus M. Simulation-based optimization of lattice support structures for offshore wind energy converters with the simultaneous perturbation algorithm. *Journal of Physics: Conference Series* 2014; **555**: 012075:1-8.

Paper 7 Pasamontes LB, Torres FG, **Zwick D**, Schafhirt S, Muskulus M. Support structure optimization for offshore wind turbines with a genetic algorithm. *Proceedings of the 33rd International Conference on Ocean,*

Offshore and Arctic Engineering 2014, San Francisco, USA, OMAE; **9B**: V09BT09A033:1-7.

Contributions to related publications not appended in the thesis

- Chew KH, Ng EYK, Tai K, Muskulus M, **Zwick D**. Offshore wind turbine jacket substructure: a comparison study between four-legged and three-legged designs. *Journal of Ocean and Wind Energy* 2014; **1**: 74-81.
- Schafhirt S, **Zwick D**, Mukulus M. Reanalysis of jacket support structure for computer-aided optimization of offshore wind turbines with a genetic algorithm. *Journal of Ocean and Wind Energy* 2014; **1**: 209-216.
- Dalhaug OG, Berthelsen PA, Kvamsdal T, Frøyd L, Gjerde SS, Zhang Z, Cox K, Van Buren E, **Zwick D**. Specification of the NOWITECH 10MW reference wind turbine. *NOWITECH Report*, 2012, Trondheim, Norway.
- Muskulus M, Christensen E, **Zwick D**, Merz K. Improved tower design of the NOWITECH 10MW reference turbine. *Proceedings of the European Wind Energy Association Conference Offshore* 2013, Frankfurt, Germany, EWEA; **PO127**:1-8.

Abbreviations

API	application programming interface
COM	component object model
DEL	damage equivalent load
DLC	design load case
DNV	Det Norske Veritas
DTU	Technical University of Denmark
FLS	fatigue limit state
GRD	sea ground
HDD	hard disk drive
HSS	hot spot stress
IEC	International Electrotechnical Commission
LSM	linear statistical model
MSL	mean sea level
NOWITECH	Norwegian Research Centre for Offshore Wind Technology
NREL	National Renewable Energy Laboratory
PLR	piecewise linear regression
RAM	random-access memory

RNA	rotor nacelle assembly
SCF	stress concentration factor
SPSA	simultaneous perturbation stochastic approximation
SSD	solid state drive
ULS	ultimate limit state

Contents

1

Introduction

The worlds population is in a continuous growth, and with its industrial development, the demand for energy has been following this trend [1]. Making use of both limited resources (as coal, oil or gas) and unlimited resources (as solar, wind or water) has been the basis for energy production over the centuries. Over time, issues of limited resources as pollution or shortage have become evident and have put focus on the expanded use of unlimited resources, today better known as renewable energy resources [2].

In a global perspective, different renewable energy resources have typically been exploited based on their regional dominance. Solar energy at locations with strong solar radiation, onshore wind energy along coasts and water energy in mountain regions. As new technical solutions were developed, extracting energy from the wind at offshore locations has become feasible [3]. Several advantages compared to onshore wind, as stronger and more steady winds as well as the reduced need for land area, make it favorable to utilize wind energy offshore [4].

Since the exploitation of wind energy offshore is rather new, compared to onshore wind facilities, various structural concepts have been presented and installed so far [5]. The main difference of these concepts lies in the implementation of the structure supporting the wind energy converter itself, the so-called rotor nacelle assembly (RNA). Depending on the water depth at the installation site, structures are designed as bottom-fixed or floating. So far, only bottom-fixed constructions were erected in larger wind farms, while the floating technology is still in a prototype phase due to a large number of engineering challenges and high costs [6]. Both categories are covering a number of several design possibilities, as for example a monopile, lattice tower, tripod, tripile or gravity base structure for bottom-fixed

designs (Fig. 1.1). Following the definition of a support structure of a bottom-fixed offshore wind turbine in international standards as IEC 61400-3 [7], the support structure consists of several parts: (1) tower, (2) sub-structure and (3) foundation, as shown in Figure 1.1. However, this definition is not consistently used in the research field since other standards, as for example DNV-OS-J101 [8], are not treating the foundation as part of the support structure. For support structures with differing concepts for part (1) and (2), the connection is realized by a transition piece, which is located above the mean sea level (MSL). For the concept of a full-height lattice tower, part (1) is not existing as part (2) goes all the way from sea ground (GRD) up to the RNA.

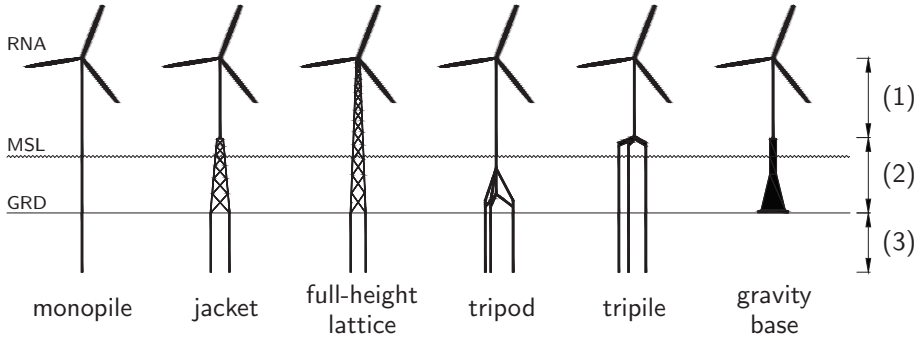

Figure 1.1: Various bottom-fixed support structure concepts (not to scale)

The work described in this thesis was performed on bottom-fixed support structures with a lattice tower design (named as 'jacket' and 'full-height lattice' in Figure 1.1). As a simplification, the design of the tower and foundation part was not analyzed or optimized. Hence, the focus of this thesis lies on bottom-fixed support structures for offshore wind turbines by investigating a lattice type part (2), the sub-structure, in detail.

1.1 Outline

The scope of this thesis is presented as a collection of research articles. The structure is based on an introduction, presenting mainly the motivation and objectives of this work. It is followed by a theory chapter, giving the reader the relevant and needed scientific background to be able to understand the performed analyses. As the appended papers give a detailed insight to the research results achieved, chapter 3 describes each paper by a small overview only. The introductory part of this thesis

is closed by concluding remarks and a recommendation for further work. In total seven research papers are appended which can be found in Appendix A. In addition, the author contributed to four other related publications which are not appended in the thesis. Abstracts of those publications can be found in Appendix B.

1.2 Motivation and objectives

Driven by debates about the impact of pollution on the world climate as well as the increasing demand for energy, the interest for renewable energy is omnipresent. Several governments in Europe have named offshore wind power as a potential future energy source, powerful enough to be able to cover a significant share of the total energy production [9]. As an example, the United Kingdom has announced ambitious plans in their Round 3 program [10, 11], focusing on energy production by large offshore wind farms far away from shore to be able to achieve their climate goals. The above mentioned opportunities of offshore wind resources are promising in this sense. However, going offshore brings up several challenges as additional structural loads due to the marine environment [12], as well as installation and maintenance issues [13]. Taking into account better wind resources on the one hand, and additional challenges on the other hand, produced offshore wind power is by a factor of about 2 more expensive than onshore wind power [14]. Therefore, a cost reduction is strongly needed to be able to increase the economic feasibility of offshore wind power [15].

Several reasons for the increased cost of energy when going offshore are discussed, as for example the material cost, design and installation of the support structure, or loading issues related to the marine environment [16]. In a general perspective, also standards drive the extensive use of material for support structures, among other things based on large safety factors or uncertainties in the calculation of loads [17]. The offshore oil and gas industry has accepted these conditions so far as it is a high risk business, related to possible accidents both in terms of human and environmental aspects. However, the offshore wind industry has a much stronger focus on economic feasibility, as wind turbine installations are unmanned and environmental accidents are less severe. This puts more focus on the need of cost efficient designs construed for relevant loads.

As a central tool in the design process of offshore wind turbines, time-domain simulations are often performed [18]. This technique is based on state descriptions of the complete simulated system in each individual time step, calculated and solved in an iterative process. Alternatively, analyses can be performed in frequency-domain [19–21], a technique which is not further investigated in this thesis. The main

reason for the choice of the time-domain is the challenge in frequency-domain analyses to correctly represent structural response loads resulting from simultaneously applied stochastic wind and wave loads. For complex structures, such as lattice towers, with a large number of nodes and members and additional various load influences, time-domain simulations can be a time consuming task. This is an undesirable situation in the context of cost reduction. Issues related to simplifications in time-domain simulations, their validity and accuracy as well as their efficiency are leading to the first objective of this thesis:

A better understanding of complex time-domain simulations is of central interest. Research questions addressed are as following:

- To which extent has the represented variability of input loading consequences on the simulation results, e.g., is a simulation error to be expected and eventually in which quantity?
- Can time-domain simulations in the design situation of power production be simplified in a fatigue load assessment, to be able to reduce the number of simulations needed significantly?
- What are limitations of sequential analyses, e.g., a decomposition of the RNA and support structure, versus integrated analyses in terms of structural load representations?

Several studies related to this research field can be found in the literature. Kvittem and Moan [22] investigated the influence of input loading variability on floating offshore wind turbines, focusing on simulation length and bin sizes of wind and wave input data. Simplified approaches for wind turbine load cases were studied by Manuel et al. [23], Fitzwater [24] and Dong et al. [25]. In these studies, load case results were estimated by regression methods or the use of probability distributions. Böker [26] studied load simulations and local dynamics of both integrated and sequential models. New contributions presented in this thesis are related to the application of such analysis methods to lattice type sub-structures with focus on simulation accuracy and efficiency. The to be expected error which may result from simplifications made in the simulation setup is an important information for the evaluation of numerical models and simulation results.

Another aspect of an efficient design process is the structural optimization towards a minimized cost of energy of the whole system [27–30]. Relevant loads for the structural optimization are in the case of offshore wind turbines represented by irregular input loading of wind and wave forces. Such structures are concerned as

complex coupled structures, where different parts of the structure are exposed to different loading characteristics. Due to the rotational movement of the rotor during operation, additional loading frequencies are applied to the system which have to be taken into account in the analysis. Optimization of lattice towers under these conditions is challenging, leading to the second objective of this thesis:

The adaptation of optimization approaches in the analysis of complex coupled structures can lead to an efficient design. This is investigated by the following analyses:

- How can automatic optimization approaches be used for the efficient design of lattice type sub-structures for offshore wind turbines?
- What kind of optimization approach is favorable in terms of number of iterations or total analysis time?
- To which extent can the structure be optimized, e.g., what is the material utilization by applying ultimate and fatigue loads to the structure?

Optimization studies for wind turbine structures have been performed on several aspects and components of the system. Yoshida [31] used a genetic algorithm for the optimization of the tower. Long et al. [32, 33] worked on structural optimization of a full-height lattice tower under static and dynamic loading. Ashuri et al. [30] investigated a multidisciplinary design optimization of the complete offshore wind turbine system for minimum levelized cost of energy, using gradient-based optimization. The in the following presented results on optimization aspects show the application of different optimization approaches to lattice type sub-structures, focusing on an efficient design in terms of minimized weight by providing sufficient ultimate resistance and fatigue lifetime. New contributions by this thesis are the development of a local optimization approach for offshore wind turbine sub-structures as well as the application of stochastic optimization approaches to such complex systems.

1.3 Research results

It requires a detailed understanding of the time-domain simulation process, as well as the dynamic behavior of offshore wind turbines to be able to achieve efficient support structure designs. In this thesis, both mentioned aspects were investigated in detail using the example of a lattice type sub-structure. Achieved research results can be summarized as following:

- The input loading variability of turbulent wind and irregular waves was investigated based on a large simulation study with about 30,000 time-domain simulations. It was found that the variability due to finite sampling of this input loading is an important source of simulation error; for ultimate loads, an error of 12-34% and for fatigue loads, an error of 6-12% can occur when following international standards with a total simulation length of 60 minutes and various load cases. This work is documented in Paper 1.

- The potential reduction of the computational effort needed for time-domain simulations was investigated by proposing a method using statistical regression models for a simplified fatigue load assessment in the design situation of power production. It was shown that by reducing the number of simulated load cases from 21 to 3, the total fatigue damage estimate exhibited a maximum error of 6% compared with the complete assessment. Consequently, the simulation time could be shorted by a factor of 7. The detailed development of the method is described in Paper 2.

- Using the design of a commercial lattice type sub-structure, different approaches to load calculations were studied with respect to sequential and integrated simulation setups. Integrated analysis seems to generally predict less fatigue damage than sequential analysis, decreasing by 30-70% in two power production cases with small waves. This finding and other comparisons, as for example discrepancies of different simulation software packages, are shown in Paper 3.

- A first attempt to apply automatic optimization approaches on a lattice type sub-structure in time-domain simulations is described in Paper 4. This study was performed using a genetic model of a 10MW offshore wind turbine, supported by a full-height lattice tower. A local optimization approach was developed and applied for the identification of optimal member dimensions in each section of the structure, aiming for a full material utilization in terms of fatigue damage over the lifetime of the structure.

- Focusing more on different optimization techniques, three studies were investigated with the aim of structural optimization in terms of fatigue damage, using automatized approaches. Paper 5 goes into detail of the local optimization approach, which is based on the principle of decomposition. It was found to be very efficient, resulting in a nearly full utilization of fatigue resistance. Another optimization technique based on a stochastic approximation method was used in Paper 6. The study shows the application and feasibility

of a simulation-based optimization of lattice type sub-structures with the simultaneous perturbation algorithm. Considerably improved designs could be achieved. However, the method was found to be very time consuming. A third optimization study was performed using a genetic algorithm (Paper 7). It was shown that member dimensions could be optimized for a complex lattice tower structure following the stochastic nature of the process. Again, the stochastic selection of new designs, as in the simultaneous perturbation algorithm, resulted in a time consuming but successful structural optimization.

1.4 Readership

This thesis is focused on the application of time-domain simulations for the optimization of lattice type sub-structures for offshore wind turbines. This includes a better understanding and documentation of time-domain simulations of offshore wind turbines in general, but also the fatigue assessment of such complex structures. The readership is students, researches and engineers in both academia and industry working with computer simulations of wind turbines. It addresses topics as the application of simulations, the fatigue assessment as well as automatic optimization approaches.

2

General scientific background

2.1 Offshore wind turbine model

Affected by the offshore oil and gas industry with its experience over several decades, sub-structures for offshore wind turbines have been presented and installed in a variety of different concepts, known from the oil and gas sector [34, 35]. Beyond the bottom-fixed lattice tower structures, two types have been used for the research investigations in this thesis, as shown in Figure 2.1: firstly, the so-called jacket, a hybrid structure which supplies support for a traditional tubular tower above the water surface (known from onshore wind turbine installations). It is shaped as a lattice tower from slightly above the water surface down to the sea ground [36–38]; and secondly a full-height lattice tower, which supports directly the RNA and goes all the way down to the sea ground without structural transitions to other conceptual elements [32, 33, 39, 40]. Both concepts were realized in a four-legged configuration, which counts as industry standard for installed wind farms today. In addition, also three-legged configurations have some potential [41], but are not further presented in this thesis.

An advantage of lattice tower structures compared to other sub-structure concepts (cf. Fig. 1.1) is their suitability for the installation in a large range of water depths, from shallow waters of around 15-20m to deep water sites of up to 70m or more, depending on their economic feasibility. Another advantage is the good stiffness-to-weight ratio as well as their transparency to wave loads. Drawbacks of lattice towers are the increased structural complexity, related to both design and fabrication process, and the need for a transition piece from a space frame structure to a tubular tower, in cases where such a combination is used.

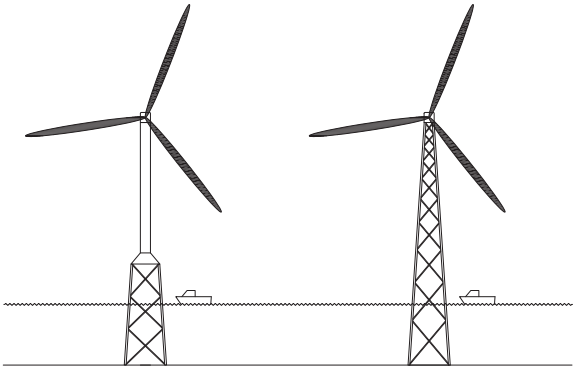

Figure 2.1: Concepts of jacket and full-height lattice tower. Details such as secondary structures or foundation piles are not shown.

For the definition of the topology of a lattice tower structure, several parameters are essential, as for example the number of legs, top and bottom distance of the legs, number and height of sections as well as diameter and thickness of legs and braces. Based on the parameterization of the lattice tower structure, the numerical model of the sub-structure can be established. Additional information is needed about the foundation concept used. In practice, lattice tower structures are connected to piles which are driven into the sea ground. While this realistic representation was used in some studies, other results were obtained by modeling a simplified foundation, represented by a fixed connection in all degrees of freedom of the bottom of the lattice tower structure with the sea ground [38, 42].

The accurate simulation of offshore wind turbines is dependent on a realistic representation of the wind energy converter in the numerical model. In general, commercial data for the RNA and its specification is not available from the suppliers due to confidential restrictions. In an attempt to overcome this lack of information, NREL [43] has come up with a generic model of a 5MW wind turbine, while NOWITECH [44] and DTU [45] have specified a 10MW wind turbine. These wind turbine concepts are aiming for a realistic representation of today's industry standard type, a three-bladed upwind horizontal axis wind turbine. The control system is based on variable speed with blade pitch. Specifications are public available in enough detail to be able to model the RNA for integrated analyses. For studies presented in this thesis, generic models of the 5MW NREL turbine and the 10MW NOWITECH turbine were used. Selected specifications of the two turbine representations are given in Table 2.1.

Table 2.1: RNA specifications for the NREL 5MW [43] and NOWITECH 10MW [44] offshore wind turbine.

Property	NREL 5MW	NOWITECH 10MW
Rotor diameter	126m	141m
Hub height	90m	101m
Cut-in, Rated, Cut-out wind speed	3,11.4,25m/s	4,15,30m/s
Tip speed ratio	7.55	7.80

Uncertainties about the simulation model in terms of a realistic representation of an offshore wind turbine are one of the reasons for the use of prescribed safety factors in international standards. Simulation errors can for example be caused by the modeling approach, by the implementation of the structural model, by uncertainties about material properties and environmental conditions, or by simplifications and approximations used.

2.2 Loading conditions

When the numerical offshore wind turbine model is defined and established in the software, loading conditions can be applied during the simulation. A first definition is the selection of the design load case (DLC). The DLC characterizes the status of the wind turbine, which can be in operation, during fault conditions or standing still. The international standard IEC 61400-3 [7] gives a comprehensive overview over defined DLCs with their applied conditions. Each DLC is also categorized by its main structural loading in the classes of ultimate or fatigue, respectively.

A central design situation is *power production*, listed as DLC 1.x in the standard. For fatigue analyses, which are dominant in this thesis, DLC 1.2 was applied. In this case, wind conditions are modeled by a normal turbulence model for wind speeds between cut-in and cut-out wind speed, while waves are represented by normal sea state conditions. For the estimation of structural responses to ultimate loading, two additional DLCs were selected: DLC 5.1, the emergency shut down; and DLC 6.1, idling in storm conditions.

Offshore wind turbines are exposed to the marine physical environment, including both meteorological as well as oceanographic aspects. In general, environmental conditions occur in a stochastic manner and are time dependent, as indicated by the time series data for wind and wave loading shown in Figure 2.2.

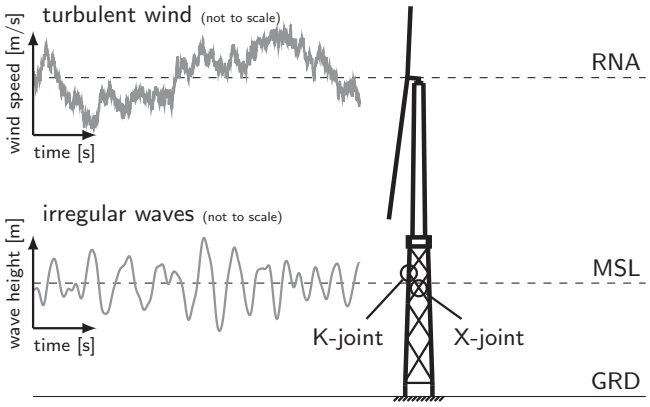

Figure 2.2: Offshore wind turbine model with representation of input loading time series.

Meteorological aspects

The most important factor of the meteorological aspects is the wind. It is caused by pressure differences in the atmosphere, acts in various directions and with a turbulent pattern [46]. Wind is the source of natural energy which is needed for a wind turbine to produce electricity. Hence, strong and steady winds are of high priority for the planning of a wind turbine installation. However, strong winds reaching wind speeds above the cut-out wind speed of the turbine are of no use, as the wind turbine cannot withstand the loading resulting from the situation of power production under such wind loading. Another unwanted wind characteristic is the phenomena of wind shear. It is caused by the boundary layer of the water surface and results in various horizontal wind speeds over the rotor height from bottom to top. Such different flow and loading conditions, both in time and space, have to be accounted for when designing a wind turbine.

Other meteorological aspects as the variation of temperature, humidity or pressure are of small influence to structural analyses and are normally neglected in simulation studies.

Oceanographic aspects

As the production of electricity of an offshore wind turbine is purely directed on the incoming wind loading, all oceanographic aspects are additional loading conditions, not contributing to the energy production. The sub-structure is first of all exposed

to wave loading, which occur in an irregular pattern. Other loading effects by the surrounding water mass acting on the structure can be caused by tidal variations, sea currents, scouring around the foundation piles [47] or drift ice, depending on the location of the offshore wind turbine installation [48].

Marine growth is another aspect and can be observed on marine structures in different thicknesses depending on the water depth. As the thickness layer of marine growth can reach a thickness of 10cm and more on the submerged part of the structure [49,50], it has a significant weight which is influencing the dynamic behavior of the structure, as for example the eigenfrequency. In addition, the thickness layer increases the drag diameter of the structural element, resulting in a larger drag force.

For the studies presented in this thesis, wind and wave directions were assumed to be aligned. This simplification of the required load case investigations was made under consideration of the comparable small impact of wind-wave misalignment on the structural response loads [41, 51].

Site specific data

While RNA components of the wind turbine are normally mass produced, support structures are not and are often designed for one specific site only. In general, a site specific optimization of the whole system could be favorable in terms of energy production [52], however, it will also increase the cost of installation. Both wind and wave conditions as well as geotechnical properties of the soil are important parameters for the design of offshore structures. This requires sufficient knowledge about the environmental conditions at the specific site in the design phase.

For simulations, a realistic representation of the environmental conditions is as important as a detailed implementation of the structural model. Site specific data are in general not public available. However, some project reports can be found in the literature including actual measured data, or extrapolated data. As an example, the UpWind design basis [53] lists measurement data for two sites in the Dutch North Sea. For a third site for deep water studies, the data was correlated to an extended water depth.

2.3 Wind turbine design and analysis software

Due to the complexity of an offshore wind turbine with its mechanical and electrical components, as well as the simultaneous loading by wind and wave forces, simulations of such integrated structures require advanced analysis software. The analysis relies on aero-hydro-servo-elastic simulation codes, taking into account the interaction of the complete structure and its applied environmental conditions. Integrated

simulations based on this principle are performed in time-domain. The analysis software is calculating loading conditions in each time step and is updating the dynamic behavior of the structure correspondingly. Typically, a time step between Δt=0.025s and Δt=0.050s is used for wind turbine analyses. The size of the time step has to be chosen carefully to be able to capture high frequent excitations in the structure.

Simulation codes which are capable to solve the dynamics of offshore wind turbines in time-domain have been established both by academic institutions and commercial companies. Examples for academic developments are FAST from NREL [54], HAWC2 from DTU [55] or 3Dfloat from NMBU [56]; on the commercial side, Bladed from DNV GL [57], Fedem Windpower from Fedem Technology AS [58] or ASHES from Simis AS [59] are examples of available tools. An international research activity which received attention was a large benchmark study of such simulation codes on the example of a jacket type sub-structure for an offshore wind turbine [60]. Results showed differences in the modeling background of the simulation codes, and stated the importance of the modeling of local dynamics of the structure.

Fedem Windpower

The selected simulation code for the time-domain analyses presented in this thesis is Fedem Windpower. Fedem stands for *Finite Element Dynamics in Elastic Mechanisms*. The software package provides the capability to model complex structures and to simulate their dynamic behavior based on a nonlinear structural dynamics approach [58]. The code includes modeling features for control systems and predicts the dynamic response of elastic mechanisms experiencing non-linear effects such as large rigid-body motions [61]. The structural modeling is based on Euler-Bernoulli beam theory [62]. Hydrodynamic forces due to drag and added water mass acting on the structure are computed based on the Morison equation [63], using drag and added mass coefficients of 1. Beyond the windpower features, blade geometries and properties can be modeled for load calculations based on blade-element momentum theory of the incoming wind loading; the control system of a wind turbine can be applied; realistic rotor dynamics are transferred to the support structure, therefore, local dynamics caused by rotor frequencies can be studied.

Efficient simulation setup

The cost of computation time is a critical point in the application of time-domain simulations. Tasks as the simulation of a complex offshore wind turbine might take up to three times real time (depending on the available hardware, as shown in Paper

1 in Appendix A), e.g., a simulation of for example 1 hour real time needs the computational effort of 3 hours processing time. For large simulation studies based on the same topology of the structure, parameter variations can be simulated in parallel by so-called *events* in Fedem Windpower. The use of events allow for parallel computing of somehow similar simulations and can reduce the total computational effort of such studies significantly.

As Fedem Windpower was used in this work as a modeling tool and dynamic solver only, all file handling and post-processing was performed in Matlab (The Mathworks, Inc., Natick, USA) by in-house written codes, as described in Section 2.4 and 2.5. When using a high-end workstation for simulations with a significant number of processor cores, an efficient setup for the simulation process is of importance. This includes both the simulation performance, as well as the file handling. Parallel performed simulations generate a large amount of result data simultaneously, which has to be processed by the hardware.

As an example, the available workstation for most of the studies presented in this thesis was equipped with two Intel® Xeon® processors, a 512GB solid state drive (SSD) storage, an 8TB hard disk drive (HDD) storage and 128GB random-access memory (RAM). When storing the model file on the HDD, as usually done, the file processing of result data from 15 parallel time-domain simulations couldn't be handled fast enough by the HDD, e.g., the bottleneck was not the processor speed as one would assume. This issue could only be slightly improved by storing the model file and result data on the SSD, even if reading and writing speed is much higher on SSDs versus HDDs. The real improvement when it comes to simulation speed was first achieved when the model file was stored on a RAM drive, which is a block of RAM allocated as storage media and available for computer media [64]. RAM is order of magnitudes faster than other forms of storage medias, which allows much higher reading and writing speeds. As storage space on RAM is rather limited, the time-domain simulation in Fedem Windpower was monitored by a Matlab script running in the background. This script was looking for completed event runs which could be moved from RAM to the HDD for storage and further post-processing. This setup was found to be the most time efficient solution for performing a large number of simulations on the available hardware. The workflow of this simulation setup is presented in Figure 2.3 by a flowchart. Matlab code examples for the implementation are given in Appendix D.1 and D.2.

From release 7.1 on, Fedem Windpower supports the Component Object Model (COM) for programmatic/scripting automation [65]. This is a very useful tool for the creation of models and a powerful control possibility for simulation setups. With the implementation of scripts, fully-automatic optimization approaches by combining the finite element solver of Fedem Windpower with in-house programmed post-processing

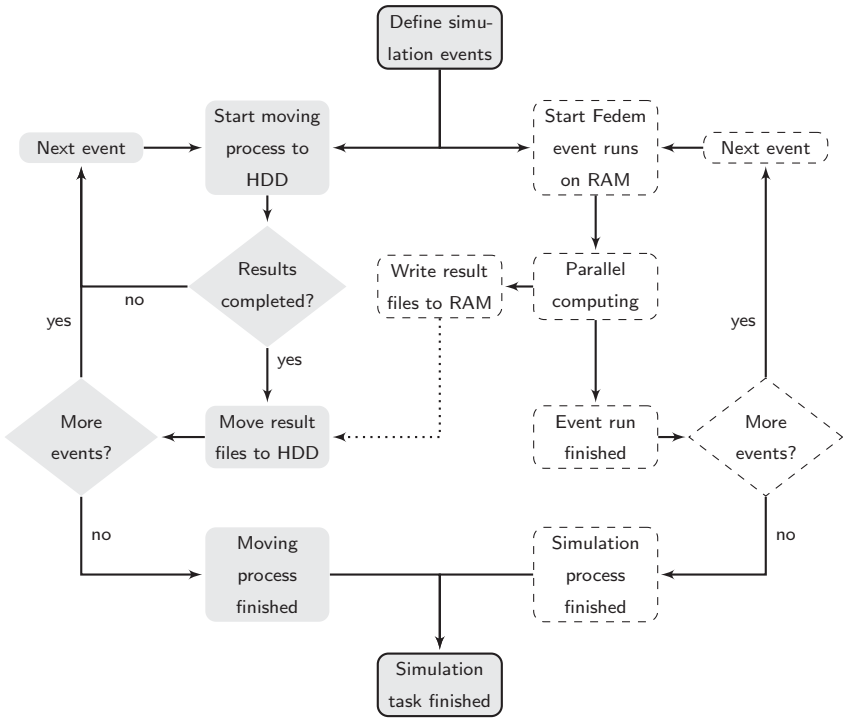

Figure 2.3: Workflow for the time efficient processing of a large number of simulations. Matlab tasks are shown with gray background without border; Fedem Windpower tasks are shown without background and dashed border.

scripts can be improved significantly. An example for a fully parameterized jacket model established by the COM-API (application programming interface) in Fedem Windpower is given in Appendix D.3.

2.4 Structural analysis

When the stochastic input loading acting on the structure is exceeding limits of the material properties, damage and a failure of the structure can occur. These limits are analyzed for ultimate and fatigue loading, and are described by the ultimate limit state (ULS) and the fatigue limit state (FLS), respectively. In ULS-analyses, response loads of the structure are investigated for the exceeding of elastic deformations,

while in FLS-analyses, the impact of cyclic loading on the lifetime of the structure is calculated.

Stress calculation

The stress calculation for tubular beam elements is in general a simple task. Axial stresses are calculated by the division of axial force and structural area; in-plane and out-of-plane bending stresses are calculated by the division of bending stress and moment of inertia, multiplied by the radius of the beam cross section. However, due to the connection of several members in one tubular joint, the calculation of stresses is more complex in the joints of lattice tower structures. 4 or 6 members are typically connected in X- and K-joints (cf. Fig. 2.2), respectively. The interaction of several members in one joint leads to stress concentrations. Therefore, stress concentration factors (SCF) have to be calculated by dedicated formulas for tubular joints, as for example described in DNV-RP-C203 [66]. SCFs are defined as the ratio of hot spot stress (HSS) to local nominal stress.

The superposition of stresses in tubular joints is calculated at in total eight different points around the circumference of the intersection. HSS $\sigma_{1..8}$ are derived by the summation of the single stress components from axial, in-plane and out-of-plane action. Therefore, the structural analysis of a multi planar joint such as a K-joint in lattice tower structures is a comprehensive task. More details about the number of stresses to be evaluated in such structures are described in Paper 2 in Appendix A.

Ultimate loads

Each HSS time series obtained by the stress calculation is analyzed on its maximum absolute stress, representing the ultimate load of the limited time series. Expected ultimate loads for longer periods, as for example the 50 year recurrence period, are calculated based on statistical extrapolation of ultimate loads, adapted to the procedure described in Annex F of IEC 61400-1 [67]. This method extracts a selection of extreme loads from the response time series and calculates their probabilities of occurrence. By the use of fitting functions, the expected ultimate load for the probability of the 50 year recurrence period can be calculated.

Fatigue assessment

For cyclic loading with a constant stress range, fatigue damage occurs when the number of applied load cycles is exceeding the maximum allowable number of cycles

before fatigue failure for this specific stress range. Fatigue properties of materials are documented in standards and are typically given as S-N-curves (S-stress range, N-number of cycles), as for example in DNV-RP-C203 [66]. The fatigue investigation of stochastic responses is based on the same principle; however, each individual stress range of the time series has to be analyzed. This is done by performing a rainflow counting analysis [68]. This analysis extracts all load cycles with its stress ranges from the response time series. Due to the large amount of data for longer time series, results are normally collected in a histogram for stress range bins with its summed up number of cycles.

A common method for fatigue damage calculation has been defined by Palmgren [69] and Miner [70]. The method is based on the definition that a fatigue failure occurs when the number of applied load cycles divided by the maximum allowable number of cycles exceeds $\mathrm{D} = 1$ (D-damage). This simple definition is valid for cyclic loading with a constant stress range, and has to be extended for the application of stochastic loading with various stress ranges (Eq. 2.1).

$$\mathrm{D} = \sum_{i=1}^{k} \frac{n_i}{N_i} \tag{2.1}$$

where D is the accumulated fatigue damage, k is the number of stress range bins, n_i is the number of stress cycles in stress range bin i and N_i is the number of cycles to failure at constant stress range $\Delta\sigma_i$.

The above mentioned histogram data is used for the total fatigue damage calculation based on the Palmgren-Miner rule. Therefore, each stress range bin contributes with a fraction of fatigue damage to the total fatigue damage D of the analyzed time series. The result obtained by the total fatigue damage D can be put into context to the expected lifetime of the cyclic loaded material by dividing the length of the analyzed time series by the fraction D. For results with $\mathrm{D} < 1$, the material can survive a corresponding loading longer than expected; for $\mathrm{D} \geq 1$, the lifetime is actually shorter than expected.

For analyses with focus on relative comparisons only, a simplified fatigue assessment can be performed based on a so-called damage equivalent load (DEL) [71]. This method is not following the complete fatigue assessment with stress analyses and lifetime calculations, but is only focusing on the fatigue characteristics of the stochastic response load time series. The basis of this method follows the Palmgren-Miner rule, too. However, results are treated differently in the DEL-analysis. For a defined reference number of cycles, the fraction of total fatigue damage can be transferred back to a specific load cycle range, assuming that this constant load cycle range (=DEL) causes the same amount of fatigue damage as the stochastic response

load time series. The so found DEL can be used as a fatigue characteristic of the response time series. By this, the DEL allows for example for direct comparisons of several simulation results in a parameter study.

2.5 Structural optimization

Although only 17 percent of the total capital cost of an offshore wind turbine installation are related to the sub-structure and foundation, a significant potential for cost reductions is identified in this area [15, 72]. One of the main interests of this thesis are therefore structural optimization approaches for lattice type sub-structures. Optimization is in this context defined as optimization for material cost, e.g., the structural weight is a central parameter for the analyses performed. The optimization goal in general was a full material utilization over the lifetime of the structure in terms of ultimate and/or fatigue resistance, realized by the lightest structure possible. An optimized structure is normally achieved after several iterations in optimization studies, calculated and designed by an automatic process.

The application of structural optimization approaches in the wind turbine design process has so far been limited, compared to automotive or aerospace industry. It is a highly relevant research field with several open questions due to the complexity of the dynamic system [29]. Structural optimization approaches from static load cases, as for example gradient-based techniques [73] are difficult to transfer to the dynamic behavior of wind turbines. Firstly, time-domain simulations would to too time consuming in order to obtain necessary gradient information; and secondly, ULS and FLS as optimization parameters are not generic constraints, e.g., structural sensitivity information could hardly be obtained. One possible solution in this case is the application of simulation-based optimization approaches. Optimized designs can be obtained by dedicated or stochastic choices in an iterative process. This idea was the basis for three investigated optimization approaches, as described below.

When optimizing the structure, dimensions of legs and braces are changed by varying diameter and/or thickness of the member. This modification can influence both structural weight as well as axial and bending stiffness, at the same time, or independently of each other. Figure 2.4 shows the dependency of diameter to thickness combinations in terms of weight and stiffness characteristics. Taking the example of P_0 as initial dimensions, several pathways can be chosen during optimization: a change $\mathrm{P}_0 \rightarrow \mathrm{P}_1$ keeps weight and axial stiffness on a constant level, but increases bending stiffness; a change $\mathrm{P}_0 \rightarrow \mathrm{P}_2$ decreases weight and axial stiffness, but keeps bending stiffness on a constant level; a change $\mathrm{P}_0 \rightarrow \mathrm{P}_3$ decreases both weight, axial and bending stiffness at the same time.

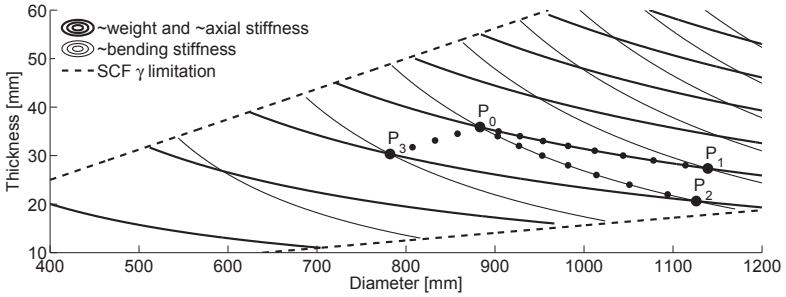

Figure 2.4: Dependency of weight and stiffness characteristics as well as SCF-limitations on member dimensions by diameter (d) and thickness (t). SCF $\gamma = \mathrm{d}/(2\mathrm{t})$ is limited by a validity range defined in DNV-RP-C203 [66]: $8 \leq \gamma \leq 32$

Dimensional changes of the members will not only influence structural weight and stiffness, but also the eigenfrequency of the structure. For a somehow realistic start configuration of the optimization process, changes to the eigenfrequency are normally small. However, in cases where the optimization approach selects a design with an eigenfrequency with risk for resonance due to a matching excitation frequency, the calculated fatigue lifetime will be comparable small and the design will be rejected by the process.

The in the following discussed optimization approaches differ mainly in their strategy for the selection of new designs, their number of iterations needed and performance in terms of computation speed. In each optimization iteration, parts of the structure, or its complete design, are redesigned by the selection of new member dimensions. In the case of a dedicated choice of member dimensions (as used for the local optimization approach), the selection is based on the analyzed loading distribution in each member of the previous simulation run. Another approach is the stochastic choice (as applied for the simultaneous perturbation and genetic algorithm), where the selection of new member dimensions is performed randomly within given limits.

Local optimization

The main idea of the local optimization approach developed for this thesis is that the knowledge of a loading distribution on a given structure should be sufficient information to be able to optimize each member of the structure [74, 75]. In detail, the ultimate and fatigue loading of each member can be extracted from a simulation

run and put into context to the actual capacity of the member. Depending on this result, the member can either be decreased or increased in its stiffness properties. When concerning the complete structure as a frame of independent members, this analysis should result in a perfectly optimized structure [76]. However, dependencies of one member to another are not taken into account by this approach. Therefore, the local optimization requires several iterations for a convergence since dependencies in the structure often require a redesign of a member after the initial optimization iteration. The local optimization approach was applied in studies presented in Paper 4 and 5 in Appendix A.

Simultaneous perturbation

The simultaneous perturbation stochastic approximation (SPSA) has been documented in detail by Spall [77–79] and was in this thesis the first time applied to a structural optimization task for offshore wind turbines. The approach can be described as a pseudo-gradient method that evaluates only two functions per iteration for all design parameters at the same time. Normally, gradient-based search algorithms need to evaluate changes in each parameter independently [80]. The pseudo-gradient of the SPSA is determined by a perturbation vector and the simulation result of the previous iteration. The perturbation vector is randomly generated in each iteration of the algorithm. More details of the method are given in Paper 6 in Appendix A.

Genetic algorithm

Another optimization approach based on the stochastic selection of new designs is the genetic algorithm [81–83]. Its principles are the natural selection and survival of the fittest. The approach has its origin in biological evolution, also indicated by the terms used for the selection of designs: genes, chromosomes, individuals, generation, population, etc. The idea is that subsections of the structure, which perform well in the structural analysis, should be combined with other well performing subsections of another design, leading to an overall optimized structure. All parameters of the structure are binary coded in one string. This string is so combined for two structures by crossover and mutation operations, resulting in a new string representing the parameter set of a new design. The detailed combination technique as well as the application of the genetic algorithm is described in Paper 7 in Appendix A.

3

Research findings

Within the field of complex time-domain simulations and structural optimization aspects, the two central topics of this thesis, several research tasks were investigated. Findings are documented in detail in the appended seven papers in Appendix A, which are described shortly in this chapter.

Common for all papers is that the analyses were performed by time-domain simulations on lattice type sub-structures for offshore wind turbines. Both fatigue analysis and the design situation of power production were of central interest for most of the work. For the representation of realistic loading frequencies, two different wind turbine models were used: the NREL 5MW baseline turbine [43] and the NOWITECH 10MW reference turbine [44]. Table 3.1 gives an overview over the field of interest of the different papers as well as the offshore wind turbine model used.

3.1 Simulation aspects

Paper 1: The simulation error caused by input loading variability in offshore wind turbine structural analysis

A large simulation study with about 30,000 simulations was performed to investigate the influence of input loading variability to the structural response of the sub-structure. Wind and wave time series representing the input loading are in general obtained by pseudo-random generators using a certain initial seed number. For a significant number of wind and wave seeds, 2 design load cases and 11 different wind speeds with their respective sea state data were simulated.

Table 3.1: Paper overview for aspects of simulation (Paper 1-3) and optimization (Paper 4-7).

	Field of interest	Sub-structure	Turbine
Paper 1	Input loading variability	OC4 reference jacket	5MW
Paper 2	Simplified fatigue load assessment	OC4 reference jacket	5MW
Paper 3	Integrated and sequential analysis	OWEC Quattropod jacket	5MW
Paper 4	Local optimization	Full-height lattice tower	10MW
Paper 5	Local optimization	OC4 reference jacket	5MW
Paper 6	Simultaneous perturbation	Full-height lattice tower	10MW
Paper 7	Genetic algorithm	OC4 reference jacket	5MW

The first result of the analysis was that the influence of wind seed variability is more important than wave seed variability. Therefore, in the case of a limited simulation setup, it is recommended to simulate several wind seeds for one wave seed only. This finding is related to a relatively calm sea state used in the simulation study, which was defined for a deep water site in the UpWind project [53].

The main investigation of the paper was the estimation of simulation error caused by the use of different seed numbers for the generation of input loading time series. The simulation error was defined by the discrepancy between results obtained by a limited simulation task compared with results obtained by theoretically infinitely long simulations. The analysis was divided into short-term simulations of 10 minutes, and long-term simulations of 60 minutes. As one would expect, the analysis confirmed that both approaches lead to relatively similar results for the same total simulation length, as for example 6x10min and 1x60min. However, the fatigue analysis of several short-term simulations has to be performed carefully, to avoid a systematical error in the calculation.

Another important result of this paper was the dependency of simulation error to the total simulation length. The recommendation given in IEC 61400-3 [7] requires for example a total simulation length of 60 minutes, either obtained by short-term 6x10min or long-term 1x60min simulations. The found simulation error converges from for example 10 to 60 minutes. However, the retaining simulation error was of a significant order which is not documented in the standard.

Paper 2: Simplified fatigue load assessment in offshore wind turbine structural analysis

In an attempt to reduce the number of simulations required for a DLC analysis in the situation of power production, a simplified fatigue load assessment was proposed. Opposite to traditional methods of linear or exponential fitting curves, a new approach based on statistical methods was presented in the paper. The idea was based on the accurate estimation of total fatigue damage over a number of load cases, for example from cut-in to cut-out wind speed of the turbine. This implies that the individual fatigue damage for each wind speed was of minor interest, as long as the summed up total fatigue damage over all wind speeds was estimated with high accuracy.

Two statistical methods were applied and discussed in this study: the piecewise linear regression (PLR) and the multivariate linear statistical model (LSM). The PLR on the one hand is a more traditional regression method, based on the estimation of fatigue damage for each individual load case. A few data points have to be simulated, so that others can be linearly interpolated. The LSM on the other hand is a more flexible regression method in statistics. It also requires a few simulated data points, but not all individual fatigue damages for all load cases are estimated. The total fatigue damage over all load cases was so calculated by the sum of the few known points, multiplied by coefficients obtained from a training of the method with known data sets.

The application of these two statistical methods was tested on a load spectrum of 21 load cases between cut-in and cut-out wind speed of the NREL 5MW baseline turbine. Of these 21 load cases, a selection of n=3,4,5,6 load cases was chosen for the estimation of the total fatigue damage by statistical methods, which was evaluated against the sum of individual fatigue damages of all 21 load cases. Results for the estimation accuracy were obtained in percentage deviation from the 'known' value over all 21 simulated load cases. Already for only 3 out of 21 simulated load cases, the total fatigue damage could be estimated with a maximum error of 6.4%. Compared to a traditional analysis, this increased the speed of the fatigue analysis by a factor of 7.

Paper 3: Comparison of different approaches to load calculation for the OWEC Quattropod jacket support structure

In the course of time-domain analyses of offshore wind turbines, the topic of integrated versus sequential simulations is of high interest. Integrated analyses include all components of the structure and wind turbine in one simulation model,

which should be the natural approach for the modeling of such complex structures. For sequential analyses, only some components of the structure are represented by a simulation model, while influences from other components are represented by extracted displacement time series from integrated analyses. In general, integrated analyses can be simplified to sequential analyses, provided that the same simulation software is used, identical environmental conditions are applied and the structural model of the analyzed component is modeled with same detail. An example of such a comparison for a simple beam model is shown in Appendix C.

However, integrated analyses are difficult to achieve for commercial projects as each industry partner normally not wants to give away his detailed computer model [84]. This often results in that analyses are performed sequential, where each industry partner uses its own detailed model and simulation software and relies on displacement time series for a specified interface. Sequential analyses are therefore in practice not directly comparable to integrated analyses, due to several simplifications or different modeling approaches in the work process.

The issue of integrated versus sequential analysis was investigated in this paper by the example of a commercial jacket design, the OWEC Quattropod structure. The influence of different simulation codes for the analysis was studied, too. ANSYS ASAS (ANSYS, Inc., Canonsburg, USA), Fedem Windpower and Bladed were used for the comparison of response loads of the in principle same structural model. However, each simulation code showed some implementation limitations which required to simplify a few features, as for example the use of a reduced midsection.

Both test of eigenfrequency, two static load cases and free decay behavior showed good agreement between the simulation codes. An issue which couldn't be resolved in detail was that structural responses to wave loads were in general found to be significantly higher in ANSYS ASAS than in Fedem Windpower. For the analysis of two power production cases, the integrated analysis resulted in general in less fatigue damage than the sequential analysis, decreased by 30-70 percent. The implementation of a reduced midsection model showed only slight differences in eigenfrequencies. Therefore, in simulation codes which not allow for the modeling of shell elements, reduced midsection models might be used if they are calibrated carefully.

The analysis showed limitations in each of the used simulation codes, related to the modeling of the wind turbine, shell elements, or the implementation of mass, stiffness and damping matrices. It is of general interest that simulation codes intended for the use of integrated analyses allow for such features in new releases.

3.2 Optimization aspects

Paper 4: Iterative optimization approach for the design of full-height lattice towers for offshore wind turbines

A NOWITECH research activity was to define a 10MW reference offshore wind turbine [44]. As part of this activity, an initial design of the sub-structure was established and documented in this paper. The design process was based on a novel support structure concept where the RNA is directly supported by a lattice tower structure, going all the way from sea ground up to the RNA.

In this initial study, an iterative optimization approach was applied, which was based on the evaluation of ultimate and fatigue loads due to wind and wave loading on the structure. This approach is understood as *local optimization* in Section 2.5 of this thesis. The minimum total weight of the structure was the overall optimization goal. Since fatigue loading was estimated as the design driver, the lifetime of the tubular joints was the optimization criterion. Three optimization parameter groups were studied: the number of sections; leg and brace member dimensions; and the setup of constant brace angle versus constant section height.

For the comparison of different tower designs in terms of their ULS- and FLS-performance, results were normalized by the yield strength of the material (ULS) or the requirement of 20 years lifetime (FLS). Results larger 1.0 were judged as valid, while results smaller 1.0 led to a failure of the structure. Optimization results were obtained for a design with constant member dimensions over the tower height, as well as with optimized member dimensions in each section according to loads.

Optimization results showed clearly that fatigue is the design driver, as FLS-results for K-legs as well as X-braces were close to 1.0 in FLS, but were in the range of 2-5 for ULS. FLS-results showed additionally that dependencies caused by brace members, which are connected to both K- and X-joints with their same dimensions, prevent the structure from being optimized in all members and connections.

Paper 5: Two-stage local optimization of lattice type support structures for offshore wind turbines

The local optimization approach was further investigated in this study, with the central interest in the accuracy and validity of the proposed method. Two aspects of the optimization approach were studied in detail: the principle of decomposition which is the basis of the idea of local optimization; and a two-staged approach based on simulations by an external finite element solver, followed by an internal sizing process of the structure. The study was performed with the example of the

OC4 reference jacket, slightly modified by the introduction of chords and stubs as structural features. During the optimization, each member of the structure was optimized locally and simultaneously.

Compared to the study described in Paper 4, loading investigations were more comprehensive by the investigation of three DLCs: power production, emergency shut down and parked under extreme conditions. In addition, the DLC in the situation of power production was performed for the complete load case spectrum with wind speeds from cut-in to cut-out wind speed of the NREL 5MW baseline turbine. Simulations of power production load cases were based on the simplified fatigue load assessment described in Paper 2.

The optimization of the structure was controlled by the ULS, FLS and buckling conditions of the members. The influence of the change of member dimensions by diameter and thickness was discussed due to resulting changes of cross sectional area as well as moment of inertia. Largest improvements for the performance of the structure, in terms of material utilization as well as structural weight, were achieved from iteration 1 to 2. Results were converging for several iterations. Interestingly, the sizing of members influenced central parameters as ULS, FLS and buckling performance differently.

The study concluded with that the application of decomposition is a useful technique in local optimization and leads to good material utilization in terms of fatigue capacity over the whole lattice tower structure. In addition, the two-staged approach showed large advantages in terms of computation time, compared to a conventional approach, by maintaining an accuracy of the sizing process of $\pm 20\%$.

Paper 6: Simulation-based optimization of lattice support structures for offshore wind energy converters with the simultaneous perturbation algorithm

By using the simulation setup and post-processing framework established for the analysis of a full-height lattice tower (described in Paper 4), a different computer-assisted optimization algorithm was applied and tested on its performance in this study. The simultaneous perturbation stochastic approximation (SPSA) was used to optimize the sub-structure in terms of member thickness and diameter, aiming for a minimized structural weight.

The SPSA depends on a few parameters and an objective function for the structural optimization. Its functionality is based on a pseudo-gradient which was determined from only two analysis runs. The objective function was defined by variables for weight and joint fatigue lifetime, where the tower weight was the indicator of cost, and the joint lifetime was the limitation for allowable fatigue loading. The perturbation vector of the analysis was generated as a random sample

independently for each component. The objective function used in this study led to a substantial number of infeasible designs, but showed at the same time some interesting results for valid designs.

Optimized structures were compared to results achieved by the local optimization approach, both in terms of final structural weight and number of iterations. In a direct comparison, the SPSA was by a factor of about 10 slower than the local optimization. However, the stochastic nature of the process resulted in optimized structures which were slightly lighter than those obtained by the local optimization. The topology of the structure optimized by the SPSA showed highly nontrivial dimension selections, again based on its stochastic approach.

Overall, the application of the SPSA in structural optimization of offshore wind turbines showed the potential of stochastic optimization approaches. Solutions which a human designer would not consider so quickly can be achieved, and by this new structural solutions could be established. The drawback of this analysis is its extensive computational effort, for example compared to the local optimization, and its need of a careful calibration of the SPSA optimization parameters.

Paper 7: Support structure optimization for offshore wind turbines with a genetic algorithm

As a third technique applied for structural optimization of offshore wind turbines in this thesis, a study with the application of a genetic algorithm was performed. The genetic algorithm is a gradient-free method for optimizing complex structures. Optimization parameters were member diameter and thickness, as discussed in Paper 4-6. In addition, the vertical location of K-joints along the legs was optimized as a new parameter. The optimization was performed based on the topology of the OC4 reference jacket. For the evaluation of structural performance, both ULS and FLS were estimated in all tubular joints.

The population size of the algorithm was chosen to be 15, as the available workstation for simulations provided 16 processor cores. Therefore, a batch of simulations for all individuals of the population could be simulated in parallel for the in total same computational cost (e.g. simulation time) as one single simulation. Due to the interest of performing an optimization study with a large number of iterations (several hundreds), a very short load case in the design situation of power production was chosen to obtain force and moment time series data in all members connected to a tubular joint. The optimization criterion was the structural weight as an identification of material cost, as applied in previous studies.

Similar to the optimization progress in Paper 5, large weight reductions could be achieved for the first few iterations. A convergence of minimum structural

weight could be seen from about 50-100 iterations. Several features of the genetic algorithms were tested in terms of convergence speed and general performance, such as the idea of mutation, immigration, as well as a varying population size.

In general, the structural optimization by use of a genetic algorithm was feasible. The approach can be used for basic member dimension scaling, as well as topology optimization, as shown by the example of K-joint locations. However, the stochastic nature of the approach still requires a significant number of simulations to obtain a reasonable solution. Some aspects of the approach have to be applied carefully. The example of binary thresholds in the encoding of design variables was such a case, which is described in detail in the paper.

4

Concluding remarks and future perspectives

This doctoral thesis gives an overview over the work performed within the field of simulation and optimization in offshore wind turbine structural analysis. Results were obtained by experiments, e.g., computer simulations on high-end workstations with efficient soft- and hardware, and post-processing routines established by the author. The conclusion of the work is presented separately for the aspects of simulation and optimization below.

Simulation aspects

Interests within the aspect of computer simulations are the simulation setup and efficiency on the one hand, and the resulting accuracy of results on the other hand. For the example of input loading variability, investigations showed that the simulation setup recommended by widely used standards led to a significant simulation error in both ULS and FLS, which is not documented by the standard today. The simulation accuracy is also of main interest for simplified load assessments, as documented for a fatigue dominated design load case. The investigation showed a significant improved simulation speed, by observing a reasonable accuracy of fatigue damage results. A third simulation study highlighted challenges of sequential versus integrated analyses, as well as the discrepancy which may result from the application of two different software packages, performing the same task.

Optimization aspects

The structural optimization of offshore wind turbine support structures has a large potential for cost reductions of such installations. Efficient optimization approaches for time-domain simulations are needed to be able to design a structure for the applied highly dynamic loading by wind and waves. Within this thesis, three optimization approaches were developed and/or applied to the optimization task of a lattice tower structure: the local optimization, the simultaneous perturbation stochastic approximation, and the genetic algorithm. Of these approaches investigated, the local optimization was the most promising technique, especially in terms of convergence speed to an optimized structure. However, stochastic approaches as the SPSA and the genetic algorithm showed interesting design solutions, which may not be obtained directly by a human designer.

Future perspectives

When working with simulations of offshore wind turbines, interesting questions arise frequently. Some of them were investigated in detail and are documented by this doctoral thesis. However, there are still several interesting aspects not investigated, which are listed as future perspectives below:

- The simulation setup is of high importance in terms of result accuracy. Besides the in detail investigated wind and wave input loading variability, other uncertainties as soil parameters, the modeling approach, simplifications or approximations are of interest for further work. This is also closely related to the need for a more precise definition of safety factors.

- As all analyses were performed on jacket type or full-height lattice tower structures, it is of interest to apply the approaches presented for other substructure types, as monopiles, tripiles or tripods, too. Linked to this, also a different analysis software, more advanced control systems or environmental load models are topics to discuss. In addition, the applicability of the proposed analysis and optimization methods to floating offshore wind turbines is of interest.

- The case study of the full-height lattice tower in the course of the NOWITECH 10MW reference wind turbine showed promising results. A complete load assessment and detailed design of this structure is proposed as a next step in the development of the concept.

- The optimization of the sub-structure was based on the cost model of structural weight only, e.g., the lightest structure was defined as the most optimal structure. In reality, this is a simplification of the design process. A more advanced cost model is of high interest, taking into account not only the design process, but also fabrication and installation aspects. Topics to investigate are for example the number of tubular joints, the use of standard pipe diameters, the effect of topology changes and welding and manufacturing constraints for the connection of members with different diameter and/or thickness.

- The local optimization approach developed in this work could be investigated further by testing several local optimization parameters, several pathway directions, the scaling technique as well as the optimization stability. The obtained optimization results showed also dimensional limitations which were given by the standard in terms of SCF validity. Such limitations might be able to overcome by considering joint detailing, leading to an even better material utilization for the applied loading.

Appendix A

Appended publications

Paper 1 **Zwick D**, Muskulus M. The simulation error caused by input loading variability in offshore wind turbine structural analysis. *Wind Energy* 2014; DOI: 10.1002/we.1767.

Paper 2 **Zwick D**, Muskulus M. Simplified fatigue load assessment in offshore wind turbine structural analysis. *Wind Energy* 2015; DOI: 10.1002/we.1831.

Paper 3 **Zwick D**, Schafhirt S, Brommundt M, Muskulus M, Narasimhan S, Mechineau J, Haugsøen PB. Comparison of different approaches to load calculation for the OWEC Quattropod jacket support structure. *Journal of Physics: Conference Series* 2014; **555**: 012110:1-10.

Paper 4 **Zwick D**, Muskulus M, Moe G. Iterative optimization approach for the design of full-height lattice towers for offshore wind turbines. *Energy Procedia* 2012; **24**: 297-304.

Paper 5 **Zwick D**, Muskulus M. Two-stage local optimization of lattice type support structures for offshore wind turbines. Submitted to *Ocean Engineering* 2014.

Paper 6 Molde H, **Zwick D**, Muskulus M. Simulation-based optimization of lattice support structures for offshore wind energy converters with the simultaneous perturbation algorithm. *Journal of Physics: Conference Series* 2014; **555**: 012075:1-8.

Paper 7 Pasamontes LB, Torres FG, **Zwick D**, Schafhirt S, Muskulus M. Support structure optimization for offshore wind turbines with a genetic

algorithm. *Proceedings of the 33rd International Conference on Ocean, Offshore and Arctic Engineering* 2014, San Francisco, USA, OMAE; **9B**: V09BT09A033:1-7.

Paper 1

The simulation error caused by input loading variability in offshore wind turbine structural analysis

Zwick D, Muskulus M
Wind Energy 2014; DOI: 10.1002/we.1767

Wind Energy

WIND ENERGY
Wind Energ. (2014)
Published online in Wiley Online Library (wileyonlinelibrary.com). DOI: 10.1002/we.1767

RESEARCH ARTICLE

The simulation error caused by input loading variability in offshore wind turbine structural analysis

Daniel Zwick and Michael Muskulus

Department of Civil and Transport Engineering, Norwegian University of Science and Technology (NTNU), Høgskoleringen 7A, 7491 Trondheim, Norway

ABSTRACT

Stochastic representations of turbulent wind and irregular waves are used in time domain simulations of offshore wind turbines. The variability due to finite sampling of this input loading is an important source of simulation error. For the OC4 reference jacket structure with a 5 MW wind turbine, an error of 12–34% for ultimate loads and 6–12% for fatigue loads can occur with a probability of 1%, for simulations with a total simulation length of 60 min and various load cases. In terms of fatigue life, in the worst case, the lifetime of a joint was thereby overestimated by 29%. The size of this error can be critical, i.e., ultimate or fatigue limits can be exceeded, with probability depending on the choice of number of random seeds and simulation length. The analysis is based on a large simulation study with about 30,000 time domain simulations. Probability density functions of response variables are estimated and analyzed in terms of confidence intervals; i.e., how probable it is to obtain results significantly different from the expected value when using a finite number of simulations. This simulation error can be reduced to the same extent, either using several short simulations with different stochastic representations of the wind field or one long simulation with corresponding total length of the wind field. When using several short-term simulations, it is important that ultimate and fatigue loads are calculated based on the complete, properly combined set of results, in order to prevent a systematic bias in the estimated loads.

KEYWORDS
offshore wind turbines; simulation error; wind and wave variability; fatigue loads

Correspondence
Daniel Zwick, Department of Civil and Transport Engineering, Norwegian University of Science and Technology (NTNU), Høgskoleringen 7A, 7491 Trondheim, Norway.
E-mail: daniel.zwick@ntnu.no

Received 18 December 2013; Revised 20 February 2014; Accepted 6 May 2014

1. INTRODUCTION

1.1. Relevance of input loading variability in numerical simulations of offshore wind turbines

Sources of uncertainty relevant to the design process of a structure are considered by international standards, e.g., by prescribing safety factors that aim to guarantee a design with a conservative probability of failure (e.g., International Electrotechnical Commission (IEC) 61400-3[1]). However, the ambition of designing efficient structures requires to reduce uncertainties as much as possible and by this safety factors. Errors in the results of numerical simulations can be caused, among other things, by the modeling approach, by uncertainty about the environmental conditions, by simplifications and approximations used, by rounding-errors adding up or by a wrong interpretation of results. By *simulation error*, the topic of this paper, we understand here the discrepancy between the results of a limited, finite simulation-based sampling of input loading in terms of the system's response, compared with the response due to an ideal statistical sampling of the input, assessed, e.g., through a hypothetical, infinitely long simulation.

Simulation errors can be typically reduced by estimating them by way of a large number of simulations. The number of simulations used is crucial for the computational effort needed and has to be limited in practice. This discrepancy between,

on the one hand, the requirement of small simulation errors and, on the other hand, a low number of simulations with which to analyze a structure, forms the motivation for this study. The importance of *random variation* and *simulation length* for the simulation error is highlighted, and a recommendation for the designer for the setup of offshore wind turbine simulations is given.

Wind turbines in an offshore environment are exposed to combined wind and wave loading, both of which are natural phenomena occurring in a stochastic, irregular manner.[2] The stochastic fluctuations of the wind are considered to be one of the most serious load problems for wind turbines and contribute considerably to material fatigue.[3] In numerical simulations, wind and wave loading are difficult to reproduce accurately, and this is therefore a significant cause of simulation error.[4] Motivated by this, a large simulation study with about 30,000 simulations was performed. As an exemplary result, for a single run of 10 min simulation length, we found a maximum simulation error of 35% for fatigue loading in the substructure, which results in a reduction in lifetime of the joint in question of up to 59%. Putting this result into relation, Veldkamp[5] showed that wind loading-related parameters (number of random seeds, average wind speed and turbulence intensity) account for only 15% of the total 'uncertainty importance' for fatigue loading on a tubular tower. The main contribution of more than 50% is related to uncertainties regarding material behavior, but these are rather more difficult to understand and address than simulation error.

The generation of wind and wave data as input loading for short-term simulations is based on the assumption that the underlying stochastic processes are stationary and Gaussian.[6–8] Wind and wave time series are obtained with the use of pseudo-random generators, whose sequence is completely determined by their initial values, typically a single *random seed*.[9] The idea of this approach is that the user can reproduce the same realizations of the process when using the same seed number, although this cannot be guaranteed when running different software or on a different computer. A practical compromise that has been commonly made is to assume that 10 min are enough (for wind simulations) in order to sufficiently sample the variability of the underlying stochastic process.[10] In recent standards, however, at least 6×10 min of stochastic realizations, or a continuous 1 h period, is required.[1] This requirement has been variously exceeded; e.g., some authors expect to accurately estimate fatigue damage with a single realization of turbulent wind using a very long simulation length of 6 h,[11] a standard time period for simulations of floating offshore structures.[12] On the other hand, Stewart *et al.*[13] discussed simulation time for a floating offshore wind turbine and concluded that a length of 10 min is sufficient for an OC3 spar buoy model to study the effect of input loading variability. The approach of splitting a 1 h simulation into 4×15 min simulations with different random seeds, and to merge these time series into a 1 h segment, is also present in the literature.[14]

Summing up, there is no consensus in the literature regarding best practices for time domain simulations. Nowadays, computational resources as well as analysis tools that allow for performing comprehensive simulation studies are available. The reader will be guided through a number of exemplary results, based on estimating probability distributions for response variables by the use of a large number of such time domain simulations.

Offshore wind turbines installed in intermediate water depths greater than 20 m can, among other types, be founded on bottom-fixed lattice tower substructures, so-called jackets. Examples are found at the wind farms Beatrice, Thornton Bank, or Ormonde.[15] The study is performed with a special concern on fatigue loading for joints in such a structure. Simulations were realized with a structural model presented in the course of the OC4 code comparison project.[16] The wind turbine itself is modeled as the NREL 5 MW baseline turbine.[17] Environmental data for a deep water site were taken from the Upwind project.[18] Aero-servo-hydro-elastic simulations of a fully integrated model were performed with the flexible multibody simulation tool Fedem Windpower (Fedem Technology AS, Trondheim, Norway, Ver. R7.0.2).[19]

1.2. Objectives

The aim of this work is to raise awareness for the role of variability (of input loading) and simulation length on the simulation error, when analyzing offshore wind turbine substructures. The main questions addressed are as follows:

- What is the relative importance of variability in wind and wave input loading?
- To what extent can simulation error be limited when using several realizations of wind and/or wave processes? Is it preferable to run several short-term or one long-term simulation with corresponding total length?
- How large a simulation error can potentially arise when using a certain number of random seeds or a certain length of the simulations, e.g., when following the IEC 61400-3 recommendation?

2. SIMULATION AND ANALYSIS FRAMEWORK

2.1. Simulation model

As reference structure, the OC4 model, placed in a water depth of 50 m, is used here (Figure 1). The structure is, for simplicity, fixed to the sea bottom in all degrees of freedom in the lowest nodes; i.e., the soil-structure interaction is

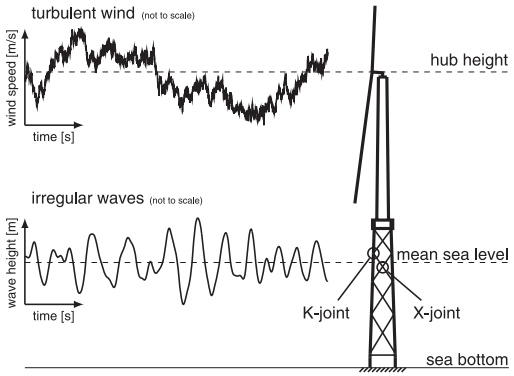

Figure 1. Nature of input loading (both turbulent wind and irregular waves) for the offshore wind turbine structure considered.

Table I. Selected design load cases, from IEC 61400-3.[1]

Design load case	Description	Wind turbulence	Sea state
DLC 1.2	Power production	NTM[a]	NSS[b]
DLC 1.3	Power production	ETM[c]	NSS[d]

[a]Normal turbulence model.
[b]Normal sea state, Pierson–Moskowitz with peak enhancement factor $\gamma = 1.0$.
[c]Extreme turbulence model.
[d]Normal sea state, JONSWAP with peak enhancement factor $\gamma = 3.3$.

Table II. Lumped scatter diagram of the K13 deep water site.[18]

V_m (m s^{-1})	4	6	8	10	12	14	16	18	20	22	24
TI_{normal} (%)	20.4	17.5	16.0	15.2	14.6	14.2	13.9	13.6	13.4	13.3	13.1
TI_{extreme} (%)	53.1	37.1	30.0	25.4	22.3	20.1	18.5	17.2	16.1	15.3	14.6
H_s (m)	1.10	1.18	1.31	1.48	1.70	1.91	2.19	2.47	2.76	3.09	3.42
T_p (s)	5.88	5.76	5.67	5.74	5.88	6.07	6.37	6.71	6.99	7.40	7.80

The lumping of wind and wave data results in a set of load cases where each mean wind speed is linked to a turbulence intensity and one specific sea state. Results for different load case simulations are identified by their respective wind speed.

neglected. The jacket is orientated with one of the side planes perpendicular to the incoming wind and wave loading, and the fully integrated simulation model has been validated to the results of OC4 phase I.[20] The structural model consists of 112 beam elements and 64 nodes and is based on Euler–Bernoulli beam theory. Beams between the nodes are not further discretized to keep the complexity of the structural model simple. The model of the NREL 5-MW baseline turbine is slightly modified, since the use of a gearbox with ratio 1:97 between low-speed and high-speed shaft can cause numerical instabilities. The gearbox has therefore been replaced by a mathematical function that multiplies the rotational velocity by the 97:1 factor, before it is used as input for the control system, with an accordingly adjusted feedback to the generator. A time step of 0.025 s was used for all simulations.

2.2. Design load cases and lumped load case table

Two design load cases (DLCs) with different turbulence models were chosen; see Table I.

Turbulent wind can be characterized by its mean wind speed V_m and the turbulence intensity TI. Irregular waves are described by significant wave height H_s and wave period T_p, as well as by the dimensionless peak enhancement factor γ. A representation for the environmental loading was taken from the Upwind design basis,[18] as shown in Table II. All load cases were realized for mean wind speeds assessed in steps of 2 m s^{-1} in the range between cut-in (3 m s^{-1}) and cut-off

(25 m s^{-1}) wind speeds for the NREL 5 MW baseline turbine. Time series for the input loading of turbulent wind, based on the IEC Kaimal model, and irregular waves, based on the Pierson–Moskowitz or Joint North Sea Wave Project (JONSWAP) sea wave spectrum, were generated in Turbsim[10] and Fedem,[19] respectively. Directions of wind and wave loading were assumed to be aligned. Other parameters for the aerodynamic setup and the sea environment like wind shear, current definition or marine growth are kept constant for all simulations.

2.3. Analysis of time series response data

Post-processing was performed using a custom code in MATLAB (The Mathworks, Inc., Natick, Massachusetts, Ver. R2013a), which extracts statistical information for the axial force time series F_x from the beam element located below the given node, i.e., a leg element below K-joints and one of the brace elements below X-joints. Results are discussed for reference check points close to the mean sea level (K-joint and X-joint in Figure 1). Other check points distributed over the height of the substructure were analyzed as well and are exhibiting similar characteristics.

Ultimate limit state (ULS): The analysis is based on statistical extrapolation of ultimate loads, adapted to the procedure described in Annex F of IEC 61400-1.[7] From the response time series, the largest values between successive upcrossings and successive downcrossings of the mean ± 1.4 times the standard deviation are selected (both maximum and minimum values). The selected extreme values are sorted in bins, normalized to the probability of the bin and fitted by an exponential function of type $y = ae^{bx}$, which was judged to provide a reliable estimation of the behavior of the tail. This relationship is solved for the probability $P_{50} = 3.8 \times 10^{-7}$ for the 50 year recurrence period, resulting in the expected extreme load.

Fatigue limit state (FLS): The damage equivalent load (DEL) analysis is based on a rainflow counting algorithm[21] and linear damage summation by the Palmgren–Miner rule. The reference number of load cycles for a simulation length of 60 min is $N_r = 2 \times 10^8$, and a negative inverse slope of $m = 3$ was used.

2.4. Scope of study

2.4.1. Part a) – the importance of wind versus wave variation.

For each load case, results from short-term simulations with a length of 10 min and for 2500 different combinations of stochastic realizations of wind and wave processes (characterized by their random seeds) were analyzed in terms of their probability densities. These probabilities were evaluated at 100 equally spaced points that cover the range of the data, using a kernel density smoother with default bandwidth.[22] The contribution of isolated wind or wave seed variability is investigated, in order to understand which source of variation has more influence on the structural results.

2.4.2. Part b) – simulation error and relevance of simulation length.

The required number of stochastic realizations and/or simulation length needed to obtain ('match') the arithmetic mean of the result distribution with a certain probability, within a defined uncertainty interval around the 'true' mean, was studied (Figure 2). For the investigation of variability, data from the short-term simulations in part a) with 50 different random wind seeds were used. Data for the discussion of simulation length were obtained by long-term simulations with a simulation length of 100 min, using 100 different random seeds for the wind time series. The means estimated from the complete simulation set were used as assumed 'true' mean values in both cases.

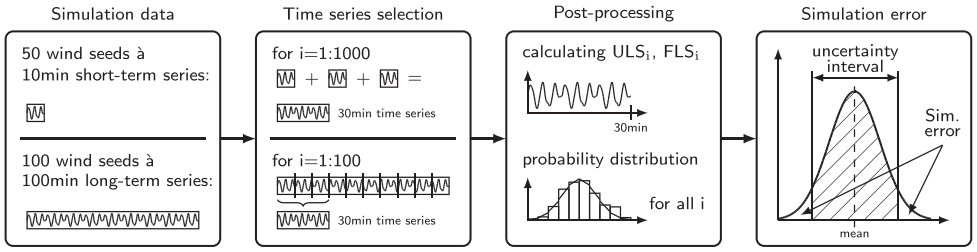

Figure 2. Schematic explanation of the simulation error analysis shown for an example of 3 iterations of short term simulations and a 30 min segment of long term simulations.

Table III. Number of simulation runs performed.

DLC	Simulation length (min)	Load cases	Wind seeds	Wave seeds	Total	Used in part
1.2	10	11	50	50	27,500	a), b), c)
1.2	100	11	100	1	1100	b), c)
1.2	360	11	3	1	33	c)
1.3	100	11	100	1	1100	c)

- The variability was analyzed in 10 iterations, where $1, 2, \ldots, 10$ randomly chosen combinations of random seeds were selected. This selection process was performed 1000 times. In each iteration, stored time series data for the analysis results of the selected random seeds were combined to one single time series.
- The impact of the simulation length on the simulation error was checked by splitting the time series. Results from long-term simulations for all 100 wind seeds were divided into segments of 10 min, where the first segment is equal to the results from the short-term simulation, and successively longer simulations were analyzed by extracting the first n 10 min segments of the original time series for $n = 2, 3, \ldots, 10$.

Each resulting analysis length was processed for the expected extreme and fatigue load, and a distribution curve was estimated by a kernel density smoother. The area under the distribution curve within the uncertainty interval was divided by the area under the complete curve, resulting in the matching probability. Results are indexed by the mean over all wind seed combinations, separately for short-term and long-term simulations.

The maximal simulation error that could obtain with a predefined significance probability of 1% or 5%, respectively, was assessed by finding the confidence interval of the response variables around the true mean that contains $\pm 49.5\%$ or $\pm 47.5\%$ of the simulation results, respectively.

2.4.3. Part c) – additional results.

As a reference check for findings obtained in parts a) and b), three more investigations with the same structural model were performed:

- Changing the response load characteristic by analyzing bending moment time series rather than the axial force.
- Analyzing a different DLC with increased turbulence intensity.
- Running 6 h simulations as very long-term simulations.

2.4.4. Number of simulations.

The large number of simulation runs listed in Table III was realized by parallel computing on two high-end workstations with two Intel® Xeon® processors and 128 GB random-access memory each, running and storing all simulation results completely in memory, and asynchronously transferring results to a network server. The average simulation time for a single simulation with analysis length of 10 min and timestep of 0.025 s was about 29 min on one core, which equals around three times real time. The total computational simulation effort of this study can be summed up to a continuous simulation time of about 35 days based on the previously mentioned computer resource or, theoretically, to about 2.9 years on a single-core machine.

3. RESULTS

3.1. Model startup phase

Initial conditions used for dynamic simulations have an impact on the structural response. This requires to eliminate the first part of time series results from consideration for the load analysis. Depending on the simulation setup, typically, the first 30–60 s is neglected, in order to remove the transient. As shown in Figure 3, this is *not sufficient* for all wind speeds for our simulation model. Especially in the case of a standstill rotor at the beginning of the simulation, low wind speeds require a longer startup phase of up to 200 s. Other simulation models might well achieve steady-state conditions within shorter time, especially if using a static calculation to initialize the structural model, a different control system or other such techniques. However, the length of the transient is expected to be dependent on the wind speed also in such cases.

3.2. Analysis of input loading time series

Variability of V_m and H_s caused by the generation of input loading time series of finite length is shown in Figure 4 (left). The range of the short-term mean is 5–20% for V_m and 5–7% for H_s. Peaks for very high wind speeds in the maximal

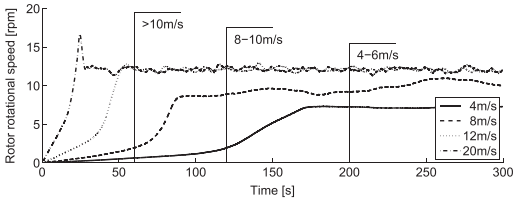

Figure 3. Startup of wind turbine rotor from standstill to steady-state operation for several load cases (the peak at 25 s for 20 m s^{-1} is caused by a time lag of the control system). Vertical lines indicate length of transients that need to be removed from analysis results, indexed by wind speed.

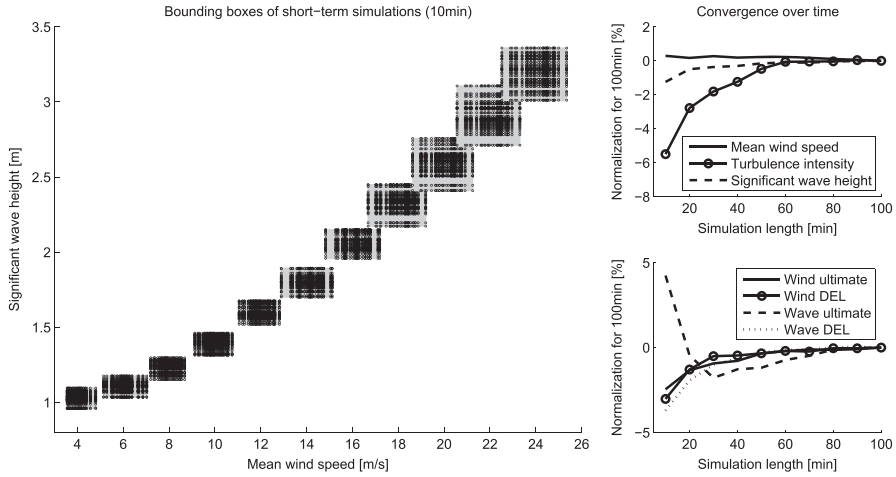

Figure 4. Input loading variations for short-term simulations (left) and convergence of mean values over all load cases and random seeds for long-term simulations (right). Parameters include turbulence intensity and wave period, as listed in Table II.

input loading range are exceeding the operational range of the turbine for power production for short time periods and local regions on the rotor plane. In these cases, the baseline control system of the turbine will not intervene and change the status of power production.

The mean of both V_m and H_s is almost constant with ±0.5–1.0% deviation over all simulation lengths and load cases, while the TI is increasing by about 6% from 10 to 60 min simulation length (Figure 4, right). This reflects the fact that variation is typically underestimated in records that are shorter than an intrinsic time scale. Ultimate and fatigue loading is converging over simulation time, too. The DEL of both wind and wave loading is somewhat underestimated for short-term simulations with a deviation of 3–4% compared with long-term simulations. While ultimate loads of the wind follow the same trend, ultimate loads of the waves are overestimated for short-term simulations by 4%.

3.3. Part a) – the importance of wind versus wave variation

3.3.1. Structural response and distributional analysis.

The structural response is heavily influenced by the variability in input loading. In Figure 5 (left), the mean of the time series has a relative deviation within ±10% of the mean for load cases with low and high wind speeds in the presented K-joint, while a deviation of up to 200% for wind speeds of 8–14 m s^{-1} was found. This high value is caused by the fact that axial forces are getting closer to zero in this range. Global ultimate loads vary significantly for different seed combinations, and the amplitude range of loads is increasing for higher wind speeds. For the DEL (Figure 5, right), a maximum deviation of 35% was found for the upper limit at 4 m s^{-1} for the reference K-joint. For other wind speeds,

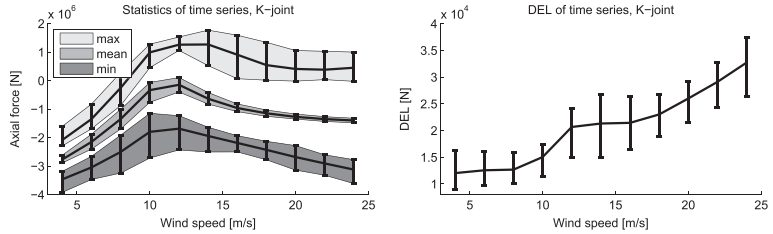

Figure 5. Mean and confidence intervals of time series results for all wind and wave seed combinations.

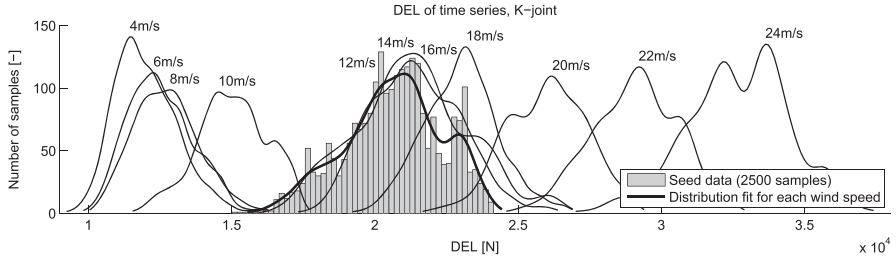

Figure 6. Result distributions. Estimated by a kernel density smoother using all wind and wave seed combinations, for different wind speeds. (For 12 m s^{-1}, the distribution is additionally given in the form of a histogram, as example. The deviation around the mean of the DEL for this load case is −27% to +17%).

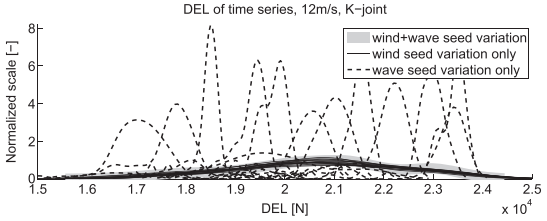

Figure 7. Distribution curves over specific wind and wave seed combinations. Varying only the wind seed, the resulting distribution is shown for 13 different wave seeds (a random choice from the 50 available seeds). Vice versa, varying only the wave seed, the distribution is shown for 13 different wind seeds. The single curve obtained when varying both seeds is added for comparison. Y-axis values are normalized to the maximum of the distribution over all random seed variations, by ensuring the area under the curves to remain the same as for the reference case.

DELs are within ±12–30% of the mean. The influence of the variability is somewhat smaller for the DEL in the X-joint, as deviations are in the range of ±7–15% (not shown). As the relative standard deviation is by a magnitude of 1.9–2.7 larger for the K-joint compared with the results for the X-joint, the variability in the selected DLC has stronger impact on K-joints, and further results are presented for this check point only.

By smoothing result data for all load cases, no clear distribution type could be identified (Figure 6). However, a trend to a normal distribution is visible. The assessment of kurtosis shows that the result distributions are less outlier prone than a normal distribution with a kurtosis of $k = 1.48$–2.07 over all wind speeds. Skewness was estimated at $s = 0.11$–0.54, suggesting a trend of the data to exhibit slightly larger tails on the right (for normal distributions, $k = 3$ and $s = 0$).

3.3.2. Comparison of isolated wind and wave variation.

The distribution for variations over all random seeds at 12 m s^{-1} from Figure 6 is shown in Figure 7 by the gray line (further referred to as reference case). In addition, distribution curves over samples with wind seed variation only (using a single-wave realization) as well as the opposite combination are drawn.

When varying the wind seed number only, by keeping the wave seed number constant, the distribution follows the reference case closely, with approximately the same mean (±1.5%) and slightly changed standard deviation (±10%). On the other hand, varying the wave seed number, by keeping the wind seed number constant, results in distributions spread over the whole bandwidth of the reference case. Different mean values (±15%), smaller standard deviation (−20% to −70%) and up to eight times larger probability density values for their respective expected value are found. It can be stated that simulations with wind seed variation only represent the reference case with very good approximation. Based on this observation, runs for long-term simulations (100 min analysis length) were performed with variation of wind random seeds only. Further results for parts b) and c) are focused on wind seed variation only, too.

3.4. Part b) – simulation error and relevance of simulation length

3.4.1. Increasing the accuracy of simulations.

A single randomly chosen wind seed may apparently end in quite uncertain results. The question is how this accuracy can be increased by analyzing an extended amount of simulation data. Results are shown in Figure 8 in terms of the probability of matching the 'true' mean within a given uncertainty interval. The more data are taken into account, the smaller the standard deviation. At the same time, the probability of finding the results within the uncertainty interval is increasing. The mean of the DEL is slightly increasing by 3.7% when going from 1 to 10 short-term simulations used in its estimation and by 4.3% for long-term simulations when going from 10 to 100 min. The latter is due to the non-locality of the rainflow counting algorithm, i.e., the occurrence of load cycles that span over several 10 min segments.

3.4.2. Simulation error.

The absolute number of the uncertainty interval is further understood as the maximal error that can be potentially made in ultimate and fatigue loads. Results for a simulation setup recommended by IEC 61400-3 are shown for all load cases in Figure 9 (left). This is a probabilistic result, when loads occur or are exceeded with 1% or 5% probability, respectively; i.e.,

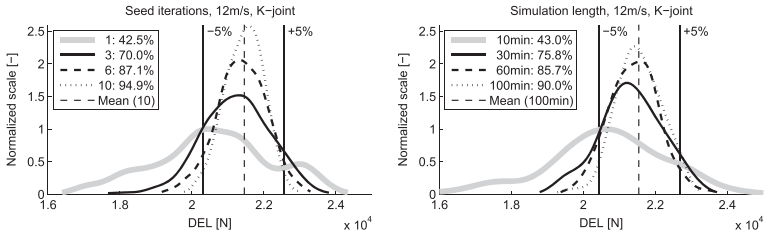

Figure 8. Improvement by using several random seeds or increasing simulation length. Results are for a wind speed of 12 m s^{-1} and an uncertainty interval of ±5%. To the left, 1, 3, 6 and 10 distinct random seeds were used with a simulation length of 10 min each. To the right, 10, 30, 60 and 100 min of continuous simulation length were used, respectively, with a single random seed.

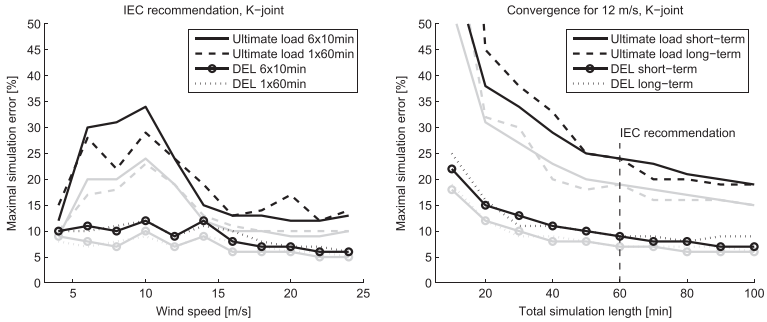

Figure 9. Relation between wind speed, total simulation length and simulation error. Results are maximum deviations from the 'true' mean that were obtained or exceeded in 5% (gray curves) or 1% (black curves) of all analysis runs.

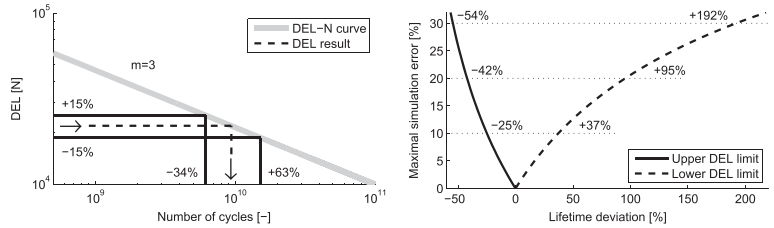

Figure 10. Fatigue assessment with simulation error in DEL results.

the minimum or maximum (or fifth lowest or highest value) is chosen from 100 simulations. Short-term simulations (6×10 min) are compared with one long-term simulation (60 min). As the IEC recommendation is only one particular choice for the simulation setup, the convergence of the simulation error for further increasing total simulation length is analyzed, too (Figure 9, right).

The convergence of ultimate loads for increasing simulation length can clearly be seen. However, even when basing the analysis on a simulation length of 100 min, a simulation error of 20% or more can still occur with a probability of 1%. DEL results can be estimated with a much smaller simulation error already for short simulation lengths but show less improvement over time. Exponential curve fitting leads to the prediction that these worst-case simulation errors for both ultimate and fatigue loading can be reduced to less than 5% after a simulation length of 6 h.

It can be concluded that combining results for several short-term simulations result in an assessment closely comparable with what is obtained from a single long-term simulation, especially for fatigue calculations. The relative standard deviation is similarly reduced (not shown).

3.5. Part c) – additional results

Time series data for local bending moments M_y and M_z at the reference K-joint were analyzed, too, for short-term simulations. Local moments M_y at this joint are caused by the side-to-side movement of the structure, while local moments M_z are caused by fore-aft movement. Results for M_y follow the characteristics found in the analysis of F_x. However, responses in M_z are slightly different with the main interesting feature that the wind versus wave seed variation shows small differences only.

The convergence over time for both DLC 1.2 and DLC 1.3 follows the same trend, independent of the load case. Because of the increased turbulence intensity of the wind, absolute DEL values are larger for DLC 1.3 compared with DLC 1.2. The standard deviation is similarly reduced by increasing simulation length for both DLCs.

A few 6 h simulations were checked for their convergence over time. The worst-case simulation error at the 1% probability level was reduced to less than 5% after 5 h for ultimate loads and after 3.5 h for fatigue loads, thereby confirming the prediction made in Section 3.4.2.

3.6. Significance of the simulation error for fatigue lifetime calculations

Consequences for the fatigue lifetime of the structure can be illustrated in a diagram that shows DEL versus number of cycles N. The DEL–N curve defines the maximum number of cycles allowable for a certain DEL. Figure 10 (left) shows a simulation error of 15% of the DEL in double logarithmic scale. The resulting number of cycles varies from −34% to +63% of the value obtained by using the original value of the DEL. The large amplification of the uncertainty in this calculation is caused by the negative inverse slope of $m = 3$, i.e., by the non-linear relation between DEL and N. The effect of different values of simulation errors is given in Figure 10 (right).

As presented in Figure 9 (left), the IEC recommendation results in a simulation error of 6–12% for most of the load cases at the 1% probability level. In the worst case, this results in a reduction of the fatigue lifetime by 16–29%, which is significant.

4. DISCUSSION

This investigation is based on a large database of simulation results. In order to manage the computational effort needed, simplifications were made to reduce the required number of simulations. A selection of load cases, spread by 2 m s^{-1}, was

used. This lumping of load cases is based on fatigue estimates performed by Kühn for a different turbine.[23] As no exact procedure of lumping load cases is known, it is an additional source of error. However, the added complexity of this effect has been left out for further studies. Results show that simulation errors for wind speeds in between the analyzed speeds can be interpolated linearly with reasonable accuracy (not shown). Additional variability of the input loading, due to wind shear, currents, marine growth, etc., has been neglected; it is expected that this will further increase the simulation error. The misalignment of wind and wave direction, or a variation of the orientation of the jacket footprint in the wind direction, was not analyzed. It is assumed that these variations have negligible influence on the variance of the results, which is dominated by the variation in the wind.[24] The study is based on the deterministic approach used for certification of turbines, whereas the probabilistic design of wind turbines (e.g., Sørensen and Toft[25]), although a more natural framework, is not considered.

An interesting observation is that the variation resulting from using different stochastic realizations of wind and wave processes is not normally distributed but results in a somehow distorted normal distribution. This is probably a consequence of nonlinearities, e.g., in the control system or from unsteady aerodynamic effects.

This paper documents the dominance of wind variation, in contrast to variation from wave loads. This finding is related to the selected DLCs and the environmental loading. The impact of the variation from wave loads is expected to be increasing for more severe sea states. The comparability of several short-term simulations and one long-term simulation can be confirmed, based on comparison of simulation error and the relative standard deviation. An important observation was made, however. When comparing, e.g., 6×10 min and 1×60 min simulation data, the short-term data have to be combined into a single time series before analyses for ultimate and fatigue loads are performed, or results will be unreliable. For example, when adding the FLS results of six separately analyzed simulations and comparing with the results for the combined time series, a systematic bias of about 4% is identified (Figure 8, left), which is due to large load amplitudes spread over several simulation segments that are not taken into account when analyzing the smaller time series separately. Similarly, the load variability is underestimated for a short-term simulation, indicating that the results based on a single 10 min load case will be unreliable. Time series segments of short-term simulations can be combined without special treatment of the first and last time steps, as the error made by this is negligible. Overall, this is consistent with the result that stationary Gaussian processes with continuous spectrum are ergodic.

With the additional results in part c), it is shown that the simulation error for both axial loads and bending moments, as well as for different DLCs with either normal or extreme turbulent wind, behaves in a similar manner. Hence, the significant input loading variability found has to be taken into account for power production, independent of the analyzed DLC. The analyses of very long simulations show that the convergence of the fatigue estimates is much slower when increasing the simulation length beyond 100 min. These results are dominated by the turbulence in the wind (with a higher frequency) rather than the irregular sea state (with a lower frequency), as wind loading contributes to a larger extent to the results and develops the full spectrum over a shorter simulation period.

An interesting point for discussion is how the simulation error would behave for other concepts and structural models of bottom-fixed substructures, as, e.g., monopiles, tripods or tripiles. These models have fewer members, but with larger diameters, compared with a jacket structure. Especially, the increase in diameter of the column(s) at the height of the mean sea level will lead to larger wave loads, which could increase the relevance of wave seed variations. On the other side, the variability of the turbulent wind will be present, independent of the used type of substructure.

5. CONCLUSION

In the current framework, the design of offshore wind turbine substructures is ideally performed by a very large number of short-term simulations, or a very long simulation in each DLC and wind speed set. Thereby, the simulation error due to the stochastic input loading of turbulent wind and irregular waves can be reduced to a desired target accuracy. However, computational efforts have to be limited in practice. We conclude with the following recommendations for numerical simulations of offshore wind turbines:

- The length of start-up transients can be significantly longer than one might expect, especially for lower wind speeds. This need to be checked when performing simulation-based analysis.
- The use of wind seed variation only, keeping the wave seed number constant, is sufficient. Simulation runs contain the same information as obtained by runs with variations of both wind and wave seeds numbers.
- By following the recommendation in IEC 61400-3 of 6×10 min or 1×60 min simulations, one has to account for the possibility of a simulation error of 12–34% or more for ultimate loads and 6–12% or more for fatigue loads over all wind speeds, in the situation of power production, that will occur with a probability of 1%. Simulation errors can be reduced by either increasing the number of short-term simulations or increasing the simulation length and only depend on total simulation time. The latter case has the advantage that transients need to be only removed once, but on the other hand, longer wind fields need to be used, which can be a limiting factor in practice.

- Attention has to be paid to the calculation method for ultimate and fatigue loads when using several short-term simulations. It is important that time series results are properly combined before the analysis, to avoid significant bias in fatigue estimates.
- When following the recommendations of IEC 61400-3, the consequences of variability and limited simulation length for the estimate of fatigue lifetime of the structure were shown to lead to a 1% probability of obtaining a 16–29% or larger reduction in fatigue lifetime, compared with what the numerical results indicate. The magnitude of this effect might be larger than most realize.

Further work should focus on the reduction of other uncertainties and a more precise definition (or recalibration) of safety factors. It is also of interest to perform simulations with different substructure types and analysis software, for a verification of the simulation error in these cases.

ACKNOWLEDGEMENTS

Support by NOWITECH, the Norwegian Research Centre for Offshore Wind Technology, is gratefully acknowledged (Research Council of Norway, contract no. 193823). We thank in particular Fedem Technology AS for providing software licenses and quick and helpful feedback.

REFERENCES

1. International Electrotechnical Commission. *Wind Turbines - Part 3: Design Requirements for Offshore Wind Turbines*, International Standard, IEC 61400-3. IEC Central Office: Geneve, Switzerland, 2009.
2. Vorpahl F, Schwarze H, Fischer T, Seidel M, Jonkman J. Offshore wind turbine environment, loads, simulation, and design. *Energy and Environment* 2013; **2**: 548–570.
3. Hau E. *Wind Turbines Fundamentals, Technologies, Application, Economics*. Springer-Verlag: Heidelberg, Germany, 2013.
4. Saranyasoontorn K, Manuel L. On the propagation of uncertainty in inflow turbulence to wind turbine loads. *Journal of Wind Engineering and Industrial Aerodynamics* 2008; **96**: 508–523.
5. Veldkamp D. A probabilistic evaluation of wind turbine fatigue design rules. *Wind Energy* 2008; **11**: 655–672.
6. Naess A, Moan T. *Stochastic Dynamics of Marine Structures*. Cambridge University Press: New York, USA, 2013.
7. International Electrotechnical Commission. *Wind Turbines - Part 1: Design Requirements*, International Standard, IEC 61400-1. IEC Central Office: Geneve, Switzerland, 2007.
8. Hasselmann K. *Measurements of Wind-wave Growth and Swell Decay During the Joint North Sea Wave Project (JONSWAP)*. Deutsches Hydrographisches Institut Hamburg: Hamburg, Germany, 1973.
9. Veers PS, Three-dimensional wind simulation. *Sandia Report SAND88-0152·UC-261*, Sandia National Laboratories, 1988.
10. Jonkman BJ, Turbsim user's guide. *NREL/TP-500-46198*, National Renewable Energy Laboratory, 2009.
11. Norton EJ. Recommendations for design of offshore wind turbines (recoff), D3 Deliverable - Collated Sensitivity Studies, document no. 2762/BR/16, Garrad Hassan and Partners Ltd, 2003.
12. Det Norske Veritas AS. Design of Floating Wind Turbine Structures. Offshore Standard, DNV-OS-J103, 2013.
13. Stewart G, Lackner M, Haid L, Matha D, Jonkman J, Robertson A, Assessing fatigue and ultimate load uncertainty in floating offshore wind turbines due to varying simulation length. *Report NREL/CP-5000-58518*, National Renewable Energy Laboratory, 2013.
14. Karimirad M, Moan T. Wave- and Wind-induced Dynamic Response of a Spar-type Offshore Wind Turbine. *Journal of Waterway, Port, Costal, and Ocean Engineering* 2012; **138**: 9–20.
15. Higgins P, Foley AM. Review of offshore wind power development in the United Kingdom. *Proceedings of 12th International Conference on Environment and Electrical Engineering (EEEIC)*, Wroclaw, Poland, 2013; 589–593.
16. Vorpahl F, Popko W, Kaufer D. *Description of a Basic Model of the 'Upwind Reference Jacket' for Code Comparison in the OC4 Project under IEA Wind Annex XXX*, IEA Wind Annex XXX. Fraunhofer Institute for Wind Energy and Energy System Technology (IWES): Bremerhaven, Germany, 2011.
17. Jonkman J, Butterfield S, Musial W, Scott G, Definition of a 5-MW reference wind turbine for offshore system development. *NREL/TP-500-38060*, National Renewable Energy Laboratory, 2009.

18. Fischer T, de Vries W, Schmidt B. *Upwind Design Basis*. WP4: Offshore Foundations and Support Structures, Endowed Chair of Wind Energy (SWE) at the Institute of Aircraft Design Universität Stuttgart: Stuttgart, Germany, 2011.
19. Fedem Technology AS. *Fedem User's Guide*, Release 7.0.2. Fedem Technology AS: Trondheim, Norway, 2013.
20. Popko W, Vorpahl F, Zuga A, Kohlmeier M, Jonkman J, Robertson A, Larsen TJ, Yde A, Sætertrø K, Okstad KM, Nichols J, Nygaard TA, Gao Z, Manolas D, Kim K, Yu Q, Shi W, Park H, Vásquez-Rojas A, Dubois J, Kaufer D, Thomassen P, de Ruiter MJ, Peeringa JM, Zhiwen H, von Waaden H. Offshore code comparison collaboration continuation (OC4), phase I - results of coupled simulations of an offshore wind turbine with jacket support structure. *Proceedings of the Twenty-second (2012) International Offshore and Polar Engineering Conference*, Vol. 1, Rhodes, Greece, 2012; 337–346.
21. Amzallag C, Gerey JP, Robert JL, Bahuaud J. Standardization of the rainflow counting method for fatigue analysis. *International Journal of Fatigue* 1994; **16**: 287–293.
22. Silverman BW. *Density Estimation for Statistics and Data Analysis*. Taylor & Francis: London, United Kingdom, 1986.
23. Kühn MJ. Dynamics and design optimisation of offshore wind energy conversion systems, *PhD Thesis*, DUWIND Delft University Wind Energy Research Institute, 2001.
24. Dong W, Moan T, Gao Z. Long-term fatigue analysis of multi-planar tubular joints for jacket-type offshore wind turbine in time domain. *Engineering Structures* 2011; **33**: 2002–2014.
25. Sørensen JD, Toft HS. Probabilistic design of wind turbines. *Energies* 2010; **3**: 241–257.

DOI: 10.1002/we

Paper 2

Simplified fatigue load assessment in offshore wind turbine structural analysis

Zwick D, Muskulus M
Wind Energy 2015; DOI: 10.1002/we.1831

Wind Energy

WIND ENERGY
Wind Energ. (2015)
Published online in Wiley Online Library (wileyonlinelibrary.com). DOI: 10.1002/we.1831

RESEARCH ARTICLE

Simplified fatigue load assessment in offshore wind turbine structural analysis

Daniel Zwick and Michael Muskulus

Department of Civil and Transport Engineering, Norwegian University of Science and Technology (NTNU), Høgskoleringen 7A, Trondheim 7491, Norway

ABSTRACT

The estimation of fatigue lifetime for an offshore wind turbine support structure requires a large number of time-domain simulations. It is an important question whether it is possible to reduce the number of load cases while retaining a high level of accuracy of the results. We present a novel method for simplified fatigue load assessments based on statistical regression models that estimate fatigue damage during power production. The main idea is to predict the total fatigue damage only and not also the individual damage values for each load case . We demonstrate the method for a jacket-type support structure. Reducing the number of simulated load cases from 21 to 3, the total fatigue damage estimate exhibited a maximum error of about 6% compared with the complete assessment. As a consequence, a significant amount of simulation time can be saved, in the order of a factor of seven. This quick fatigue assessment is especially interesting in the application of structural optimization, with a large number of iterations. Copyright © 2015 John Wiley & Sons, Ltd.

KEYWORDS
offshore wind turbines; fatigue estimation; regression models; load simulation

Correspondence
Daniel Zwick, Department of Civil and Transport Engineering, Norwegian University of Science and Technology (NTNU), Høgskoleringen 7A, Trondheim 7491, Norway.
E-mail: daniel.zwick@ntnu.no

Received 11 April 2014; Revised 19 October 2014; Accepted 5 January 2015

1. INTRODUCTION

Motivated by the general goal of cost saving in the offshore wind industry,[1] we address an important challenge in the design phase of support structures. The complete fatigue load assessment of an offshore wind turbine is often based on time-domain simulations of an integrated wind turbine model, which results in a comprehensive, time-consuming task.[2] An important question is therefore if and how it is possible to reduce the number of load cases needed while retaining a high level of accuracy of the results for fatigue load.[3] Another efficient technique for fatigue load estimation is the frequency-domain approach.[4–6] Such spectral analyses could be used for a simplified fatigue load assessment too. However, their drawbacks are the challenge to accurately represent simultaneously applied stochastic input loading from wind and waves, as described by Naess and Moan[7] for other types of structures, as well as a more conservative fatigue load estimation.[6]

When using time-domain simulations, the variability of input loading causes a simulation error when results are based on finite time series, and an accurate analysis therefore requires not only different load cases but also relatively long simulations.[8] Our aim is to efficiently and accurately estimate fatigue damage during power production (Design load case (DLC) 1.2, International Electrotechnical Commission (IEC) 61400-3[9]). We present a novel method for a simplified fatigue load assessment, by which the fatigue lifetime of a jacket-type support structure can be calculated seven times faster than usual, based on a certain simulation setup. This approximate analysis estimates the total fatigue damage with a maximal error of less than 6.4%, compared with the more comprehensive analysis.

The idea of approximate and fast fatigue damage estimation in the design phase of structures is not new, and simplified methods for assessing wind-induced fatigue damage have already been used for buildings[10] as well as for offshore structures[11] some decades ago. More recent work on wind turbines has focused on the prediction of actual loading curves, e.g., in the study of Manuel and Veers,[12] limited to a wind speed range between 15 and 19 m/s. Fitzwater[13] has studied

fatigue and extreme loading for both operational and parked conditions by fitting quadratic Weibull models. Dong *et al.*[14] used both two-parameter Weibull and generalized Gamma functions for modeling long-term fatigue damage. Two main approaches can be seen in these studies. Firstly, results for each individual load case are either simulated or estimated by regression methods, based on simulations of a selection of load cases. Secondly, a more general way uses probability distributions with only a few parameters to estimate the fatigue load, which allows for quick but not too accurate estimates. The accuracy depends on the data used for estimating the parameters; the aforementioned studies relied on many hundred load cases in the time-domain to achieve acceptable accuracy. It is not clear how this methodology can be used to efficiently estimate fatigue damage when the design of the structures is changed.

As a new approach, we present a more efficient method for simplified fatigue load assessment. We focus on the estimation of the total fatigue damage of the structure. The main idea is that a few selected load cases in combination with a regression model are sufficient for the estimation of the total fatigue damage. Thereby, fatigue damage results for all load cases are not required nor predicted. This approach offers the possibility of using more powerful statistical methods, since not the complete damage curve (fatigue damage versus wind speed) has to be predicted well everywhere, but the value of the total damage only. Such statistical methods either use a small set of coefficients that are calibrated in a training phase or some assumptions about the shape of the damage curve. The assessment of the same or a similar structure is then based on a small number of specifically selected load cases for power production in the range of cut-in to cut-out wind speed. We evaluate this method in terms of the number of load cases that should be simulated, as well as with regard to the expected maximum regression error. The latter is the expected deviation of the total damage predicted by regression from the summation of each individual damage value over all load cases during a complete damage assessment. The robustness of the statistical methods is evaluated on result data obtained by simulations of different structural configurations of the support structure model to ensure their ability to cope with changes in the structural design. More robust versions of statistical methods, which can mitigate the effect of outliers in the data, also exist,[15] but are more complex and difficult to apply, compared with the presented methods. Two statistical methods are applied and discussed in this study:

- Piecewise linear regression (PLR): a traditional regression method that calculates the total damage as the sum of individual damage values for each load case, of which a few are known and the others are linearly interpolated.[16]
- Multivariate linear statistical model (LSM): a popular and flexible regression method in statistics that calculates the total damage as the sum of a few individual known damage values multiplied by coefficients.[17]

By using such methods, the computational cost for the lifetime validation of a structural design can be reduced significantly. This approach can, e.g., be beneficially applied in simulation-based optimization routines, which so far were limited in their load case assessment.[18–23]

For the efficient lifetime analysis of integrated offshore wind turbine models, based on time-domain simulations, simplifications in the load case assessment are needed. This fact constitutes the motivation of this work, formulated in the following objectives:

- Can the total fatigue damage in all joints of the support structure during power production be estimated with reasonable accuracy from a small number of simulated load cases?
- Are regression methods feasible for the estimation of the total fatigue damage not only for a reference model but also for systematically or randomly modified structural models, with overall reasonable accuracy?

2. STRUCTURAL MODELS AND SIMULATION SETUP

This study is based on the offshore wind turbine structure of the Offshore Code Comparison Collaboration Continuation (OC4) project,[24] situated in a water depth of 50 m. The simulation model was built and analyzed in FEDEM Windpower (Ver. R7.0.2 to R7.0.4, Fedem Technology AS, Trondheim, Norway[25]) and was verified within OC4 phase I.[26] The jacket structure is divided into different levels, connected to each other by leg and brace elements (Figure 1, left). Secondary steel structures such as boat landings or ladders were not included in the model. Further details of the simulation model have been described in earlier work.[8] To be able to achieve a proper calibration of the statistical models, responses from all tubular joints in the support structure were analyzed. Sensors for the analysis of fatigue damage are numbered into two sequences, first the Y-joints/K-joints and then the adjacent X-joints. All joints in each level, starting from the lowest level, are numbered in the mathematically positive direction around the tower axis (z-direction). The detailed numbering is shown in Figure 1 (right).

2.1. Modified jacket structures

In order to evaluate the performance and robustness of the statistical methods on an extended data set, in total seven different structural models were analyzed. These models were established in two series: systematically modified models with the

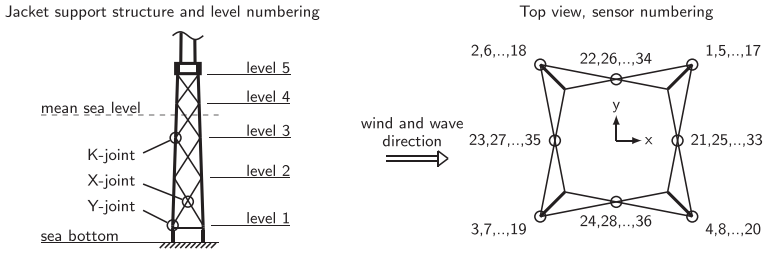

Figure 1. Simulation model for jacket support structure (model of tubular tower and rotor nacelle assembly not shown) and numbering of sensors for fatigue analysis (Y-/K-joints: $1, 2, \ldots, 20$; X-joints: $21, 22, \ldots, 36$). Sensor numbers along one leg or side plane from bottom to top are obtained by an offset of 4 between adjacent levels.

name Mx (in total five models, including the original OC4 definition as reference model, named M100) and randomly modified models with the name Rx (two models). Modifications were implemented by varying the outer diameters of the main members (legs and braces) of the original OC4 jacket definition. This results in a change of cross-sectional area while keeping the thickness of the members constant, for simplicity.

The outer diameters of the systematically modified models, in addition to the reference model, are listed in Table I. The nomenclature Mx refers to a modification of the parameters to $x\%$ of the reference model. These models are used for sensitivity tests and the calibration of the statistical models. The structural parameters of the random models Rx are given in Table II. In contrast to the systematically modified models, the randomly modified models have separate member definitions for each bay between levels 1 and 5, which might be the case for realistic designs or in optimization studies. The outer diameters for the Rx models were chosen with uniform probability within $\pm 20\%$ of the OC4 reference model.

2.2. Wind and wave loading

The representation of wind and wave loading was extracted from the UpWind design basis.[27] Environmental loads were applied unidirectional to the structure. As load cases in the lumped load cases table of the UpWind project are given for wind speed bins of 2 m/s only, linear interpolation was performed to determine representative load cases for all integer wind speeds between cut-in (3 m/s) and cut-out (25 m/s) wind speed for the National Renewable Energy Laboratory 5 MW baseline turbine.[28] This refinement was performed to increase the accuracy of the original data before testing the regression methods. Regarding the number of occurrences per year, a renormalization was performed such that the total number of hours for the total load case set was kept constant. For the here-presented simulation and regression results, there is a unique load case for each wind speed, and each load case is therefore indexed by its wind speed.

Table I. Systematic modification of OC4 model, in terms of outer diameters (m). In addition, the first global fore-aft eigenfrequency of the structure is given (Hz).

	Systematically modified models				
Component	M80	M90	M100	M110	M120
Legs	0.96	1.08	1.20	1.32	1.44
Braces	0.64	0.72	0.80	0.88	0.96
Eigenfrequency	0.296	0.305	0.312	0.319	0.324

Table II. Random modifications of OC4 model, in terms of outer diameters (m). In addition, the fist global fore-aft eigenfrequency of the structure is given (Hz).

Random models	Component	Level 1–2	Level 2–3	Level 3–4	Level 4–5	Eigenfrequency
R1	Legs	1.40	1.03	1.27	1.10	0.312
	Braces	0.82	0.95	0.70	0.90	
R2	Legs	1.16	1.09	1.43	1.12	0.311
	Braces	0.69	0.89	0.80	0.65	

Table III. Simulation effort for reference model and modified models, both systematic and random modifications.

	Load cases	Wind seeds	Number of models	Total
Reference model	21	100	1	2100
Modified models	21	10	6	1260

2.3. Performed simulations

The basis of this study consists of in total 3360 simulations that were performed on two high-end workstations with two Intel® Xeon® processors with 128 GB random-access memory each (Intel Corporation, Santa Clara, CA, USA). Simulation details are listed in Table III. Following the recommendation of the IEC 610400-3 standard, simulations with a continuous analysis length of 60 min (plus additional transient) were carried out for each wind seed. By applying a time step of $t = 0.025$ s, the computational simulation time for a single analysis was about 165 min. Summed up for all simulations, this results in a continuous computation time of 13 days on the described hardware, or theoretically of 385 days on a standard computer, using one processor core only.

2.4. Fatigue damage calculation

For each member connected to a Y-joint, K-joint or X-joint (Figure 1, left), FEDEM Windpower outputs time series data for the axial force as well as in-plane and out-of-plane bending moments. From the raw time series data, a transient of 60–200 s was cut off depending on the wind speed.[8] This results in a total analysis length of 60 min. Force and moment time series were converted to sectional stresses, using beam cross-section data for the specific members. Both the fatigue damage calculation and later regression analyses were performed using custom code in MATLAB (Ver. R2013b, The Mathworks, Inc., Natick, MA, USA), as described in the following paragraph and in Section 3.3, respectively.

Based on the topology and member dimensions of the structure, structural stress concentration factors (SCFs) were calculated for the tubular joints, using an established formula framework from DNV-RP-C203.[29] SCFs are defined as the ratio of hot spot stress (HSS) to local nominal stress. For K-joints, SCFs were obtained at all four intersections (Y-joints two intersections) of leg and brace members (upgoing and downgoing members, as well as in two side planes). For X-joints, all four connected braces have the same dimensions in the model. Hence, for the calculation of SCFs at X-joints, a pair of braces was treated as a continuous leg in one step, before analyzing the opposite configuration in the next step. Member stresses were combined to eight HSSs at each side of the weld of each intersection of brace and leg members in tubular joints, using the SCFs in the calculation. This results in the following total amount of HSS time series: 32 at Y-joints, 64 at K-joints and 64 at X-joints. In addition, a superposition of normal and bending stresses was calculated in butt joints of continuous leg members supporting Y-joints and K-joints.

For all calculated HSS time series, a fatigue assessment based on a rainflow-counting algorithm[30] and linear damage summation by the Palmgren–Miner rule[31,32] was performed. For the damage evaluation, S-N curve data for tubular joints in air and in seawater with cathodic protection were used.[29] The number of extracted load cycles was scaled accordingly to the number of occurrences per year of each load case. The highest damage of all HSSs at each sensor was extracted and further processed in the load case evaluation, representing the fatigue damage of the specific sensor. Values obtained for the damage were scaled to a structural lifetime of 20 years, e.g., a damage value smaller than 1 signifies a longer lifetime, while a damage value larger than 1 indicates a shorter lifetime, i.e., the fatigue resistance is exceeded earlier than 20 years.

3. STATISTICAL METHODS AND LOAD CASE SELECTION

As introduced in Section 1, two statistical methods are applied in this study, which are explained in detail later in the text: the PLR and a multivariate LSM.

3.1. Piecewise linear regression

PLR is a method to predict the dependent variable (fatigue damage) by examining several intervals of the independent variable (wind speed) and fitting linear functions to the data in each of these intervals.[16] The resulting piecewise function is continuous, but not continuously differentiable. As a basic limitation of PLR, the load case spectrum must be described by at least the first and last load case, to be able to linearly interpolate intermediate load case results. Consequently, two

load cases are fixed in the load case selection, and reasonable results can first be obtained for three or more load cases. For the application of the PLR in a load case assessment, the only requirements are the number and definition of load cases to be used. Another, unknown load cases will be interpolated, and the total damage D_{tot} is calculated as the sum of damages from in total $m = 21$ individual load cases (Equation (1)), containing both simulated and linearly estimated damage values.

$$D_{\text{tot}} = \sum_{j=1}^{m} D_j \tag{1}$$

3.2. Multivariate linear statistical model

In contrast to linear regression, where a response variable is regressed from the two closest single observations only, the LSM takes several observations (values of fatigue damage for different wind speeds) into account.[17] These observations are multiplied by regression coefficients, and all these individual contributions are linearly added. Even if the method has a linear structure, each term can appear also in higher order or as an interaction term that multiplies two or more observations. Examples are given for a linear (Equation (2)) and quadratic (Equation (3)) use of observations, the latter including linear, interaction and quadratic terms:

$$D_{\text{tot}} = C_1 + C_2 \cdot D_4 + C_3 \cdot D_{10} + \epsilon \tag{2}$$

$$D_{\text{tot}} = C_1 + C_2 \cdot D_4 + C_3 \cdot D_{10} + C_4 \cdot D_4 D_{10} + C_5 \cdot D_4^2 + C_6 \cdot D_{10}^2 + \epsilon \tag{3}$$

D_{tot} is the estimated total damage over all load cases; C_i are the regression coefficients; D_j are individual damage values obtained by the analysis of simulation data, as an example indexed by a wind speed of 4 and 10 m/s; ϵ describes a random component, i.e., the regression error, which is assumed to be Gaussian with an unknown, constant variance. The LSM requires the calibration of the regression coefficients before it can be used in a load case assessment.

3.3. Application of statistical methods

The application of statistical methods was performed in three phases: training, evaluation and validation. In the first phase, parameters were calibrated with training data, which here means observations obtained by simulations. This first phase is followed by an evaluation phase to determine the load case combination with the best performance, e.g., the smallest regression error. The validation as the last phase is using the identified best combination in order to calculate the expected maximum regression error. In both training and evaluation phases, all possible load case combinations were analyzed for a total of $n = 3, 4, 5, 6$ load cases (Table IV). The number of simulated load cases was chosen based on the minimum requirement of reasonable results for the PLR (Section 3.1) and on the ambition to keep the number of required simulations small, e.g., the accuracy achieved by more than six simulated load cases was not of interest in the analysis. Figure 2 gives an overview over the performed analysis.

The main intention of the training phase is the calibration of the coefficients of the LSM. Each load case combination and sensor number results in a specific set of coefficients, which was further used in the evaluation phase. The PLR is not dependent on coefficients, e.g., a calibration in the training phase was not required. During the evaluation phase, the load case combination resulting in the smallest deviation of the predicted total damage by regression methods to the summation of each individual damage over all load cases was determined. This so-called best load case combination was found by minimizing the maximum absolute total damage deviation over all sensors. The evaluation phase can either be based on the same data set as in the training phase or can use an extended data set that includes new data. The statistical model thereby defined was further validated with known and new data sets in the validation phase (using all seven structural models). An overview of all statistical models and analysis phases is given in Table V.

Table IV. Number of possible load case combinations, calculated by the binomial coefficient of the number of variable load case selections and the number of used load cases.

	Load case selection		Number of used load cases			
Regression method	Fixed	Variable	Three	Four	Five	Six
PLR	2	19	969	3876	11628	27132
LSM	—	21	1330	5985	20349	54264

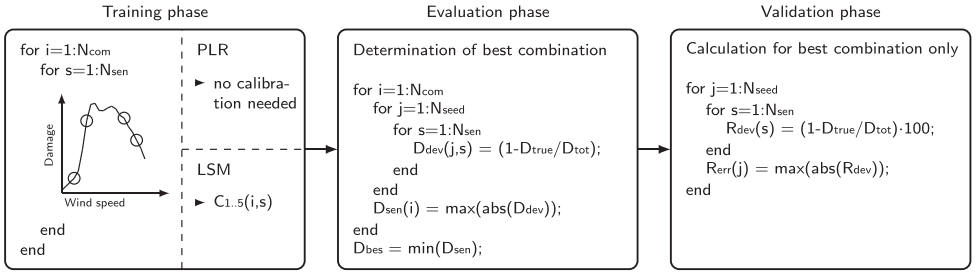

Figure 2. Schematic explanation of the application of statistical methods for an example of four simulated load cases; programming examples are following MATLAB notation. The following parameters are used: n, number of simulated load cases; N_{com}, number of possible load case combinations (Table IV); N_{sen}, total number of sensors; C, regression coefficients for the LSM; N_{seed}, number of wind seeds; D_{dev}, damage deviation; D_{true}, total damage calculated based on the original data of all simulated load cases; D_{tot}, estimated total damage over all load cases; D_{sen}, maximum absolute deviation over all sensors; D_{bes}, minimum deviation over all combinations; R_{dev}, regression deviation in per cent; and R_{err}, maximum regression error over all sensors (%).

Table V. Simulation data from reference model (M100), systematically modified models (M80, M90, M110 and M120) and randomly modified models (R1 and R2) used for the different regression methods in the phases of training, evaluation and validation.

		LSM			
Phase	PLR	Basic	Version 1	Version 2	Version 3
Training	M100	M100	M100	M90 M100 M110	M100 M110 R1
Evaluation	M100	M100	M90 M110	M80 M120	M80 M120
Validation	All	All	All	All	All

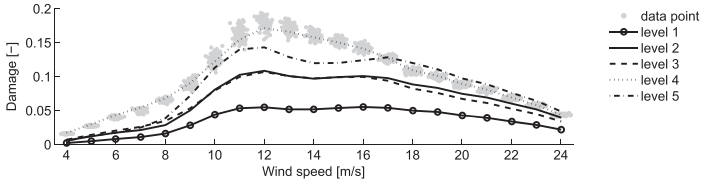

Figure 3. Simulation results for the OC4 original model definition (M100). The mean of all Y-joints/K-joints in each level is indicated as level curves; scatter points are given for K-joint number 13 as a representative sensor in level 4. Each wind speed has been analyzed with 60 min load cases, for 100 different random representations of the wind field.

When comparing validation results of the PLR and LSM, one has to be aware that the calculation of all individual sensor damages was based on a global set of parameters for the PLR, while more sensor specific information was provided by the regression coefficients of the LSM. These coefficients were trained for each individual sensor independently and were applied sensorwise in the regression analysis.

4. ESTIMATION OF FATIGUE DAMAGE

Individual damage results for the OC4 original model definition for each load case and wind seed simulation for a single representative data sensor are given in Figure 3. In addition, arithmetic mean values of the four sensors in each Y-joint/K-joint level are shown, with level numbering according to Figure 1. Different curve shapes with respect to the tower height are found. This makes it impractical to define a specific regression curve valid for all sensors, and the definition of the best load case combination has to be a compromise in terms of matching the properties of all sensors.

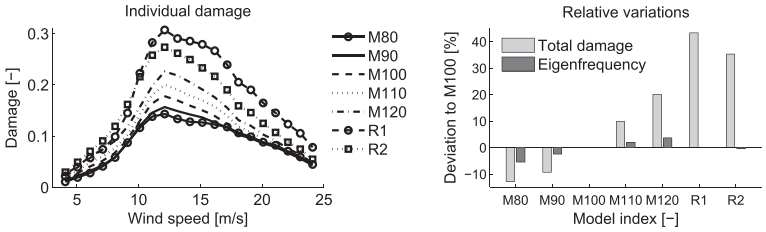

Figure 4. Variance of both individual and total damage, as well as first global fore-aft eigenfrequency for all analyzed structural models. Examples are given for K-joint sensor number 13.

4.1. Systematically and randomly modified models

The modified models are compared with the reference design in Figure 4 (left). The curves exhibit similar behavior but show different quantities over the set of load cases. Especially, the random models R1 and R2 show a significant increase of individual damage values, for wind speeds higher than 10 m/s. This observation is confirmed by the comparison of total damage for the different models (Figure 4, right). The large increase in fatigue damage for R1 and R2 cannot be explained by a global resonance problem. The change of eigenfrequency of these models compared with the reference model is with less than 0.5% negligible (absolute values given in Tables I and II). We assume therefore that the random choice of member dimensions leads to an unbalanced structural behavior. Interestingly, the total damage is systematically decreased for the systematically modified models M80 and M90 with smaller diameters, while it is increased for models with larger diameters (M110 and M120). However, observations at sensors at other locations of the structure result in the opposite behavior (not shown).

4.2. Definition of the best load case combination for the PLR

The basis of the PLR method is to assume a piecewise linear shape of the fatigue damage curve (damage versus wind speed). This assumption means that the statistical model requires no coefficients to be estimated. This leads to a combined training and evaluation phases, where all load case combinations are evaluated, resulting in an expected deviation for each sensor and combination. Figure 5 gives an overview over the distribution of deviation results for several sensor types spread over the support structure.

Figure 6 illustrates the principle of the PLR, comparing all simulated data points with the linearly interpolated estimated data points. The selection of three simulated load cases (left) is quickly performed as two load cases are fixed (4 and 24 m/s) and only one is variable. The best combination is found with a third load case at 12 m/s, which also seems reasonable by visual inspection of the data. On the other hand, five simulated load cases (right) leave three load cases variable. One would assume that the shown selection is not optimal, as the selected load case at 21 m/s is not contributing significantly with new information. However, we should recall the fact that the best found combination is a global result for all 36 sensors at the same time, i.e., the estimation of the total damage for data sets of other sensors (which are not shown in the figure) does have an advantage from the additional load case at this wind speed.

Table VI gives an overview over the calculated best load case combinations for the PLR method, depending on the number of simulated load cases.

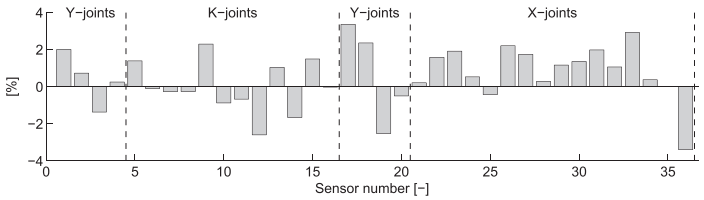

Figure 5. Deviation of estimated to known total damage for all sensors, for an example of the best load case combination with five simulated load cases.

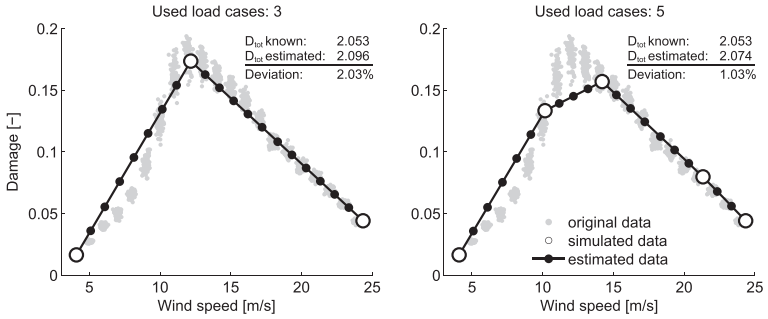

Figure 6. Regression plot for the case of three (left) and five (right) load cases in the PLR method, with interpolated estimated data for intermediate load cases. The original data are shown for all 100 wind seeds at this specific sensor number 13. As an example, results from one wind seed number are used for the calculation of the known total damage. The estimated total damage is calculated based on the sum of both simulated and estimated data points over all wind speeds. This results in the given deviation of estimated versus known damage.

Table VI. PLR: the best load case combination calculated for $n = 3, 4, 5, 6$ used load cases. Selected load cases are indexed by an 'x'.

	Wind speed (m/s)																			
n	4	5	6	7	8	9	10	11	12	13	14	15	16	17	18	19	20	21	22	23	24
3	x								x												x
4	x							x				x									x
5	x						x				x							x			x
6	x					x			x				x				x				x

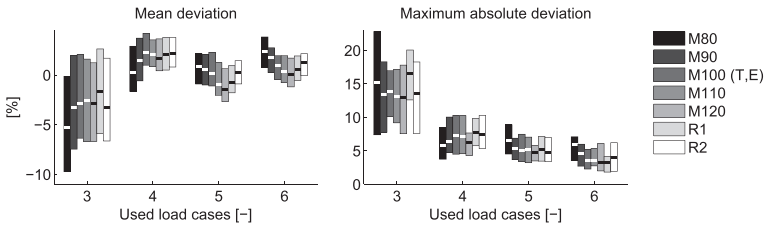

Figure 7. Performance of PLR: errorbars showing variability for 10 different wind seeds, with arithmetic mean indicated by a horizontal line. Capital letters behind the model name in the legend indicate which of the models was used in the training (T) and evaluation (E) phase (Table V).

4.2.1. Validation with systematically and randomly modified models.

After evaluating the PLR, its performance was validated by applying the best load case combination to 'unknown' data sets from both systematically and randomly modified models. Total damage deviation characteristics are extracted in terms of the arithmetic mean and maximum absolute deviation over all sensors. Results for the standard deviation are presented in a case study in Section 4.4. The validation is performed for 10 different wind seeds, resulting in errorbars showing the variability over these different wind fields (Figure 7).

Even if the PLR is trained and evaluated for the model M100 only, it performs well for all modified models too. Both mean and maximum absolute deviation show a considerable improvement when increasing the number of simulated load cases from three to four, resulting in a maximum total damage deviation of less than 10%. Further refinement leads only to slight improvements.

4.3. Performance of basic LSM model

After achieving reasonable results with the PLR model, the LSM was trained in a linear configuration (Equation (2)) with the same data resource, the model M100 only. Results are looking promising for the mean deviation in Figure 8 (left). However, the maximum absolute deviation was found to be way off for other models than the training model (right). Deviations of up to 40% are possible, and no significant improvement can be obtained when increasing the number of used load cases.

Obviously, the LSM basic model lacks the capability to predict the total damage for unknown designs, as long as training and evaluation phases are focused on one specific design only.

4.3.1. Improving regression performance.

Several versions were investigated to improve the performance of the LSM (Figure 9 and Table V). The crucial idea is to include modified models in the phases of training and evaluation too. This makes the statistical model more robust to structural modifications. It is impractical to calibrate and test the method with a very large number of additional cases; therefore, we proceeded by testing a few selected ideas. In detail, the following improvements could be achieved by each of these versions of the method:

Version 1: The basic model was only slightly improved when considering new data in the evaluation phase. For some modified models, the estimation accuracy of the total damage was actually slightly decreased. In total, a small positive effect of this version could be noted.

Version 2: By expanding the data resource in the training phase to closely modified models of the OC4 original definition, the regression error for other systematically models could be significantly decreased. However, this model still lacks the capability to predict the total damage for the randomly modified models.

Version 3: When the training phase includes the original model, one systematically modified model and one randomly modified model, the performance was in general very good and robust. A maximum regression error of less than 5% was found in the case of using five load cases, for example.

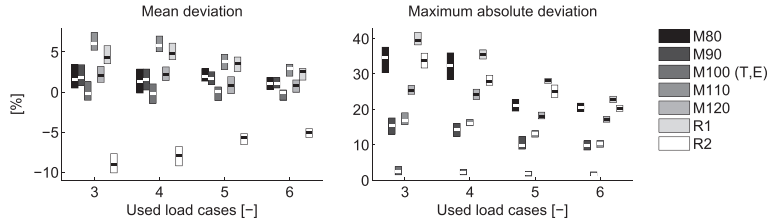

Figure 8. Performance of basic LSM model. Details of the figure are explained in the caption of Figure 7.

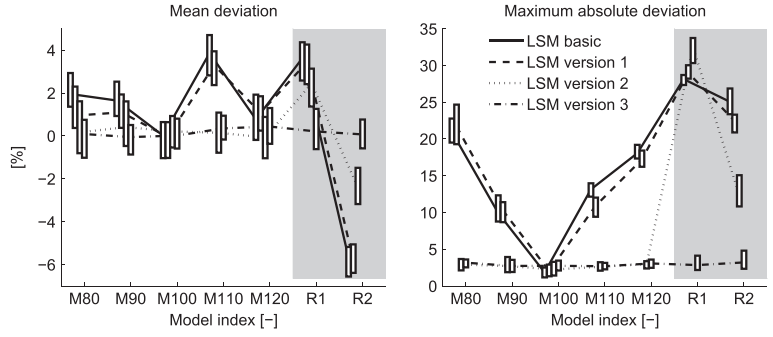

Figure 9. The performance of the LSM using five load cases, for different structural models. Results for R1 and R2 are presented on a different background color to better visualize the trend for systematically modified models for the maximum absolute deviation (M80 to M120). The errorbars show the variability for 10 different wind seeds; lines are connecting the arithmetic means.

Table VII. LSM version 3: the best load case combination calculated for $n = 3, 4, 5, 6$ load cases. The set of load cases used is a global property, valid for all sensors. The regression coefficients $C_{1..n+1}$ (Equation (2)) are local parameters, with individual values for each sensor. As an example, the table shows the values for sensor 13. Wind speeds below 7 and above 21 m/s were not relevant for the damage estimation.

		Wind speed (m/s)																
n	C_1	←	7	8	9	10	11	12	13	14	15	16	17	18	19	20	21	→
3	0.11				3.30					5.21					8.11			
4	−0.09			6.81			2.13			3.88							9.15	
5	−0.05		3.37	4.21			2.29				4.23						8.10	
6	0.12			2.12		1.68		1.41		2.12		2.61		5.78				

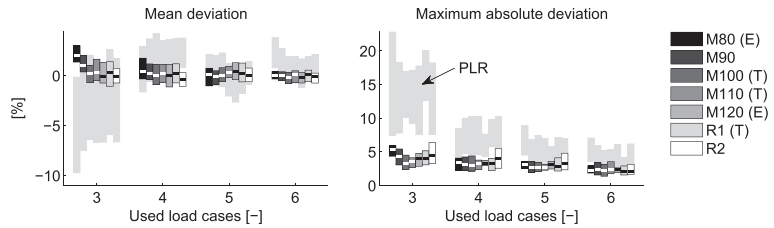

Figure 10. Performance of LSM model (version 3). Details of the figure are explained in the caption of Figure 7. Results for the PLR model are shown by the shaded area, to give a better impression of the improvement achieved by the use of the LSM.

Version 4: By focusing the training phase on the original model and randomly modified models only (R1 and R2), the regression error was increasing slightly for systematically modified models (not shown).

Summing up the approach to improve the performance of the LSM, the most successful idea was to include data from different structural models, both systematically and randomly modified, in the training phase. Of minor importance was the model selection in the evaluation phase. Slight improvements could be achieved by using additional modified models, which were not used in the training phase. However, in the case of limited simulation data as resource for the calibration of the regression parameters, models used in the training phase can be used in the evaluation phase as well, without influencing the regression error significantly. Load case combinations and examples for the regression coefficients for the most accurate LSM model (version 3) are given in Table VII. The regression error when estimating the total damage is shown in Figure 10. The development over three to six used load cases shows a more or less linear trend; therefore, the case of two load cases used was investigated too. The performance in this case decreases significantly, with larger variance and a maximum absolute deviation of up to 14% for the randomly modified model R2 (not shown in Figure 10).

Another possibility to improve the LSM is, in principle, to include interaction and quadratic terms (as in Equation (3)). While this might be promising for some statistical data sets, regression errors were increasing dramatically for the damage data in this study. This probably happened because of the much larger number of parameters that need to be estimated from the same limited data set. Based on this experience, results for this approach are not presented.

4.4. Comparison of statistical methods and performance in a case study

So far, large data resources were used for the calibration of regression parameters (100 wind seeds for M100, 10 wind seeds for other models), in order to demonstrate the feasibility of the proposed methods. In the following, a case study was performed where the data resource was limited to two or three wind seeds only, independent of the structural model. Both PLR and LSM (version 3) were tested, performing the phases of training, evaluation and validation as explained earlier. As the choice of the wind seed number has an influence on the variance,[8] the selection of two or three wind seeds out of 10 available wind seeds was performed $\binom{10}{2} = 45$ times and $\binom{10}{3} = 120$ times, respectively. Each such wind seed combination was used for the performance check of both regression methods. Results for the maximum absolute deviation were extracted in terms of the arithmetic mean and standard deviation of all possible wind seed combinations and are presented in Figure 11 for a number of three (left), four (middle) and five (right) used load cases.

When using three load cases (Figure 11, left), the LSM in general exhibits a better performance compared with the PLR. Increasing the available data from two (top) to three (bottom) wind seeds results in minor changes for the LSM only, while the performance of the PLR remains stable. In a second step, the number of used loads cases was increased to four

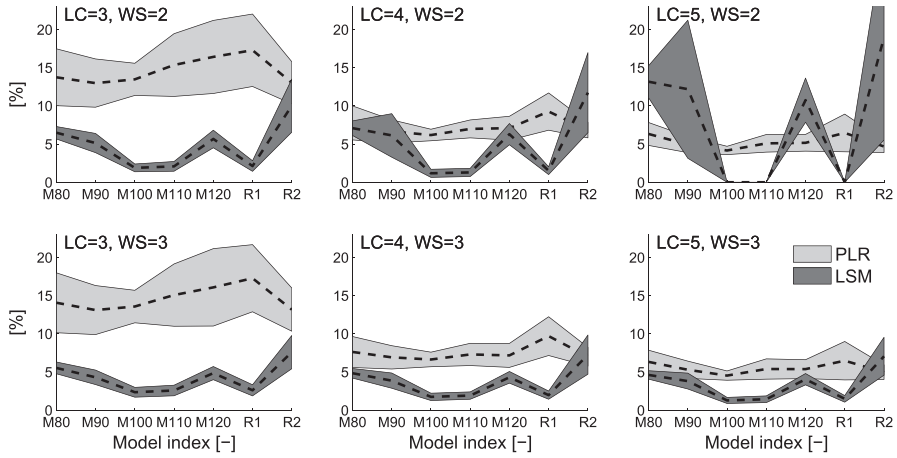

Figure 11. Maximum absolute deviation of the total damage estimation for PLR and LSM (version 3) when using three, four and five load cases (LC), and a number of wind seeds (WS) of two and three, respectively. The variance is caused by all possible seed combinations and is shown around the mean (dashed line) by $\pm 1\sigma$ (shaded area).

(middle). This results in a significant improvement of the performance of the PLR, where the mean deviation is divided in half, while at the same time reducing the standard deviation. On the other hand, the increase in the number of regression parameters means that the LSM will exhibit a more specialized response. For a small number of wind seeds (top), this results in decreased performance for models not considered in the calibration of regression parameters (M90 and R2). By further increasing the number of used load cases to five (right), this effect of limited data is clearly visible (top). The total damage of models used in the training phase (M100, M110 and R1) is calculated with zero deviation, while the unknown models (M90 and R2) show large variation in the estimation of the total damage, a clear case of overfitting. A significant improvement for this number of used load cases is achieved by increasing the data resource again, using three (bottom) instead of two (top) wind seeds.

Summing up, this case study with limited data resources for the calibration of the parameters of the statistical models demonstrates that the LSM shows a less stable behavior for modified models, whereas the PLR seems to be more robust. The latter is especially noticeable for the randomly modified model R2, where the limited data resource in the training phase leads to a decreased performance of the LSM, compared with the full analysis in Section 4.3.1. However, this case study also emphasizes the potential of these methods and their feasibility of fatigue damage estimation with reasonable accuracy, provided that enough data are available in the calibration phase.

An interesting aspect is the computational effort of the calibration phase in the case study. The potential of using statistical methods, in comparison to the traditional simulation of all individual load cases, is calculated in Table VIII. It is shown that the application of PLR and LSM can be beneficial when at least 3 or 18 analyses of such a structure need to be performed, respectively. Both cases selected for this calculation were chosen with the intention of a regression error of less than 10% (PLR: LC $=$ 5, WS $=$ 2; and LSM: LC $=$ 3, WS $=$ 3 in Figure 11). Comparing the PLR and LSM directly, the PLR is beneficial in terms of total computation time (summing up calibration and simulation phase) for a number of less than 136 simulations. For a larger number of simulations ($>$136) the LSM is, all other things being equal, more efficient.

Table VIII. Potential of regression methods in comparison to a traditional simulation of all individual load cases. The total number of simulations is calculated from the number of used load cases (LC), the number of wind seeds (WS) and the number of simulation models (SM) used for the calibration of the model parameters.

	Calibration phase				Simulation phase				Potential for number	
Method	LC	WS	SM	Total	LC	WS	SM	Total	of k simulations	
Traditional	—	—	—	—	21	1	1	21		
PLR	21	2	1	42	5	1	1	5	$42 + 5{\cdot}k < 21{\cdot}k$	$\rightarrow k >$ 2.6
LSM	21	3	5	315	3	1	1	3	$315 + 3{\cdot}k < 21{\cdot}k$	$\rightarrow k >$ 17.5

5. DISCUSSION

This study shows that statistical methods can be used for simplified fatigue load assessments with reasonable accuracy. Using the LSM linear model, an estimation of the total fatigue damage of several different structural models could be achieved with a maximum regression error of 6.4%, simulating only 3 of 21 power production load cases (Figure 10, right). This is the expected maximum absolute deviation for the sensor with the lowest estimation performance, i.e., the fatigue damage is estimated for most of the sensors with higher accuracy. This fact is extremely interesting for optimization purposes. It makes it possible to considerably reduce the number of load cases to be simulated in each iteration of an optimization routine while still providing an accurate fatigue estimate of the structural design. As a drawback of the LSM, the calibration of the regression parameters has to be performed carefully. The case study in Section 4.4 shows both potential and risk of the application of the LSM, if the data resource in the pre-processing phase of an optimization routine is limited. In this case, the PLR might be preferred, since it shows a relatively robust performance for modified structural models, even if the maximum deviation might be somewhat larger for some of the models. On the other hand, a carefully calibrated LSM will be more efficient in each optimization iteration. The most important algorithms in structural optimization are gradient-based, and estimating these with finite differences for k design variables needs $2k$ function evaluations. In such a case, the calibrated LSM will be advantageous if $nk \geq 9$, where n is the number of iterations of the optimization algorithm.

Several parameters defined in the simulation model may be subject to change in other analyses and might have an influence on the shown results. For both the structural and wind turbine models, the control system and the definition of the environmental loading have direct influence on the response in the support structure. Changes in the response may lead to a different shape of the individual fatigue damage curve over all load cases (Figure 3). This will probably directly influence the performance of the PLR, but not that of the LSM, at least not to the same extent. It is expected that the LSM is more flexible for different applications as the approach is not related to the characteristics of the individual damage curves. The latter is also the reason why polynomial or exponential fitting functions were not used in this study, as they are expected to be too inflexible in this context. Other factors, such as the investigation of wind–wave misalignment or the influence of marine growth thickness, are expected to be manageable by the proposed statistical methods. This assumption is based on the fact that the handling of in total 36 sensor responses at the same time already demonstrates that the statistical methods possess a certain flexibility.

The so-called best load case combination was defined as the combination with the smallest maximum absolute deviation over all sensors. One could argue that this is imprecise and that a statistical extrapolation of extreme values should be used instead (as applied for extreme wind speeds by the International Electrotechnical Commission[33]). However, the maximum criteria were used here to ensure that there is no total damage deviation larger than indicated by the regression error given in the results. When considering the actual choice of load cases in the best load case combination, the PLR shows a kind of logical pattern when increasing the number of used load cases (Figure 6 and Table VI). The LSM (version 3) shows a more random behavior (Table VII). However, the wind speeds of 8 and 14 m/s seem to have some importance as they were chosen by three of four performed analyses for different numbers of used load cases.

Readers may have noticed that individual fatigue damage values in this analysis are somewhat large (Figures 3 and 4, left). The summed-up total damage values over all load cases can exceed 1.0 for some sensors and models, indicating a fatigue failure of the weakest joint. This can be explained by the fact that none of the here-presented structural models were optimized or designed with a complete load case assessment. The underlying OC4 model is rather a simplification of the original Rambøll design specified in the UpWind project,[34] which among other things makes use of joint cans.

In the overall picture, it is the efficiency and accuracy of the simplified fatigue load assessment that matters. Simulating only 3 out of 21 load cases results in an analysis that is seven times faster compared with the traditional approach. Putting the resulting maximum fatigue damage estimation error of about 6% into context with the simulation error caused by input loading variability (up to 16–29% lifetime reduction in calculations that are based on widely used standards[8]), we can conclude that the latter error is dominating. The accuracy achieved for the fatigue damage estimation with statistical methods is by a factor of 2.5–4.5 better compared with the simulation error for fatigue loads.

6. CONCLUSION

The cost reduction of offshore wind turbine support structures is of current interest. The simplified fatigue load assessment presented here can contribute to a more efficient design process, reducing computational effort. The following findings are demonstrated:

- Statistical methods for the estimation of the total fatigue damage over all power production load cases, by only simulating a few of them, were successfully tested. The maximum regression error found in this study was 6.4% for

an example that uses 3 simulated load cases out of 21 and a multivariate LSM. This increases the speed of the fatigue analysis by a factor of seven in the simulation phase.
- The multivariate LSM shows large potential for performing simplified load case assessments in optimization routines. The statistical model should be applied by calibrating the regression parameters based on a combination of a reference model, a systematically modified model and a randomly modified model.
- When limited data resources might be an issue, or only a small number of fatigue analyses have to be performed, a more traditional regression method such as PLR can be favored. This model still provides a maximum regression error of less than 10% when using four or more load cases. It is in addition significantly faster in the calibration of regression parameters, compared with the statistical model.

As addressed in the discussion, it is of interest for further work to test the proposed method of a simplified fatigue load assessment with different structural models, control systems or environmental load models. Also other design load cases, e.g., idling or wind–wave misalignment, are of interest in this context.

ACKNOWLEDGEMENTS

Support by NOWITECH, the Norwegian Research Centre for Offshore Wind Technology, is gratefully acknowledged (Research Council of Norway, contract no. 193823). We thank in particular Fedem Technology AS for providing software licenses and quick and helpful feedback.

REFERENCES

1. Davey HE, Nimmo A. *Offshore Wind Cost Reduction Pathways Study.* Cost reduction study. The Crown Estate: London, United Kingdom, 2012.
2. Vorpahl F, Schwarze H, Fischer T, Seidel M, Jonkman J. Offshore wind turbine environment, loads, simulation, and design. *Energy and Environment* 2013; **2**: 548–570.
3. Muskulus M, Schafhirt S. Design optimization of wind turbine support structures - a review. *Journal of Ocean and Wind Energy* 2014; **1**: 12–22.
4. van der Tempel J. Design of support structures for offshore wind turbines, *PhD Thesis*, Delft University of Technology, Delft, the Netherlands, 2006.
5. van der Meulen MB, Ashuri T, van Bussel GJ, Molenaar DP. Influence of nonlinear irregular waves on the fatigue loads of an offshore wind turbine. *Journal of Physics: Conference Series* 2014, in press.
6. Ragan P, Manuel L. Comparing estimates of wind turbine fatigue loads using time-domain and spectral methods. *Wind Engineering* 2007; **31**: 83–99.
7. Naess A, Moan T. *Stochastic Dynamics of Marine Structures*. Cambridge University Press: New York, USA, 2013.
8. Zwick D, Muskulus M. The simulation error caused by input loading variability in offshore wind turbine structural analysis. *Wind Energy* 2014;1–12, DOI: 10.1002/we.1767.
9. International Electrotechnical Commission. Wind turbines - part 3: design requirements for offshore wind turbines. *International Standard, IEC 61400-3*, IEC Central Office: Geneve, Switzerland, 2009; 1–128.
10. Patel K, Freathy P. A simplified method for assessing wind-induced fatigue damage. *Engineering Structures* 1984; **6**: 268–273.
11. Leira BJ, Karunakara D. Estimation of fatigue damage and extreme response for a jack-up platform. *Marine Structures* 1990; **3**: 461–493.
12. Manuel L, Veers PS, Winterstein SR. Parametric models for estimating wind turbine fatigue loads for design. *Journal of Solar Energy Engineering* 2001; **123**: 346–355.
13. Fitzwater LM. *Estimation of Fatigue and Extreme Load Distributions from Limited Data with Application to Wind Energy Systems*, Sandia Report SAND 2004-0001. Sandia National Laboratories: Albuquerque, USA, 2004.
14. Dong W, Moan T, Gao Z. Long-term fatigue analysis of multi-planar tubular joints for jacket-type offshore wind turbine in time domain. *Engineering Structures* 2011; **33**: 2002–2014.
15. Wilcox R. *Introduction to Robust Estimation and Hypothesis Testing*. Elsevier Inc.: Waltham, USA, 2011.
16. Montgomery DC, Peck EA, Vining GG. *Introduction to Linear Regression Analysis*. John Wiley & Sons Inc.: Hoboken, USA, 2012.
17. Fahrmeir L, Kneib T, Lang S, Marx B. *Regression Models, Methods and Applications*. Springer-Verlag: Berlin, Heidelberg, Germany, 2013.

18. Zwick D, Muskulus M, Moe G. Iterative optimization approach for the design of full-height lattice towers for offshore wind turbines. *Energy Procedia* 2012; **24**: 297–304.
19. Yoshida S. Wind turbine tower optimization method using a genetic algorithm. *Wind Engineering* 2006; **30**: 453–470.
20. Molde H, Zwick D, Muskulus M. Simulation-based optimization of lattice support structures for offshore energy converters with the simultaneous perturbation algorithm. *Journal of Physics: Conference Series 555* 2014; **012075**: 1–8.
21. Schafhirt S, Zwick D, Muskulus M. Reanalysis of jacket support structure for computer-aided optimization of offshore wind turbines with a genetic algorithm. *Journal of Ocean and Wind Energy* 2014; **1**: 209–126.
22. Ashuri T, Zaaijer M, Martins J, van Bussel G, van Kuik G. Multidisciplinary design optimization of offshore wind turbines for minimum levelized cost of energy. *Renewable Energy* 2014; **68**: 893–905.
23. Ashuri T. Beyond classical upscaling: Integrated aeroservoelastic design and optimization of large offshore wind turbines. *PhD Thesis*, Delft University of Technology, Delft, the Netherlands, 2012, pp. 1–225.
24. Vorpahl F, Popko W, Kaufer D, *Description of a Basic Model of the 'UpWind Reference Jacket' for Code Comparison in the OC4 Project Under IEA Wind Annex XXX*, Technical Report OC4 Phase I - Jacket Model, Fraunhofer Institute for Wind Energy and Energy System Technology (IWES), Bremerhaven, Germany, 2011.
25. Fedem Technology AS. *Fedem User's Guide*, Release 7.0.3. Fedem Technology AS: Trondheim, Norway, 2013.
26. Popko W, Vorpahl F, Zuga A, Kohlmeier M, Jonkman J, Robertson A, Larsen TJ, Yde A, Sætertrø K, Okstad KM, Nichols J, Nygaard TA, Gao Z, Manolas D, Kim K, Yu Q, Shi W, Park H, Vasquez-Rojas A, Dubois J, Kaufer D, Thomassen P, de Ruiter MJ, Peeringa JM, Zhiwen H, von Waaden H. Offshore code comparison collaboration continuation (OC4), phase I - results of coupled simulations of an offshore wind turbine with jacket support structure. *Journal of Ocean and Wind Energy* 2014; **1**: 1–11.
27. Fischer T, de Vries W, Schmidt B. Upwind design basis. *WP4: Offshore Foundations and Support Structures, Endowed Chair of Wind Energy (SWE) at the Institute of Aircraft Design Universität Stuttgart*, Stuttgart, Germany, 2010; 1–140.
28. Jonkman J, Butterfield S, Musial W, Scott G, *Definition of a 5-MW Reference Wind Turbine for Offshore System Development*, Technical Report NREL/TP-500-38060, National Renewable Energy Laboratory, Golden, USA, 2009.
29. Det Norske Veritas AS. *Fatigue Design of Offshore Steel Structures.* Recommended Practice, DNV-RP-C203, 2012.
30. Amzallag C, Gerey J, Robert J, Bahuaud J. Standardization of the rainflow counting method for fatigue analysis. *International Journal of Fatigue* 1994; **16**: 287–293.
31. Palmgren AZ. Die lebensdauer von kugellagern. *Zeitschrift des Vereins Deutscher Ingenieure* 1924; **68**: 339–341.
32. Miner MA. Cumulative damage in fatigue. *Journal of Applied Mechanics* 1945; **12**: A159–A164.
33. International Electrotechnical Commission. Wind turbines - part 1: design requirements. *International Standard, IEC 61400-1*, IEC Central Office: Geneve, Switzerland, 2005; 1–85.
34. Vemula NK. *Design Solution for the Upwind Reference Offshore Support Structure*, Deliverable D4.2.5 (WP4: Offshore Foundations and Support Structures). Rambøll: Esbjerg, Denmark, 2010.

Paper 3

Comparison of different approaches to load calculation for the OWEC Quattropod jacket support structure

Zwick D, Schafhirt S, Brommundt M, Muskulus M, Narasimhan S, Mechineau J, Haugsøen PB
Journal of Physics: Conference Series 2014; **555**: 012110:1-10

Comparison of different approaches to load calculation for the OWEC Quattropod jacket support structure

D Zwick[1], S Schafhirt[1], M Brommundt[1], M Muskulus[1], Narasimhan S[2], J Mechineau[2] and P B Haugsøen[2]

[1] Department of Civil and Transport Engineering, Norwegian University of Science and Technology, Høgskoleringen 7a, 7491 Trondheim, Norway
[2] OWEC Tower AS, Storetveitvegen 96, 5072 Bergen, Norway

E-mail: daniel.zwick@ntnu.no

Abstract. Accurate load simulations are necessary in order to design cost-efficient support structures for offshore wind turbines. Due to software limitations and confidentiality issues, support structures are often designed with sequential analyses, where simplified wind turbine and support structure models replace more detailed models. The differences with an integrated analysis are studied here for a commercial OWEC Quattropod. Integrated analysis seems to generally predict less damage than sequential analysis, decreasing by 30-70 percent in two power production cases with small waves.

Additionally it was found that using a different realization of the wave forces for the retrieval run in sequential analysis leads to an increase of predicted damage, which can be explained as the effect of applying two independent wave force series at the same time.

The midsection of the detailed support structure model used shell elements. Additional analyses for a model with an equivalent beam model of the midsection showed only small differences, mostly overpredicting damage by a few percent. Such models can therefore be used for relatively accurate analysis, if carefully calibrated.

1. Introduction

The design of support structures for offshore wind turbines is based on accurate load calculations with numerical computer models. Conformity of the design to the required serviceability, ultimate and fatigue limits is thereby assessed. Different modeling approaches, computer codes, and the way in which calculations are performed can significantly influence the results. This can potentially lead to overconservative designs, and a better understanding of the issues involved might offer the possibility of further optimizing support structures and reducing their costs.

In this study we considered a commercial OWEC Quattropod® designed by OWEC Tower AS for a water depth of 26.1m in the Thornton Bank project. One of the five different structures designed for this site was selected. The load calculations and certification in this commercial project were performed in cooperation between the support structure designer OWEC Tower AS, the wind turbine manufacturer REpower Systems AG and the engineering consultancy TDA. Basis for most load calculations was a sequential analysis [9] that allows for cooperation between all parties involved without sharing detailed computer models.

Sequential analysis as pioneered by REpower consists of three distinct steps. In a first step, only the support structure model is used without a tower and wind turbine model included. Simulations were performed with ANSYS ASAS(NL) (Version 13, ANSYS Inc., Canonsburg) and result in generalized mass, damping and stiffness matrices together with a generalized load time series that essentially consists of the integrated wave loading experienced by the support structure. In a second step a wind turbine simulation is performed in a variant of FLEX5 (Stig Øye, DTU) with this reduced model for the support structure. Displacement time series at an interface node are output that reflect the response to combined wave and wind loading. In the final step these time series are applied to the detailed support structure model, including exactly the same wave loading used for the first step.

The sequential analysis replaces the earlier *semi-integrated* approach [10] in which an equivalent beam model was used for the support structure in the second step. Both approaches have in common that the wind turbine simulations are performed with a simplified model for the support structure. In contrast to this, a *fully-coupled* or *integrated* simulation will simulate the wind turbine with a detailed model of the support structure. A number of studies have hypothesized that for such a complex and tightly coupled system fully-coupled simulations are needed to obtain accurate results, especially with regard to local vibrations of the support structure [12, 2].

Even if integrated analyses are performed, the question remains how accurate and realistic the results are, compared to the actual behavior of the system. The Offshore Code Comparison Collaboration (OC3) project headed by Fraunhofer IWES (Bremerhaven) and the National Renewable Energy Laboratory (Boulder, Colorado) has performed systematic studies of differences in load calculations obtained by different simulation codes. During its successor, the OC4 project under Task 30 of IEA Wind, a prototypical support structure of the jacket type was studied [7]. Although results generally agree within 10 percent for displacements and forces, damage equivalent loads differ to a larger extent, with up to 50 percent or more in some cases.

The goal of the present study was to study differences in load simulations for a commercial OWEC Quattropod® design, which contains many more features and details than the OC4 jacket. Three main questions were addressed:

(i) What are the differences in load calculations between different analysis codes?
(ii) What differences can be seen between fully-coupled/integrated and sequential load calculations?
(iii) What is the influence of various changes in model detail?

2. Methods

Currently, not many software packages allow for an integrated analysis of a complete offshore wind turbine on a jacket structure. We have performed most analyses with Fedem Windpower (Fedem Technology AS, Trondheim), which is a flexible multibody solver that has been extended to provide both aerodynamic and wave loads. Fedem Windpower has been verified in the OC3/OC4 project and we used a pre-release version of the software. Alternatively, Bladed (Version 4.2, GL Garrad Hassan, Bristol) was used. Both simulation codes were at present not able to run all cases of this study with the OWEC Quattropod® and all its features included.

Although integrated wind turbine analyses can be performed with Fedem Windpower, it currently does not provide functionality for implementing non-diagonal elements of generalized stiffness and damping matrices necessary for the second step of the sequential analysis. The wind turbine simulations with a simplified support structure model were therefore performed by Bladed (Fig. 1).

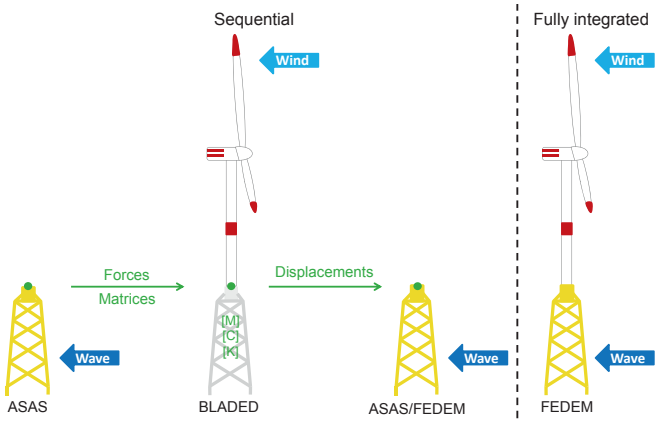

Figure 1. Sequential and integrated analysis as performed in this study.

The current version of Bladed has limitations with respect to the number of nodes and elements available. Although the support structure could be fully implemented up to mudline, it was not possible to obtain simulation results when the soil piles were included. The Bladed model of the complete wind turbine was therefore rigidly connected to the ground at mudline level. It is also not possible to include freedom releases and rigid element offsets in Bladed, and Bladed does not offer shell elements for modeling the transition piece and deck. Mass, stiffness and damping matrices for the sequential analysis were included in Bladed as a "soil model", but it was not possible to use non-diagonal elements in the mass matrix. The latter is no practical limitation since these, corresponding to the effect of geometric nonlinearities, were a factor of 1000 smaller than the diagonal elements. Finally, a short rigid element at the top of the transition piece had to be modeled with flexible material.

Retrieval runs (step 3 of the sequential analysis, Fig. 1) were performed with both Fedem Windpower and ASAS models of the support structure, since Bladed does not easily allow for structural analyses without a wind turbine, and does also not provide many of the more detailed features needed for accurately modeling the support structure.

2.1. Simulation models

The support structure models were based on the final ASAS model of the OWEC Quattropod® used in the certification analysis. This is a finite-element model with more than 900 nodes and elements, including both beam and 4–node shell elements, as well as (linear) springs and dashpot elements for the soil piles (Fig. 2*a*). The model has been exactly replicated in Fedem Windpower. This model is called FEDEM1 in the following (Fig. 2*b*). For the integrated simulations the NREL 5MW reference wind turbine [6] was implemented on top of the jacket, with an additional point mass of 100t to more closely match the REpower 6M turbine. Also the damping was adjusted (see below). This model was called FEDEM3 (not shown). The models were run for 600s with output time steps of 0.02s. The first 100s of results were discarded in order to remove possible transients. A full overview over all FEDEM models used in this study is given in Table 1.

2.2. Reduced midsection

Since Bladed does not supply shell elements, the middle section with the transition piece was represented by an equivalent beam model in Bladed (Fig. 2*c*). This reduced midsection was obtained by manually adjusting element properties in order to match mass and stiffness. The

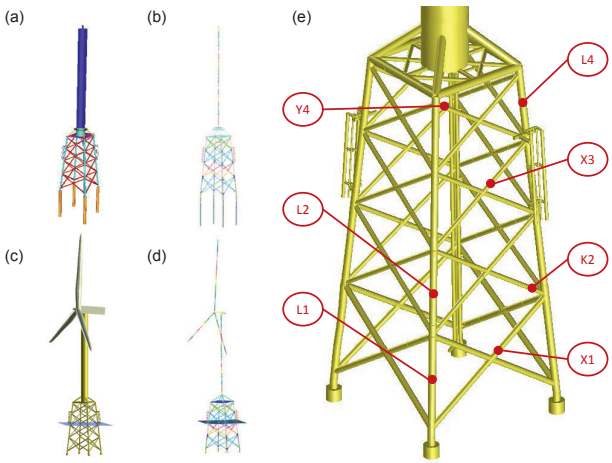

Figure 2. Simulation models in this study.
(*a*) ANSYS ASAS,
(*b*) FEDEM1,
(*c*) BLADED1,
(*d*) FEDEM4,
(*e*) Detail of the model with reduced midsection, including output locations.
FEDEM3 is a combination of the FEDEM4 turbine and the FEDEM1 jacket.
BLADED2 is BLADED1 with the jacket removed and represented by generalized matrices.
L: leg; X, K, Y: type of joint. Number denotes bay, counting from bottom.

Table 1. Overview of FEDEM simulation models.

Identification	Description
FEDEM1	configuration identical to ANSYS ASAS model
FEDEM2	as FEDEM1, with reduced midsection
FEDEM3	as FEDEM1, with modeled NREL 5MW turbine
FEDEM4	as FEDEM3, with reduced midsection

latter was assessed by comparing the first five eigenfrequencies (Fig. 3). The same integrated model was exactly reproduced in Fedem Windpower and called FEDEM4 (Fig. 2*d*). The midsection was also replaced by this reduced midsection for the FEDEM1 model, which is then called FEDEM2.

2.3. Output stations
Responses were recorded at all nodes and members of the support structure, of which only a few are discussed here (Fig. 2*e*). These output stations consist of nodes on the legs and braces, and are named either as leg (L) nodes or according to the closest joint (X-, K-, and Y-type). The jacket has four bays, which are numbered starting at the bottom, such that, e.g., K2 denotes the K-joint on the second-lowest bay.

2.4. Damping
The ASAS model of the OWEC Quattropod® was implemented with Rayleigh damping, i.e., element damping matrices are linear combinations $C = \alpha M + \beta K$ of element mass (M) and stiffness (K) matrices. This was exactly reproduced in Fedem Windpower. Bladed uses a modal basis for simulations, and a damping ratio ζ needs to be specified for each such mode.

If all elements were using the same Rayleigh damping coefficients α and β, this would be given by $\zeta(\omega) = \frac{1}{2}\left(\frac{\alpha}{\omega} + \beta\omega\right)$ [3]. In extension of this, the Rayleigh damping coefficients were

here taken as averages $\alpha = \sum_i \alpha_i m_i / \sum_i m_i$, $\beta = \sum_i \beta_i m_i / \sum_i m_i$ of the coefficients α_i, β_i of all elements, weighted by the magnitude m_i of the i-th component of the corresponding eigenvector (modeshape). Results (see below) seem to indicate good agreement. For the wind turbine, the damping was slightly adjusted and differs from the damping specified by NREL (in order to mask results for confidentiality reasons).

2.5. Damage factors

Responses were assessed by visual inspection of time series, second order statistics, probability density functions and spectra. An approximate, relative assessment of damage was obtained directly from the displacement time series. Rainflow counting was performed and damage was integrated using Palmgren-Miner's rule with a load-N curve (displacement versus allowable cycles to failure), similar to the approach in [4]. The ultimate displacement before failure was taken to be 1.0m and an inverse slope $m = 3$ was used. The results cannot be compared for different nodes because of differing geometry, but for different loadcases (as long as they are based on timeseries of the same length). For most plots (see below) the results were additionally normalized to a reference damage value such that relative changes in damage are reported.

3. Results

In the following the different models are compared, with respect to four questions:

(i) Can the support structure be analyzed in both ASAS and FEDEM with similar results?
(ii) Can the wind turbine be analyzed in both FEDEM and Bladed with similar results?
(iii) Are there differences in support structure behavior for the reduced midsection?
(iv) Are there differences between fully-coupled and sequential results?

Three classes of models were considered and directly compared:

- ASAS and FEDEM1/FEDEM2 are models of only the support structure, whereas
- BLADED1 and FEDEM3/FEDEM4 are models of a complete wind turbine.
- FEDEM4 and BLADED1 are both clamped at mudline.

Comparisons are typically only within each class. For fully-coupled simulations FEDEM3 is used, for step 2 in the sequential analysis BLADED2 is used, and FEDEM1 and ASAS are used for the retrieval runs.

Two main environmental conditions were used for the power production loadcases that are relevant for fatigue lifetime estimation:

(A) irregular waves with $H_s = 1.0\,\mathrm{m}$, $T_p = 4.95\,\mathrm{s}$ and $\gamma = 1.06$ from a JONSWAP spectrum, and turbulent wind at $U = 8\,\mathrm{m/s}$ from a von Karman spectrum with turbulence intensity $I = 0.153$;
(B) irregular waves with $H_s = 2.59\,\mathrm{m}$, $T_p = 6.99\,\mathrm{s}$ and $\gamma = 2.13$; turbulent wind at $U = 20\,\mathrm{m/s}$ with $I = 0.121$.

Many additional load cases were used for testing specific aspects of the models (see below).

3.1. Mass and center of gravity

The total mass for the ASAS model is 1337t, which is closely matched by the other models (within 1.5 percent). The center of gravity lies within 1.6 percent for the vertical axis and less than 6.0 percent horizontally. The only exception are the models with reduced midsection which exhibit a horizontal deviation of a few cm (amounting to 20 percent relative error).

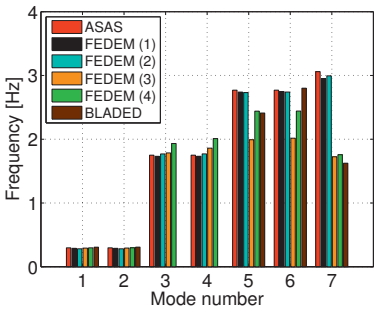

Figure 3. Comparison of first seven eigenfrequencies.

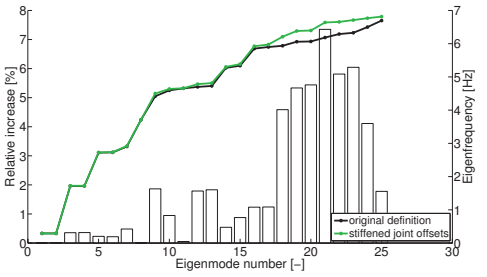

Figure 4. Eigenfrequencies and relative changes for FEDEM model with and without local element offsets.

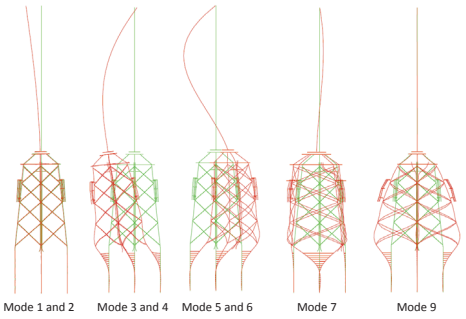

Figure 5. The first nine modeshapes of the ASAS model.

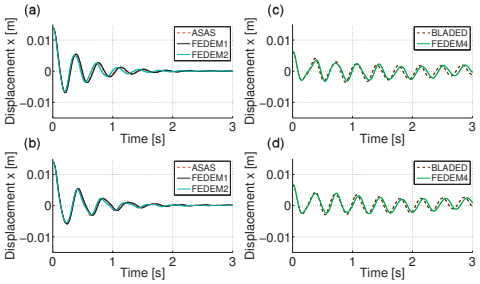

Figure 6. Decay test with a 1MN force applied at tower bottom and released at $t = 0\,\mathrm{s}$. Horizontal displacements at L4. (a, c): in air; (b, d): in still water.

3.2. Eigenfrequencies

The first seven eigenmodes were compared (Fig. 3) and showed relatively good agreement between ASAS and FEDEM1/FEDEM2, or between FEDEM4 and BLADED1. Differences between detailed models and models with reduced midsection are only evident for the complete wind turbine. It should be noted that such a comparison is at best approximate, since there exist various ways of defining dynamic modes for rotating, flexible multibody systems. For example, in Bladed the first tower modes are obtained by considering unit loads in all six degrees of freedom (with the rotor-nacelle assembly represented by a point mass and inertia), and then further modes normal to these [1]. Comparing the modeshapes visually allows to identify similar modes (Fig. 5), but cannot resolve such differences.

3.3. Static load cases

Two static load cases, with either 1MN or 1MNm applied at the tower bottom, showed good agreement between all models (in each class). The much stiffer clamped models exhibited only 50 to 25 percent of the displacements.

3.4. Free decay behavior

Free decay behavior of the support structure models was assessed by ramping up a 1MN horizontal load and releasing it at $t = 0\,\mathrm{s}$. ASAS and FEDEM1 showed excellent agreement,

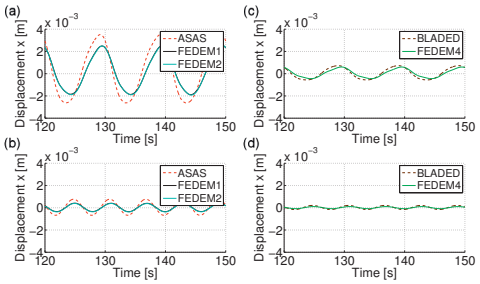

Figure 7. Response to regular wave loading at output location L2. (a, c): $H = 6\,\mathrm{m}$, $T = 10\,\mathrm{s}$; (b, d): $H = 2\,\mathrm{m}$, $T = 6\,\mathrm{s}$.

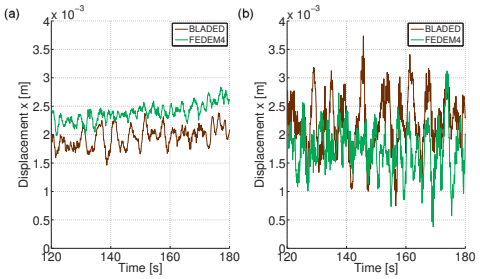

Figure 8. Integrated models BLADED1 and FEDEM4. Example response time series at output location X3. (a): Environmental conditions A. (b): Environmental conditions B.

both in air (Fig. 6a) and still water (Fig. 6b). Model FEDEM2 with reduced midsection showed a slightly shorter period due to a somewhat smaller first eigenfrequency, but with similar amplitude. The comparison between FEDEM4 and BLADED1 showed similar agreement (Fig. 6c, d). Interestingly, at first the results for ASAS did not match the FEDEM results, but after consulting with TDA it was confirmed that one needs to specify a very small wave in ASAS in order to obtain the contribution from the added mass.

3.5. Behavior under regular and irregular waves

The response was studied both for regular and irregular waves based on linear wave theory. Surprisingly, results for regular waves with $H = 6\,\mathrm{m}$, $T = 10\,\mathrm{s}$ (Fig. 7a) and with $H = 2\,\mathrm{m}$, $T = 6\,\mathrm{s}$ (Fig. 7b) showed that the response in ASAS is significantly higher (around 100 percent increase for the 2m wave, and around 40 percent for the 6m wave) than for the FEDEM models. Essentially the same difference was seen for irregular waves. In order to understand this phenomenon better, regular waves with $H = 2\,\mathrm{m}$, $T = 30\,\mathrm{s}$ were additionally studied (not shown). Such a slow wave far away from resonant frequencies leads to a quasi-static response, which is essentially due to wave forces (inertial effects are thereby avoided). Still, we found differences in response amplitude of 20-25 percent. This suggests that wave loads are generally higher in ASAS. Although the wave loads in FEDEM have been verified in the OC3/OC4 project, the details in which these are resolved and integrated might still cause such a difference.

The reduced midsection in FEDEM2 did not influence the response to the same extent, with a maximum difference of up to 20 percent for the lower bays in the 2m wave. The comparison between BLADED1 and FEDEM4 also showed a slight underestimation of wave loads of about 15-20 percent in FEDEM.

These differences were systematically larger for the smaller waves, which suggests that they might be mainly caused by the calculation of the wave forces in the splashzone. Additionally, the influence of marine growth was assessed. This generally led to larger displacement amplitude (due to higher wave loads), and showing similar differences consistent with the above.

3.6. Influence of local joint modeling

The ASAS model contains element offsets at joints to model local joint behavior. These were reproduced (manually, with rigid beams) in the FEDEM models. Since this is of general interest, we studied the behavior of the model without these offsets. For the lower eigenmodes the

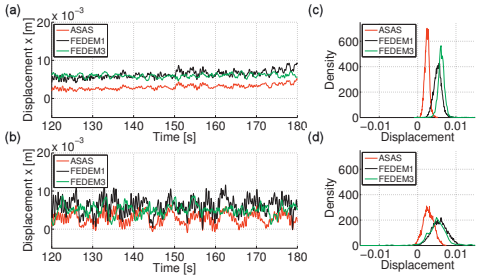

Figure 9. Results for sequential (ASAS, FEDEM1) and integrated analyses (FEDEM3) according to Fig. 1. (a, b): Example time series for X3 joint. (c, d): Probability density functions of these responses. (a, c): Environmental conditions A. (b, d): Environmental conditions B.

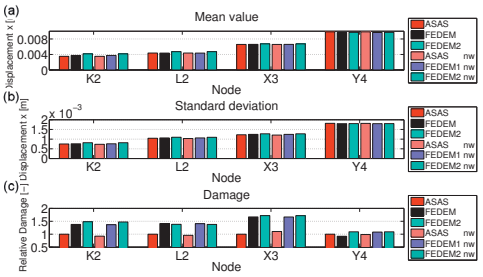

Figure 10. Comparison of responses in sequential analysis between models and for waves / no-waves (nw) in the retrieval run. Environmental conditions similar to A.

differences were minimal (below 0.5 percent), but the eigenfrequencies were increasing by 4-7 percent for higher modes that correspond to local vibrations (Fig. 4).

Running a typical power production case, no systematic, clear trend of changes was discernible. In total, however, both the standard deviations and the damage factors were higher with stiffened joint offsets, up to 20 percent, or in some cases (K2) even up to 50 percent.

3.7. Sequential analysis with a reduced model

This is the main case of interest for this study. Since the wind turbine was simulated with BLADED2 in step 2 of the sequential analysis, and with FEDEM3 in the integrated analysis, we first compared integrated analysis between BLADED1 and FEDEM4 (Fig. 8). The results showed good agreement, although a few differences (e.g., in mean displacements) existed (not shown).

The influence of correctly implementing the wave loads was separately studied. Removing the wave forces in the retrieval run led to small differences (Fig. 10); for these fatigue cases with relatively small wave height the response of the support structure seems to be dominated mostly by wind loads. In general, a small decrease in damage (up to 5 percent) seems to result.

Differences for the retrieval runs between ASAS and FEDEM were much more pronounced, with up to 60 percent higher damage in FEDEM1, and a few percent more for the reduced midsection model. Again, this could be caused by a different integration of wave forces in FEDEM. Additionally, the retrieval run is performed with displacements that ultimately were obtained from wave forces by ASAS. These changes can therefore also reflect changes due to using a different realization of irregular waves, which in effect amounts to using wave forces twice. Not using the wave forces from ASAS results in a negative response, using the wave forces from FEDEM results in a second positive response. Since these responses are completely independent of each other, on the average there will be a net effect that will be larger than for using wave forces once. In contrast, output Y4 is not directly affected by waves and therefore shows little differences.

The same comparison was used for assessing the differences between sequential and integrated analysis for both environmental conditions A and B (Fig. 11). Two additional nodes L1 and X1 were included in this comparison. For environmental condition B some convergence problems

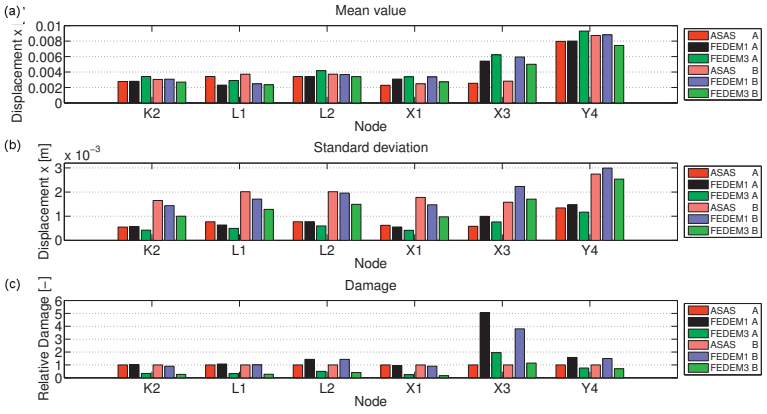

Figure 11. Comparison of sequential and integrated analysis.

were encountered, such that these results are only based on 200s of simulation time. The main result is that damages in the integrated analysis were significantly lower than in the sequential analysis (reduced by 30-70 percent), with the notable exception of the X3 brace that showed an increase of 100 percent for the small waves of environment A. As before, sequential retrieval runs with FEDEM1 suffered slightly from mismatches in wave forces. Again, the X3 brace, located relatively close to the splashzone, is an exception and exhibits the most damage.

4. Discussion

Accurate and reliable load calculations are important for the design, the optimization and the certification of offshore wind turbines. Current projects are complicated by (a) the commercial unavailability of wind turbine analysis software with all features required for integrated analyses with complex support structures, and (b) the necessity felt by the industry of keeping model details confidential. Sequential analysis has been introduced as a potential solution, but soon its limitations were detected.

4.1. Sequential analysis with a complete model

In general there seems to be some misunderstanding in literature about the conceptual foundation on which sequential analysis is based. *Substructuring methods* have been around almost since the beginning of finite element analysis [8]. When sequential analysis is performed with an identical model of the support structure and the same environmental conditions, using displacements at an interface node, results will be *identical* to an integrated analysis. This was confirmed by simulations (not shown). Differences in results will occur only because of (a) different software used for the analyses, (b) different environmental conditions (e.g., through different random number generators), and (c) because of different detail in the support structure model used.

4.2. Integrated versus sequential analysis

In this study the integrated analysis resulted in significantly reduced damage factors (with the notable exception of an X-brace in the top part of the jacket). Although the comparison is not perfect, since different software were used for the sequential and the integrated analysis, this indeed suggests the need for integrated analyses in the design of support structures for offshore wind turbines.

It is hoped that the limitations in current wind turbine analysis software will be addressed and fixed in the near future, such that integrated analyses of complex support structures become feasible and efficient soon.

4.3. Reduced midsection
The reduced midsection models showed slight differences in eigenfrequencies, so responses / excitations will generally differ to a certain extent. However, almost no influence on the response due to (regular and irregular) wave loads was detected. Also in the sequential analysis, only slight differences were observed (Fig. 10), generally overestimating the damage by a few percent.

4.4. Different analysis codes
Both FEDEM and ASAS showed larger differences in response to wave loads than expected. This should be further studied.

In general we can conclude that using different waves in the retrieval step of the sequential analysis did have a significant influence on the damage for these cases with relatively small waves, but will generally be conservative and limited to a factor of two at most. The situation should be studied more closely for larger waves and, for example, assessing the ultimate limit state behavior.

Acknowledgments
Financial support by the Research Council of Norway under grant no. 193326 ("Innovative foundation structure for offshore wind turbines") is gratefully acknowledged. We thank the Norwegian Research Centre for Offshore Wind Technology (NOWITECH) for support, in particular the helpful staff of Fedem Technology AS.

References
[1] GL Garrad Hassan 2011 *Bladed user manual* Version 4.2 (Bristol: Garrad Hassan & Partners)
[2] Böker C 2009 *Load simulation and local dynamics of support structures for offshore wind turbines* (Hannover: Institut für Stahlbau, Gottfried Wilhelm Leibniz Universität Hannover)
[3] Craig RR Jr 1981 *Structural dynamics* (Hoboken: John Wiley & Sons)
[4] Freebury G and Musial W 2000 *Determining equivalent damage loading for full-scale wind turbine blade fatigue tests* Technical Report NREL/CP-500-27510 Golden: National Renewable Energy Laboratory
[5] Hald T and Høgedal M 2005 Implementation of a finite element foundation module in Flex5 using Craig-Bampton substructuring *Proc. Copenhagen Offshore Wind*
[6] Jonkman J, Butterfield S, Musial W and Scott G 2009 *Definition of a 5-MW reference wind turbine for offshore system developmen* Technical Report NREL/TP-500-38060 (Golden: National Renewable Energy Laboratory)
[7] Popko W *et al* 2012 Offshore Code Comparison Comparison Collaboration Continuation (OC4) phase I — results of coupled simulations of an offshore wind turbine with jacket support structure *Proc. 22nd Int. Offshore Polar Engng. Conf. (Rhodes)* 337–46
[8] Przemieniecki JS 1986 *Theory of matrix structural analysis* (Mineola: Dover)
[9] Seidel M, von Mutius M, Rix P and Steudel D 2005 Integrated analysis of wind and wave loading for complex support structures of offshore wind turbines *Proc. Offshore Wind Conference 2005 (Copenhagen)*
[10] Seidel M, von Mutius M and Steudel D 2004 Design and load calculations for offshore foundations of a 5MW turbine *Proc. DEWEK 2004 (Wilhelmshaven)*
[11] Seidel M and Foss G 2006 Impact of different substructures on turbine loading and dynamic behaviour for the DOWNVInD project in 45m water depth *Proc. EWEC 2006 (Athens)*
[12] Seidel M, Ostermann F, Curvers A P W M, Kühn M, Kaufer D and Böker C 2009 Validation of offshore load simulations using measurement data from the DOWNVInD project *Proc. European Offshore Wind 2009 (Stockholm)*
[13] Seidel M 2010 Design of support structures for offshore wind turbines — interfaces between project owner, turbine manufacturer, authorities and designer *Stahlbau* **79** 631–6

Paper 4

Iterative optimization approach for the design of full-height lattice towers for offshore wind turbines

Zwick D, Muskulus M, Moe G
Energy Procedia 2012; **24**: 297-304

Available online at www.sciencedirect.com

SciVerse ScienceDirect

Energy Procedia 24 (2012) 297 – 304

Energy Procedia

DeepWind, 19-20 January 2012, Trondheim, Norway

Iterative optimization approach for the design of full-height lattice towers for offshore wind turbines

Daniel Zwick*, Michael Muskulus, Geir Moe

Department of Civil and Transport Engineering, Norwegian University of Science and Technology, 7491 Trondheim, Norway

Abstract

Among several possible support structure types for offshore wind turbines, a full-height lattice tower is one design option. Advantages of this design are the smaller amount of steel used for the structure compared to other concepts, and the possibility to install the whole structure in one operation. Based on the complexity of dynamic loadings on the support structure by wind and wave as well as operational loads, an initial lattice tower design with constant member dimensions over the tower height shows a large optimization potential and can be optimized section by section. This paper presents basic considerations for an iterative optimization approach and identifies sensitivities for the optimization process of a full-height lattice tower. It was found that an analysis with constant member dimensions over the tower height gives an indication about the required dimensions for an optimized design.

Keywords: offshore wind turbine, bottom-fixed support structure, full-height lattice tower

1. Introduction

Installations of bottom-fixed offshore wind farms in intermediate water depth of 20-70m are until now based on more or less the same construction idea: the support structure carrying the rotor nacelle assembly (RNA) is a combination of a multi-member (jacket, tripile, tripod), tubular (monopile) or gravity based sub-structure with a tubular tower [1]. A new design approach of a full-height lattice tower has been developed by the Department of Civil and Transport Engineering at NTNU [2], in which the traditional tubular tower is replaced by a space frame structure going all the way from seabed to RNA. The aims of this approach are a reduction in steel weight and a simplification of the installation, and thereby a reduction of total cost of the support structure, compared to known solutions.

An iterative method was used to optimize these designs, based on the automatic generation of tower finite element models characterized by a few parameters, the time-domain analysis of the models in FEDEM Windpower (a flexible multi-body solver developed by Fedem Technology AS, Trondheim, Norway), and post-processing of the resulting time series for the calculation of ultimate loads and fatigue properties.

*Corresponding author (phone +47 994 94 853, fax +47 735 97 021)
Email addresses: daniel.zwick@ntnu.no (Daniel Zwick), michael.muskulus@ntnu.no (Michael Muskulus), geir.moe@ntnu.no (Geir Moe)

1876-6102 doi:10.1016/j.egypro.2012.06.112

The main contribution of this paper is to show how to utilize the sensitivities for the optimization process. This helps to reduce the number of time-domain analyses necessary, thereby reducing calculation time to a manageable amount. Important design parameters are the member dimension configuration and the number of sections over the tower height. Results are presented that compare optimized designs with adapted member dimensions and different numbers of sections, with regard to the total weight of the structure. Both constant brace angle and constant section height designs were considered.

2. Full-height lattice tower design

2.1. Topology

Lattice towers are known as light weight space frame structures with a wide area of application for offshore oil and gas platform installations [3]. In the offshore wind turbine industry, lattice towers are until now only used as the sub-structure of the wind turbine installation, providing support for a traditional tubular tower. The latter is known from onshore wind turbines. A transition piece located at a certain level above the water surface is connecting the two structural parts.

The design of a full-height lattice tower presented here, as shown in Figure 1, provides directly support for the turbine nacelle, without transition to a tubular tower. The structure is characterised by leg and brace members, welded together in K- and X-joints.

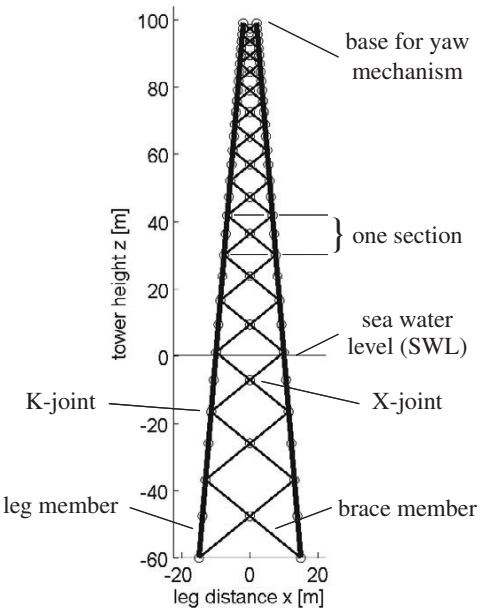

Fig. 1. Full-height lattice tower with constant brace angle

The specification of a certain site location and RNA configuration gives a first indication about the structural design of the tower. The *top distance* defines the tower width at the base for the yaw mechanism. In combination with the *tower height*, these parameters are set by the turbine manufacturer due to blade tip clearance above the water surface and turbine nacelle design. Also the *bottom distance* between the legs at sea bottom is limited by the rotor design due to a minimum required blade tip clearance to the tower structure. For the design optimization process, several parameters are available:

- *leg number*
- *section number*
- *leg and brace member dimensions*
- *constant brace angle or constant section height*

The described work was performed with a 4-legged lattice tower only, as the design base was chosen to be similar to common jackets combined with tubular towers used in offshore wind turbine installations today. The other mentioned parameters were used as optimization variables.

2.2. Simulation model and initial load conditions

A full-height lattice tower for the installation of the proposed 10MW NOWITECH reference turbine in 60m water depth was selected. This design idea of the tower was originally presented by Long and Moe [2]. Details of the analysed design in this study can be found in Table 1. The fully-coupled model of an offshore wind turbine was build in FEDEM Windpower with a blade design based on the study of Frøyd

and Dahlhaug [4]. Simulation runs with 13.5m/s turbulent wind (16% turbulence intensity) and an irregular sea state with JONSWAP spectrum (significant wave height H_s = 4m and mean wave period T_p = 9s) were performed for aligned wind and wave direction to provide initial load conditions. This load case represents a typical load on the structure at rated speed in North Sea wave conditions.

2.3. Iterative optimization approach

For the iterative optimization approach, each iteration, as shown in Figure 2, is based on two main steps. First the analysis of a specific tower design with a multi-body solver, and second the post-processing of calculated time series of forces and moments for each member and joint. Each tower model is analysed for the ultimate limit state (ULS) and the fatigue limit state (FLS). The analysis includes the calculation of stress concentration factors (SCF) to determine hot spot stresses (HSS) in the joints of the lattice tower (see Section 2.3.1).

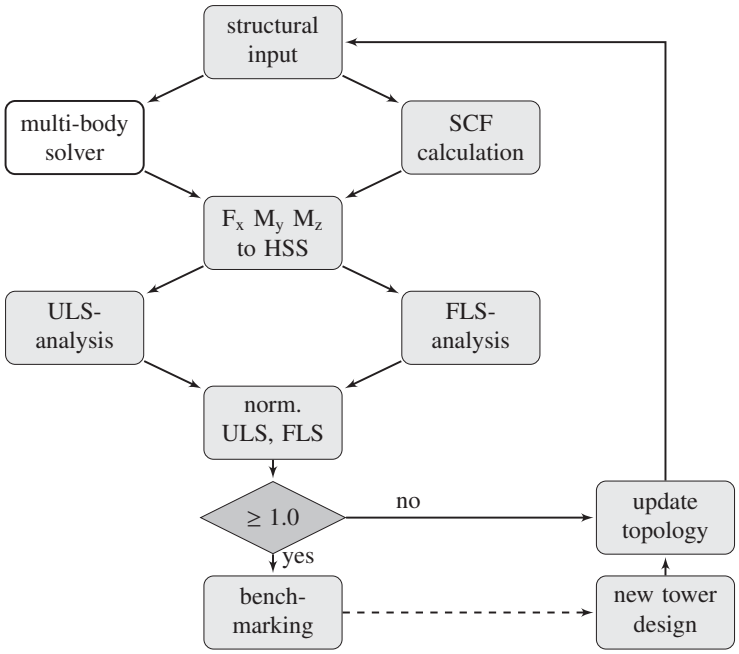

Fig. 2. Iterative optimization approach

The optimization from one iteration step to the next is based on the strategy of resizing members with lifetimes farthest away from the design lifetime. Lifetime was chosen as optimization criterion due to the fact that fatigue is one of the design drivers of support structures for offshore wind turbines [5]. During optimization, one or several members can be optimized in each iteration step at the same time. Members are resized according to their benchmark value (see Section 2.3.3) as whole numbers, from minimum 1mm to a maximum value within 10% of the benchmark result. A design is regarded as optimized when normalized lifetimes for all sections were found in an interval of 1.0 to 1.5. Limitations for the feasibility to find such designs are described in Section 4.2. As a starting point for this study, the presented optimization is based on the resizing of member thickness only, while member diameters were kept constant.

2.3.1. SCF and HSS calculation

The calculation of SCF and HSS is based on DNV-RP-C203, *Fatigue design of offshore steel structures* [6]. As shown in Figure 3, in total eight stresses are calculated at hot spots around the circumference at the

intersection of brace and leg members, as well as at brace to brace connections in X-joints. HSS at these points are derived by summation of single stress components from axial, in-plane and out-of-plane action.

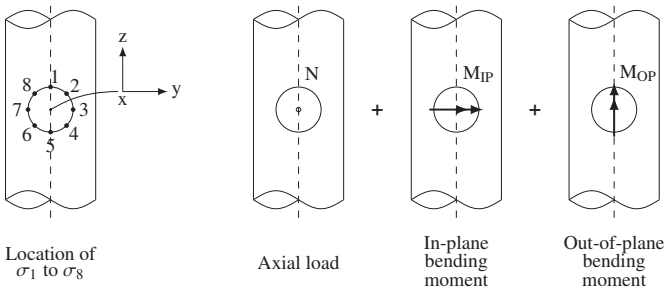

Fig. 3. Superposition of stresses for tubular joints (adapted from DNV-RP-C203 [6])

2.3.2. ULS and FLS analysis

In the ULS-analysis, extreme values for each HSS variation $\sigma_{1..8}$ are calculated. The minimum and maximum values of the time series characterize the ultimate load applied on the structure during simulation time. For the calculation of fatigue properties in the FLS-analysis, a rainflow counting process is performed [7], followed by a fatigue analysis based on the Palmgren-Miner approach [8]. Results from rainflow counting of each time series and HSS $\sigma_{1..8}$ are used to estimate the lifetime of the structure according to S-N curves for tubular joints in DNV-RP-C203.

2.3.3. Normalization and benchmarking of different tower designs

To be able to compare different tower designs in terms of their ULS- and FLS-performance as well as material weight, a normalization approach was proposed for benchmarking. Results from ULS-analysis are normalized by the yield strength for steel, while results from FLS-analysis are normalized by the requirement of 20 years lifetime [9]. These normalized values have to be ≥ 1.0 to characterize a stable design. As shown in Figure 2, values < 1.0 will require an update of the tower topology and a re-run of the simulation. These benchmark values can be regarded as additional safety factors.

3. Optimization results

3.1. Constant member dimensions over tower height

Due to simplicity in the design process, first studies of the full-height lattice tower concept were performed with constant member dimensions over tower height only [2]. The application of such a design is a rather unrealistic case due to heavily oversized members in several tower sections. However, this case also shows quite clearly where and in which order the highest potential for optimization can be found for the support structure, where both wind and wave loads are acting on different parts of the structure.

Figure 4(a) shows a typical distribution of minimum normalized HSS in each tower section over tower height for a design with constant member dimensions. For the ultimate limit state, the behavior of the main legs seems not to be dominated by wave loads, but suffers high loadings at the tower top from the transition between lattice tower and yaw mechanism. Brace members are affected by wave loading as seen in the fluctuation of the curves for K- and X-brace joints below and above sea water level (SWL). This has been checked by comparison with a simulation without wave loading. The lifetime of the braces is decreasing towards the tower top and bottom, and is higher in the middle part of the structure.

The lifetime distribution for the fatigue limit state shows a somehow different picture. It has to be noticed, that the scale of the x axis in Figure 4(a) (right) is logarithmic and so, a large optimization potential is offered by both leg and brace members. At the same time, the FLS profile shown here for a design with

Table 1. Details of the proposed 10MW NOWITECH reference turbine in this study

	Constant member dimensions	Optimized design
tower height [m]	158.70	158.70
leg/brace diameter [m]	1.6/0.8	1.6/0.8
leg/brace thickness [mm]	73/34	49..63/20..34
number of sections	15	15
tower weight [t]	3082	2283

constant member dimensions is optimized for the most critical section in terms of a lifetime close to, but above the required 20 years. While leg members show a large potential between water surface and the second last tower section below the yaw mechanism, brace members are significantly oversized in the lower half of the structure.

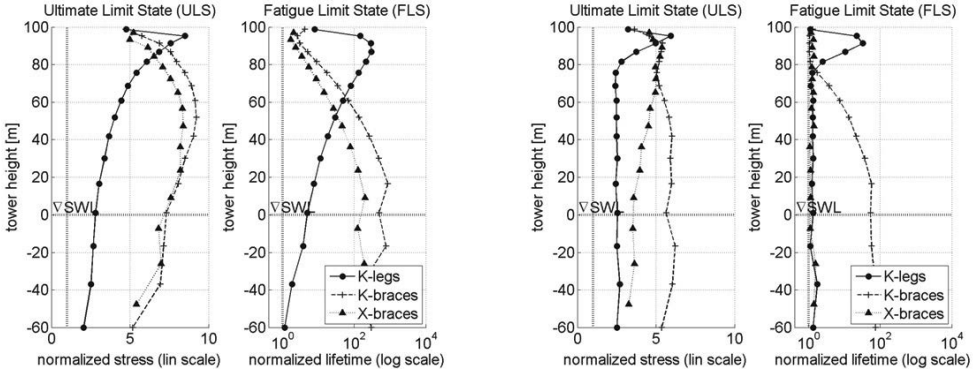

(a) constant member dimensions over tower height (b) optimized member dimensions according to loads

Fig. 4. Distribution of minimum normalized HSS and lifetime over tower height

3.2. Varying member dimensions over tower height

As expected, the possibility of introducing varying member dimensions over the tower height reduces total tower weight, while structural performance keeps ensured. Figure 4(b) shows an optimized distribution of normalized stress and lifetime over the tower height. It is interesting to see that leg-profiles are approximately the same in ULS and FLS, while those for braces are following a different trend. Since fatigue loading is the dominating design case, optimized profiles for legs and braces are close to the normalization value of 1.0 where applicable. The optimization shown in Figure 4 is based on varying member thickness, while keeping diameters constant. Figure 5(a) gives an overview over the thickness reduction during the optimization process from a constant design (straight line) to the optimized design (curved line).

4. Structural behavior of optimized designs

The responsivity of the design to changes in member dimensions (constant in each tower section) was studied with respect to fatigue lifetime estimates of joints. In addition to the fatigue properties, also ultimate loads were checked for each tower generated in the process. Based on the results presented in Section 3, ULS and FLS behaviors show different characteristics over the tower height and are discussed separately in the following. Another finding is the responsivity of the design to changes in tower parameters, which can help to narrow down the number of necessary simulation runs during the optimization needed in order to find a light-weight design fulfilling the stability and fatigue requirements.

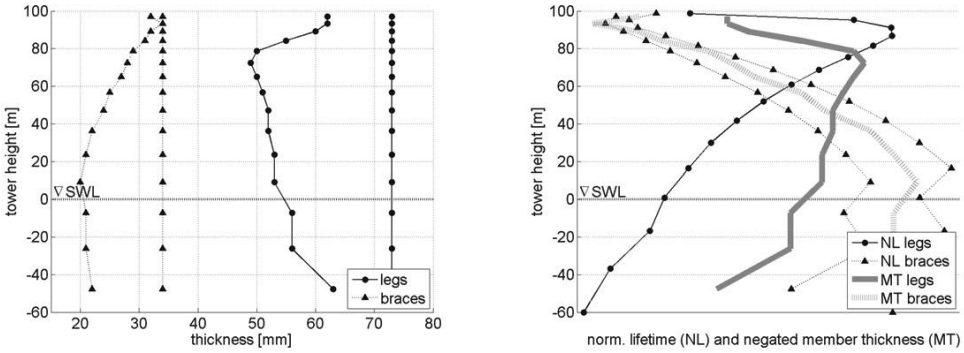

(a) thickness profiles over tower height with constant diameter (b) comparing lifetime and thickness profiles

Fig. 5. Member thickness profiles and their proposed use for the optimization approach (see Section 4.3.1)

4.1. ULS

For the ultimate limit state of a design with constant member dimensions, gravitational loads due to the weight of the structure and RNA are dominating the stress distribution in the legs. As shown in Figure 4(a), the normalized stress increases with the tower height until the tower top is reached. Close to the base for the yaw mechanism, thrust forces from the rotor are more dominating and lead to a reduction of total normalized stresses in the legs. The same behavior can be observed in the uppermost part for the optimized design with varying member dimensions. However, the lower part of the structure shows an equal stress distribution due to adapted member dimensions.

Effects of the optimization process on the ULS stress distribution of brace elements are smaller compared to leg elements. Comparing Figure 4(a) and 4(b), the optimized profile shows mainly an improvement in the middle part of the structure with reduced member thickness, where oversizing was reduced in X-joints.

4.2. FLS

The analysis of both constant and optimized designs confirmed that the fatigue lifetime is the design driver. By adjusting member dimensions to the minimum fatigue lifetime of 20 years, normalized values of the ultimate loads are still above 2.0. While the lifetime for brace connections in both K- and X-joints for a constant design follows a similar trend as in the ULS case, the optimized design gives the possibility to optimize the lifetime of X-joints over the whole tower height. However, due to the relation of legs and braces in K-joints, braces are oversized in these connections. The opposite behavior can be found at the tower top, where leg members are oversized to keep braces in K-joints above the required lifetime. The background for these dependencies lies in the basic design with constant brace member dimensions within the same section, which is explained further in the following section.

4.3. Responsivity to changes in tower characteristics

4.3.1. Member dimensions

Important relations for changes of member dimensions were observed. Members were changed section-wise with constant leg and brace dimension in each section. This leads to responsivities in the optimization process since legs and braces are physically connected in K-joints and the variation of one of these members results in a changed behavior for the connected member, too. Variations in member performance affecting neighboring members were mainly found to be a local phenomenon, however, global variations could be observed in some optimization steps and will be in the focus of further research. On the other hand, adjusting brace dimensions leads to changes in both K- and X-joints for brace elements. This limits the possibility to optimize leg and brace members for both K- and X-joints at the same time. By introducing stubs for the brace connections in K-joints, this relation can be broken and a deeper optimized design can be realized.

There is also the possibility to decouple the performance of K- and X-joints by use of cast nodes for X-joints. However, introducing stubs or cast nodes will at the same time increase the number of members and welds needed during fabrication of the structure.

An interesting correlation was found between the FLS result for a design with constant dimensions (Figure 4(a) to the right) and the thickness profile of an optimized design (Figure 5(a)). By mirroring the thickness profiles on a vertical axis, the curves for legs and braces respectively show significant similarity to the FLS profiles over the tower height. This observation is illustrated in Figure 5(b) and delivers a useful basis for the optimization approach. While the FLS profile for legs only gives an indication about the required optimization trend, the thickness profile for braces follows almost exactly the FLS profile over the tower height. By running a simulation with constant member dimensions first, the shape of the FLS profile result can be analysed and translated into required changes to the member thickness. The second attempt can so be further optimized in detail. Following this approach, the number of time-domain analyses necessary can be reduced.

4.3.2. Number of sections

Another design parameter for the tower topology is the number of sections, which defines how many X-braces are used over the tower height. This parameter has a significant influence on the behavior of the braces at, or close to the SWL, since it is changing their relative position to the waves. Naturally, the interest is to keep the number of sections small, since this will lead to a smaller number of members and a lighter tower structure. Figure 6(a) gives an overview over seven different tower designs with the number of sections varying from 12 to 18 (curves indicated in light grey to black).

The influence of this parameter on the legs is as expected small, both in ULS and FLS. For the braces, wave force interaction close to SWL can be observed in the ULS. Furthermore, trends in K- and X-joints show opposite behavior. While the K-joint performance for the braces is decreasing with increasing number of sections, values for the X-joints are increasing. This behavior can be explained by the fact that an increasing number of sections shares the applied load on several braces. However, variations in tower topology also lead to changes of the brace angles, and by this result in higher SCF for the K-joints.

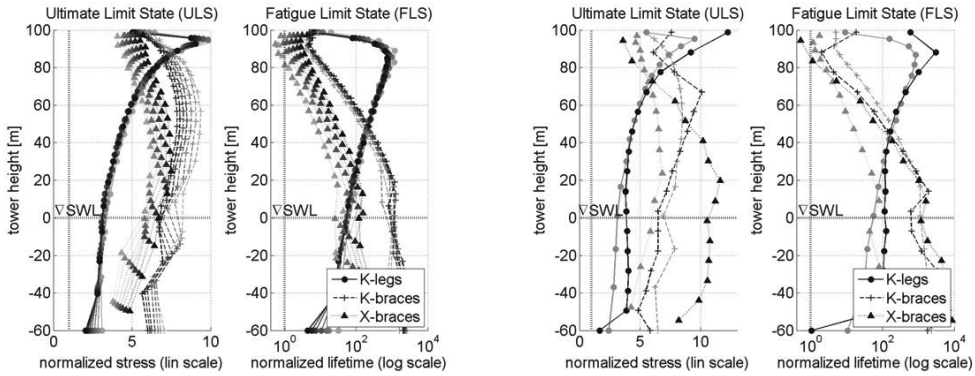

(a) varying number of sections (b) constant brace angle versus constant section height

Fig. 6. Responsivity of several towers to changes in section design

The responsivity to the number of sections in the FLS is mainly noticeable by changes of lifetime for X-joints. A reason for that can be found in a stiffer structure when the number of sections is increased, and so increased lifetime values due to less vibrations in the plane between the legs. K-joints are less affected by this variation and show only a slight improvement in lifetime for a larger number of sections.

4.3.3. Constant brace angle versus constant section height

As shown in Figure 6(b), the change of tower characteristics from constant brace angle (light grey) to constant section height (black) results in significant variations for the X-joints in both ULS and FLS. Due to the slender topology of the tower, section heights for a constant brace angle design are two times larger than those of a constant section height design at the bottom section, while they are only one third at the top section. These changes lead to the varying behavior of loads on X-joints for the two cases. At the same time, legs and braces in K-joints are not affected in the same order as the X-joints. It can be noticed that the ULS and FLS performance of braces in X-joints becomes larger for the constant section height design for most of the tower joints. However, at the tower top, where brace lengths are increasing for the constant section height design compared to the constant brace angle design, the latter delivers better performance.

Based on fabrication aspects of the structure, it is expected to be an advantage to select the constant brace angle design. This will avoid small angles between braces and legs, as they occur close to the tower top for a constant section height design. By keeping the same brace angle configuration at all K-joints, also prefabrication of geometrically similar joints will be a possibility.

5. Conclusion

Future investments in offshore wind turbine installations are highly based on the expectation that the price level for installations will decrease. Therefore, the analysis of several support structure types is an important step to be able to identify the potential in cost reduction by an optimized design. The presented full-height lattice tower is one possible design solution and should be further developed in this consideration.

Since several design parameters lead to significant changes in the tower topology of a full-height lattice tower and time-domain analyses are time consuming and expensive, an effective optimization approach is needed to be able to reduce the number of necessary simulation runs. An approach is presented in this paper, where results from the analysis of a design with constant member dimensions over tower height are analysed and translated into an expectation of the member dimension profile over tower height for an optimized design. This approach saves a significant number of iteration steps during optimization. Further detailed optimization of the design is achieved by changing member dimensions in one or several sections stepwise in each iteration step.

The paper presents a first stage of a complete analysis of the full-height lattice tower concept. Further work will focus on the improvement of the mentioned iterative optimization approach, the extension of several parameter studies and the assessment of suitability of the concept in future wind park installations. In addition, the concept has to be analysed and proven using more extensive load case simulations according to the standard [9].

References

[1] F. Cesari, T. Balestra, F. Taraborelli, Offshore wind turbine foundations in deep waters, in: J. Twidell and G. Gaudiosi (eds.): Offshore Wind Power, Multi-Science Publishing Co. Ltd, 2009.
[2] H. Long, G. Moe, Truss type support structures for offshore wind turbines, in: Proceedings of European Offshore Wind Conference and Exhibition (EOW 2007), Berlin, 2007.
[3] GIGAWIND Alpha Ventus, Ganzheitliches Dimensionierungskonzept für OWEA-Tragstrukturen anhand von Messungen im Offshore-Testfeld Alpha Ventus, Jahresbericht 2009, Leibniz Universität Hannover, Germany, 2010.
[4] L. Frøyd, O. G. Dahlhaug, A conceptual design method for parametric study of blades for offshore wind turbines, in: ASME 2011 30th International Conference on Ocean, Offshore and Arctic Engineering (OMAE2011), Rotterdam, 2011, pp. 609–618.
[5] W. de Vries, Support structure concepts for deep water sites, Project UpWind Final report WP 4.2, Delft University of Technology, The Netherlands, 2011.
[6] Det Norske Veritas, Fatigue design of offshore steel structures, Recommended Practice, DNV-RP-C203, 2008.
[7] C. Amzallag, J. P. Gerey, J. L. Robert, J. Bahuaud, Standardization of the rainflow counting method for fatigue analysis, International Journal of Fatigue 16 (1994) 287–293.
[8] M. A. Miner, Cumulative damage in fatigue, Journal of Applied Mechanics 12 (1945) A159.
[9] International Electrotechnical Commission, Wind turbines - Part 3: Design requirements for offshore wind turbines, International Standard, IEC 61400-3, 2009.

Paper 5

Two-stage local optimization of lattice type support structures for offshore wind turbines

Zwick D, Muskulus M
Submitted to *Ocean Engineering* 2014

Two-stage local optimization of lattice type support structures for offshore wind turbines

D. Zwick[a,*], M. Muskulus[a]

[a] *Department of Civil and Transport Engineering, Norwegian University of Science and Technology (NTNU), Høgskoleringen 7A, 7491 Trondheim, Norway*

Abstract

Offshore wind turbines are exposed to stochastic dynamic loading that includes non-linear aerodynamic effects. Hence, demanding time domain simulations are needed for the detailed design of support structures. Evaluation and optimization were separated into two stages, resulting in a saving of analysis time of roughly 70 percent compared to a conventional approach. The optimization was based on the principle of decomposition. This was found to be very efficient, resulting in a nearly full utilization of fatigue resistance. Fatigue damage was the design driver in this analysis, while ultimate and buckling performance were controlled within the given constraints.

Keywords: offshore wind turbines, structural optimization, decomposition, time domain analysis, numerical modeling

1. Introduction

Harvesting renewable energy by offshore wind turbines is expected to be an important energy source in the future (Hau, 2013). To be able to get a break through of this type of technology, the cost per kilowatt hour has to be reduced (Davey and Nimmo, 2012). One aspect of cost reduction is presented here: the quick sizing process of a lattice type offshore wind turbine support structure using numerical simulations, leading to an optimized design with efficient utilization of the members.

Structural optimization has been used in automotive and aerospace industry for a long time, but to a lesser extent in the wind industry (Muskulus and Schafhirt, 2014). Most existing optimization approaches have been developed for static loading, wheres the structural analysis of wind turbines is more challenging due to a highly dynamic load picture. Figure 1 illustrates the characteristics of the input loading acting on an offshore wind turbine. Due to the stochastic

*Corresponding author, phone +47 994 94 853, fax +47 735 97 021

Email addresses: daniel.zwick@ntnu.no (D. Zwick), michael.muskulus@ntnu.no (M. Muskulus)

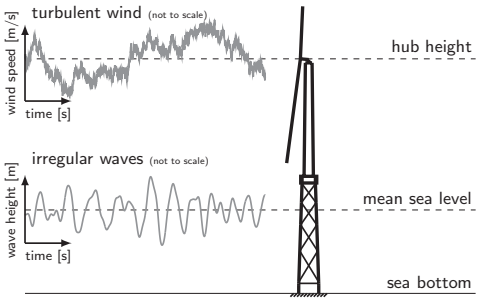

Figure 1: Offshore wind turbine model with representation of input loading time series.

nature of turbulent wind and irregular wave loading (Naess and Moan, 2013), analytic solutions of the equations of motion are impracticable. Loads with various characteristics are acting on different parts of the structure, leading to excitations of the coupled system. As the wind turbine is exposed to the wind, resulting in a rotational movement of the rotor, the structure experiences additional loading frequencies. The rotor rotation is furthermore regulated by a control system, preventing damage from the structure for wind speeds above rated speed (normally around 12m/s). Summing up, an offshore wind turbine is a highly dynamic, elastic and coupled system, subject to stochastic loading and control mechanisms. This results in the need of fully coupled time domain analyses, which require time consuming simulations compared to static load investigations. For optimization approaches, which normally require several iterations to obtain an optimized design, this is an undesirable situation. Efficient optimization approaches for the time domain are needed. Some examples for such an application can be found in the literature, using finite-difference gradients (Ashuri, 2012), a genetic algorithm (Pasamontes et al., 2014) or a simultaneous perturbation algorithm (Molde et al., 2014). These methods vary significantly in the number of iterations needed, as well as the total computation time. Due to practical limitations with time domain analyses, significant simplifications in the load case assessment are normally performed for these methods.

In an effort to reduce the computational cost for detailed analyses, an efficient optimization approach using the principle of decomposition described by Freeman and Newell (1971) and Chandrasekaran (1990) is proposed and evaluated here. The method is based on the idea of a decomposition of the structure into weakly coupled substructures. Thereby, each member of the complete structure is optimized locally and simultaneously, assuming that other members of the structure are not affected by a change of member dimensions (Haftka and Gürdal, 1991). This local optimization approach has been applied for the sizing of a full-height lattice tower in an iterative process earlier, but under the simplification of analyzing one power production load case only (Zwick et al., 2012; Muskulus et al., 2013). The method of decomposition in the local optimization

approach was now investigated in more detail and for a set of load cases that represent realistic load conditions for both ultimate and fatigue load analysis. Additionally, the method was now applied in a two-stage approach. Evaluation runs were performed by the external finite element solver Fedem Windpower (Fedem Technology AS, Trondheim, Norway, Version R7.1 beta3) in a first stage. Fedem Windpower is a multi-body solver for complex mechanical assemblies exposed to various loading and includes the functionality to calculate aerodynamic and hydrodynamic loads on the structure, as well as the capability to model a control system. Motivated by the intention of reducing the total computational effort needed for the structural optimization, the structural sizing process was performed internally in a second stage.

In this study, we present an analysis of the accuracy and validity of the proposed method for a representative set of load cases. It was found that the application of a two-stage local optimization is favorable and enables a quick evaluation and sizing of an initial design. By using the principle of decomposition, the sizing method leads to an efficient utilization of the structural members in terms of fatigue damage, which was indicated to be the design driver in this analysis.

2. Methodology

2.1. Simulation model

2.1.1. Wind turbine structure

The structural model used for the application of the local optimization is based on the OC4 reference jacket (Vorpahl et al., 2011). It is a four-legged lattice tower structure, consisting of four bays with X-brace side planes connecting the legs (Fig. 1). The connection to the tubular tower was modeled as a rigid transition piece made out of concrete. Placed on top of the tubular tower, the NREL 5MW baseline turbine defined by Jonkman et al. (2009) extracts energy from the wind. The model has been used and verified in earlier studies by Popko et al. (2014) and Zwick and Muskulus (2014a).

Differing from the jacket definition by Vorpahl et al. (2011), the lattice structure was modeled with more features in this study. K- and X-joints (Fig. 2) were improved in detail by the introduction of chords and stubs. This technique is often used in offshore industry (Standards Norway, 2004) and enables a more efficient design that takes account of concentrated stresses in tubular joints. For K-joints, chords are oriented in leg direction, while stubs are oriented in brace direction. For X-joints, two aligned members of the connected braces were treated as chord, while the connected members from the two other brace directions were treated as stubs. As a slight simplification, X-joint chords and stubs had the same structural properties in this study and are further referred to as X-joint stubs only.

During optimization, cross sectional properties of all members were modified, while the topology remained the same as for the OC4 reference jacket. The structural properties of the jacket are described by five different cross section

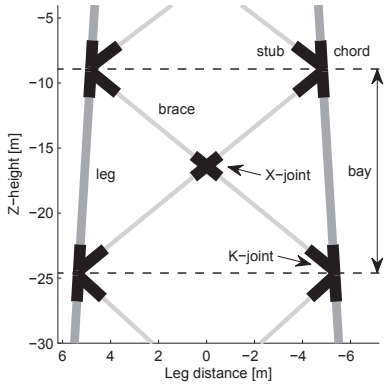

Figure 2: Section of the jacket structure with details as chords and stubs at K- and X-joints (proportions of legs, braces, chords and stubs not to scale).

Table 1: Cross section types of the jacket support structure, including total number of categories and beam elements.

Cross section type	Categories	Beam elements
Legs	4	16
Braces	8	64
K-joint chords on legs	5	64
K-joint stubs on braces	8	64
X-joint stubs	12	64
Total	37	272

types (Tab. 1). Each type has several categories based on the number of in total 4 bays of the jacket structure, e.g., cross sections are independent from bay to bay (except K-joint chords on legs connecting two bays) and from lower to upper stubs and braces within the same bay. Each category again has several beam elements assigned due to the symmetric layout of the structure, e.g., all side planes are identical.

2.1.2. Environmental loads

For the representation of a realistic load picture, three design load cases (DLC) from IEC 61400-3 (International Electrotechnical Commission, 2009) were chosen: power production (1.2), emergency shut down (5.1) and parked under extreme conditions (6.1). Beyond those, the complete assessment of DLC 1.2 is a comprehensive task (Vorpahl et al., 2013). Though, a simplified fatigue load assessment was used to cover the contribution to fatigue damage from all wind speeds in the range of cut-in (3m/s) to cut-off (25m/s) wind speed (Zwick

Table 2: Representation of environmental loads taken from the Upwind design basis documented by Fischer et al. (2011) (V_m-mean wind speed; TI-turbulence intensity; H_s-significant wave height; T_p-wave period; γ-dimensionless peak enhancement factor; F-fatigue strength; U-ultimate strength)

DLC	V_m [m]	TI [%]	H_s [m]	T_p [s]	γ [-]	Type	Description
1.2	9	15.6	1.395	5.705	1.0	F	Power production
	14	14.2	1.910	6.070	1.0	F	Power production
	19	13.5	2.615	6.850	1.0	F	Power production
5.1	14	14.2	1.910	6.070	1.0	U	Emergency shut down
6.1	42	12.0	9.400	10.870	3.3	U	Parked under extreme conditions

and Muskulus, 2014b). This approach is based on a statistical model and reduces the number of necessary power production load cases to be simulated from 21 to 3. Summing up, in total five load cases were defined and simulated, listed in Table 2.

For the simulated load cases from DLC 5.1 and 6.1, the control system of the turbine was overwritten by pitching the blades out of the wind. For DLC 5.1, the emergency shut down was performed after the turbine reached a steady state of power production.

2.2. Evaluation of structural performance

The structural response to wind and wave loading for each member was extracted as axial force and in-plane and out-of-plane bending moment from the finite element solver in each time step. Time series were converted to nominal stresses by use of cross sectional area and moment of inertia. Resulting stress time series were further processed by the superposition of stresses in tubular joints, including the impact of stress concentration factors (SCF) (Det Norske Veritas AS, 2012). The superposition of nominal and bending stresses leads to eight hot spot stresses (HSS) in each welded connection of a chord to a stub member in a tubular joint. All calculated stress time series were investigated by ultimate and fatigue limit state analyses as well as a buckling check, as described in the following.

2.2.1. Ultimate limit state

As indicated in Table 2, DLC 5.1 and 6.1 were taken as a basis for the ultimate limit state (ULS) analysis. The time series was analyzed in terms of maximum absolute stress and was evaluated to the yield strength of structural steel of 250MPa. ULS results were normalized to the yield strength, e.g., a value smaller 1 indicates that stresses are below the critical value of the yield stress, while values larger 1 indicate an ultimate failure of the structure by yielding.

2.2.2. Fatigue limit state

The structural performance in the fatigue limit state (FLS) was determined based on load cases in the design situation of power production. Time series of the HSS were processed by a rainflow counting algorithm (Amzallag et al., 1994). Extracted stress cycles and amplitudes were evaluated by standard S-N-curves (Det Norske Veritas AS, 2012), using the damage summation rule by Palmgren (1924) and Miner (1945). The resulting damage was scaled to a lifetime of 20 years and, according to the ULS normalization, takes values for categories below and above 1. Smaller than 1 indicates a not fully utilized fatigue life of the member, while a value larger than 1 indicates a fatigue failure.

2.2.3. Buckling

The loading of long and slender members in lattice structures might, due to insufficient stability, result in a buckling failure of the structure (Bleich, 1952). Therefore a buckling safety factor (BSF) was calculated for each structural design to avoid sizing of members with critical dimensions in terms of buckling. The buckling safety check was performed on a general basis using the formula derived by Euler (Domokos and Holmes, 1993). Maximum axial forces found by the finite element simulation of all load cases were considered and normalized by the critical force calculated by the Euler-formula, using the structural properties of the actual member. For buckling, safety factors larger than 1 indicate a survival of the structure, while a value smaller than 1 indicates a buckling failure of a member.

2.3. Local optimization approach

2.3.1. Decomposition and two-staged strategy

The complex pattern of the lattice tower structure results in dependencies between members as observed by Zwick et al. (2012). This challenge is partly addressed by the modeling of chords and stubs for tubular joints. In addition, decomposition was applied here to be able to quickly size structural members for an optimum performance of the jacket structure. The strategy of the approach is based on two central assumptions:

- When changing dimensional properties, such as diameter and/or thickness of a member, it is assumed that sectional response forces and moments remain constant. This assumption is made for both the actual changed member and for all other members of the structure. Additionally, this is assumed to be valid for a simultaneous change of all members all over the structure.
- It is also assumed that SCFs remain constant under the change of dimensional properties.

Obviously, both assumptions are ambitious and can only be approximately fulfilled, as basic structural equations show that both dynamic responses and SCFs are directly influenced by the dimensional properties of the members.

However, our work shows that assumptions such as these can be useful in optimization approaches. The principle of decomposition was applied in a two-stage analysis:

Stage 1) **External finite element solver:** the structural model was built in Fedem Windpower and analyzed in a time domain simulation. Structural responses to wind and wave loads are calculated in each time step of Δt=0.025s, and this analysis is rather time consuming. Simulation runs with a total length of 690s were performed, whereof the first 90s were cut off to remove transient effects. In terms of variability issues of the input loading as shown by Zwick and Muskulus (2014a), one wind and one wave seed were applied only.

Stage 2) **Internal sizing:** after the response loads of the structure were extracted from the time domain simulation results, the sizing of the structural members was performed with in-house code using MATLAB scripts (The Mathworks, Natick, Massachusetts, Inc., Ver. R2013b and R2014a). Each sizing step is based on time series results from the last time domain finite element simulation that was performed in the first stage. The above assumptions make it possible to perform the sizing internally in stage 2) without the need to run the external finite element solver for each newly established design. All in all, the internal sizing is a very fast process and requires only small computational resources compared to stage 1) with the finite element solver.

The flowchart in Figure 3 gives an overview of the optimization approach, indicating an iterative structure. The smallest number of iterations can be achieved by using an initial design in step 1, resizing the structure by the internal sizing process in step 2 and controlling the achieved structure by a new run with the finite element solver in step 3. Normally, the first control run after sizing will lead to slightly different results than expected, resulting in a new sizing process with a subsequent control run. This process might be continued several times before a valid and optimized design is achieved. It has to be mentioned that the flowchart allows for an initial design to pass the optimization directly without internal sizing, as long as the constraints of ULS, FLS and BSF are all fulfilled in the first step. However, this scenario is very unlikely as the initial design was chosen to have constant cross sectional parameters over all bays, which normally will require some resizing.

2.3.2. Objective function

Based on the main goal of cost reduction, the material utilization and steel weight of the structure are the central parameters of the objective function. Constraints are the ULS and FLS as well as the BSF indices. The optimization approach searches in each step for a lighter design that still fulfills the constraints. However, weight increases can occur to increase ultimate and/or fatigue performance. To improve material utilization, both upper and lower constraints were applied.

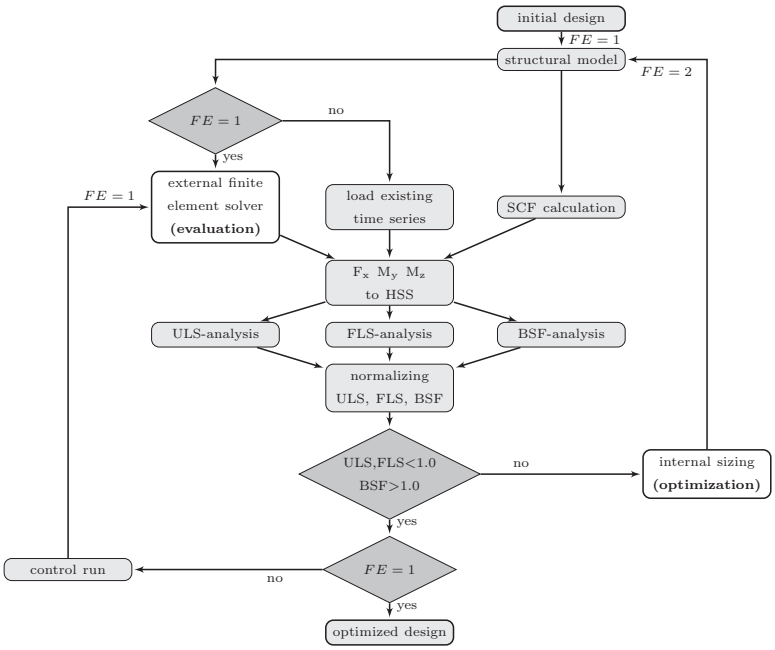

Figure 3: Flowchart of the iterative optimization approach (adapted from Zwick et al. (2012)). The parameter FE is a state description of the two-staged approach, e.g., $FE = 1$ leads to stage 1), the external finite element solver run; $FE = 2$ results from stage 2), the internal sizing, and leads to the loading of an existing times series.

2.3.3. Selection of cross sectional properties

Design parameters are the diameter (D) and thickness (T) of each cross section type and category (in total 2x37=74 parameters, see Tab. 1). For the selection of D and T of a member, several constraints are used: minimum (D=400mm, T=20mm) and maximum (D=1600mm, T=60mm) values are defined as fixed constraints; the SCF-parameter γ ($=D/(2T)$) sets an upper and lower limit; and dynamic constraints by the SCF-validity occur as for example a stub member cannot have a larger diameter or thickness as the chord member has (due to the validity of SCF-parameters α and β).

For the selection of the initial design, two start areas were defined (Fig. 4): for legs around D=1200mm and T=50mm; for braces around D=800mm and T=30mm (indicated by parameter ranges in the figure). The initial design contained also similar values for all bays over the tower height. All combinations out of these start values lead to valid SCF-parameters. Figure 4 shows in addition several dimension-specific characteristics as contour plot, which are of importance when sizing the structure internally. First, the cross sectional area,

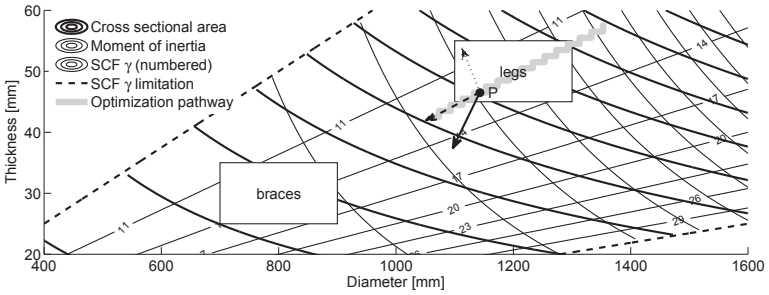

Figure 4: Diameter and thickness selection with initial ranges for leg and brace components. The optimization pathway is given as an example for possible dimensions selected for a new parameter set P' based on a FLS-result in the range of 0.01 to 3.00.

influencing the scaling of axial force to nominal stress. Secondly, the moment of inertia, scaling the in-plane and out-of-plane bending moments to bending stresses. Thirdly, the SCF-parameter γ in the validity range of 8 to 32. As an example for the parameter selection, point P is chosen as a leg property. Several interests have to be taken into account when selecting a new parameter set P': weight reduction can be achieved by following the gradient of the cross sectional area (solid arrow); stiffness reduction can be achieved by following the gradient of both cross sectional area (solid arrow) and moment of inertia (dashed arrow); reduction of SCFs can be achieved by following the gradient of the SCF γ curve (dotted arrow).

Ideally, one would chose a new D and T in a way which reduces weight, while at the same time increasing stiffness and reducing SCF γ. This is obviously not possible, i.e., the selection of new dimensions is a compromise in terms of fulfilling the goal of a lighter structure, by at the same time maintaining the required stiffness and fatigue performance. Based on experience with the local optimization approach, the optimization pathway was chosen in the direction of the gradient for the moment of inertia. By this, a weight and stiffness reduction can be achieved without an increase of the SCF parameter γ.

The implementation of the optimization pathway (Fig. 4) for the D and T selection of a new design was done by a linear scaling according to the FLS result of the previous simulation or sizing step, subtracted by a target value of 0.85. The intention of the target value is to guide the FLS result towards the threshold value of 1.00, without exceeding it after a sizing step (which is based on an approximate analysis making use of the above assumptions). For FLS results smaller than the target value, D and T were decreased; for larger FLS results, dimensions were increased. The step-wise behavior in Figure 5 can be explained by the fact that integer numbers in the unit of millimeters have to be defined for a de- or increase. This leads also to the situation that a diameter change might come along with no thickness change when the FLS result is between 0.75 and 0.95.

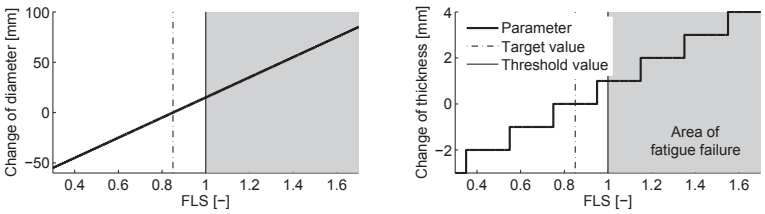

Figure 5: Choice of diameter and thickness change dependent on FLS result. The shaded area indicates FLS values which lead to a fatigue failure, e.g., the optimization drives results under the threshold value towards the target value.

2.4. Scope of analysis

Results presented in Section 3 are based on a number of in total 7 selected optimization runs, whereas each optimization run contains of five iterations. For the different optimization runs, random initial designs within the defined parameter ranges in Figure 4 were chosen. Ultimate and fatigue results are presented with their maximum value over all categories, while buckling results are presented in terms of the minimum safety factor achieved over the whole structure. The analysis was focused on the optimization progress, with special concern on the sizing process, both in terms of accuracy and cost, as a central functionality of the two-stage local optimization approach. As an important characteristic in structural design, the resulting eigenfrequency of the structure was investigated for various designs.

3. Results

3.1. Optimization progress

It is of main interest if the main idea of this study, changing all members at all locations at the same time, combined with an approximate analysis, leads to useful results. Figure 6 gives an overview over the progress of all central results in the optimization. While the structural weight is increasing for an increasing number of iterations, maximum results for FLS of all cross section categories are forced to get under the threshold of 1.0. At the same time, constraints for ULS and BSF have to be maintained. Results are given for a number of data samples, having their starting point randomly chosen within the defined parameter range for diameter and thickness. In addition, the arithmetic mean is drawn, showing the general progress of the optimization.

Central results show their largest change from iteration number 1 to 2, and converge for several iterations. All initial designs start out with too large fatigue damage as indicated by the first iteration. In fact, the fatigue damage is driving the optimization process, leading to an overall valid design after five iterations. The improvement of the structure in terms of fatigue performance leads to an increase of total structural weight, as well as buckling performance. The ULS

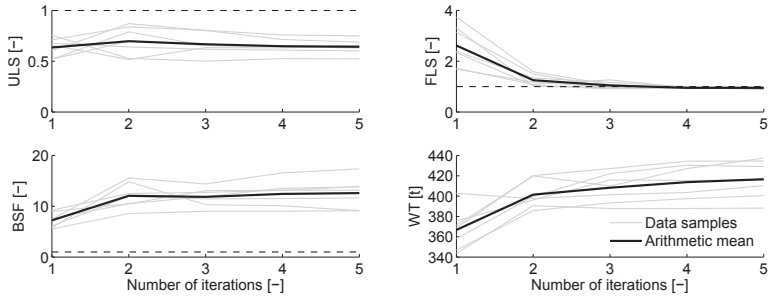

Figure 6: Optimization progress for ULS, FLS, BSF and total structural weight (WT). Data samples are presented for different, independently started optimization runs.

performance keeps more or less stable for the number of iterations performed. Overall, the simultaneous sizing process of all members shows a good progress with fast convergence. A significant fatigue damage reduction can be achieved already after two iterations. The fact that the structural weight is increasing, and not decreasing as one would assume in the sense of 'optimization', is simply related to the chosen initial designs which are obviously too weak for the applied loading. The optimization progress also shows the challenge of a large number of design parameters chosen here (different beam cross sections for several beam type categories and bays). While constraints are fulfilled after five iterations, and especially the FLS plot shows a good utilization of fatigue performance for all designs, the resulting weight for structures with different starting points varies between 390 and 440 tons. One of the reasons for this are the limitations given by the validity of several SCF-parameters which are defined in the standard. This matter is explained in more detail in Section 3.3.1.

3.2. Sizing process

3.2.1. Accuracy

The success of the strategy of the two-staged analysis is directly dependent on the accuracy which can be achieved during the internal sizing process (Fig. 7). The deviation of predicted (while sizing) versus achieved (time-domain simulation) results is normalized to simulated results, e.g., a positive deviation indicates that the result after the sizing process was expected to be smaller than what was actually found by simulation. In other words, a positive deviation is a conservative result of the sizing process for the BSF (solutions to be found >1.0), while a negative deviation is conservative for ULS and FLS performance (solutions to be found <1.0).

The overall picture confirms the expectation, that a large number of scatter points is found around the origin, where only small deviations come along with small weight changes. Though, three interesting observations can be made: first, ULS results are found on both the positive and negative side, indepen-

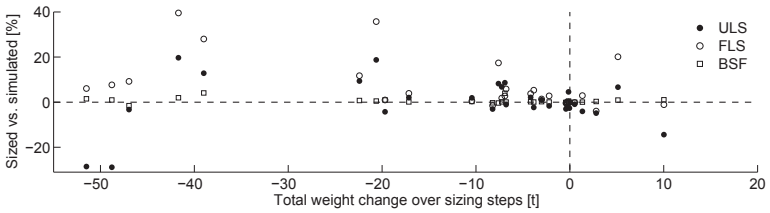

Figure 7: Accuracy of sizing process for the total weight change summed up over all sizing steps in between two iterations.

dent of the size of the weight change; secondly, FLS results are mostly found on the positive side, i.e. non-conservative; thirdly, buckling results can be predicted with high accuracy of maximum ±4% deviation even for large weight changes. This investigation shows an important characteristic of the sizing process during local optimization: the sizing influences the investigated structural performances as ULS, FLS and BSF differently. This fact is useful information for the adjustment of optimization parameters of the process.

3.2.2. Number of sizing steps

The weight change achieved during the sizing process is developed over a number of several sizing steps. Structural dimensions are changed step-wise towards the design constraints, while step quantities are dependent on the FLS result. Interestingly, large weight savings can be achieved by a small number of sizing steps (not shown). For weight changes of up to 50 tons during the sizing process, less than 10 sizing steps are sufficient (with one exception of a data sample of 33 steps). In average, 8 sizing steps are performed between each optimization iteration. Several occurrences are also observed close to the origin, where a few sizing steps lead to small weight changes only. This is often the case for a design which is close to the optimum, but still needs some adjustments to fulfill the constraints.

3.2.3. Computation time

One single finite element solver process was estimated to take about 38.5 minutes in average, while a single sizing step was calculated to take only 5.5 minutes. The external solver process contained 5 design load cases simulated in parallel, while the internal sizing for all load cases was performed in series. The comparison of a conventional approach and the two-staged approach is listed in Table 3. A conventional approach needs to run the solver in the beginning for a first evaluation of the design. Further on in the optimization, each resizing of the structure will be followed by a solver run (listed under *sizing time* in Table 3). The two-staged approach makes use of the proposed internal sizing process, resulting in a significantly reduced computation time. However, the finite element solver has to be run in each iteration before a new sizing process can be started. In total, the influence of the sizing process is crucial, showing

Table 3: Comparison of computation time in minutes needed for an optimization with a conventional approach versus the two-staged approach. The example is given for an optimization with 5 iterations, and 8 sizing steps in each of the 4 sizing processes between the solver runs. The cost of simultaneous processes on several cores in parallel is not taken into account.

Approach	Evaluation time	Sizing time	Total time	Saving
Conventional	1x38.5= 38.5	4*8*38.5=1232	1270.5	-
Two-staged	5x38.5=192.5	4*8* 5.5= 176	368.5	71%

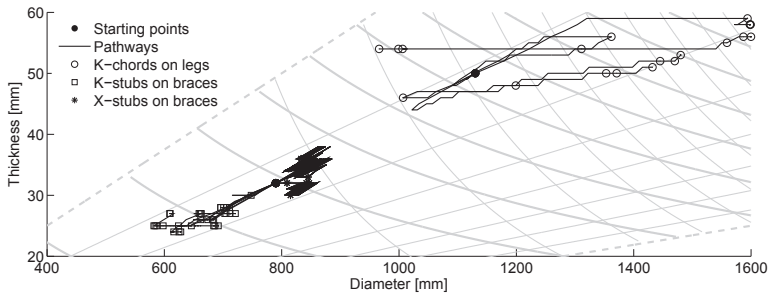

Figure 8: Selection of diameter and thickness samples during the sizing process. As a reference, curves for the cross sectional area, the moment of inertia and SCF γ parameters are indicated by the gray curves (see Fig. 4 for more details).

the large advantage of the two-staged approach compared to the conventional approach in terms of computation time.

3.3. Structural development

3.3.1. Parameter selection

The selection of member dimensions for new designs is the central tool to optimize the structure. The process is influenced by the intended direction indicated in Figure 4 and the step size shown in Figure 5. An example of the structural development for an initial design is given in Figure 8. While large sizing steps are changing both diameter and thickness, small sizing steps end up with a change in diameter only. However, limitations as maximum diameter or thickness may occur, as indicated by the development of the K-chords on legs in the figure. Scatter points are shown for the number of iterations only, not each single sizing step. Though, differing optimization directions compared to the intended optimization pathway (Fig. 4) may occur when the sizing is developing with several small steps over the complete sizing process. The stochastic behavior of the starting point leads to different pathways of the process for various initial designs, resulting in differently optimized structures (not shown).

The development of dimensional properties over the tower height was investigated, too (Fig. 9, left and middle). Both K-chords on legs and X-stubs

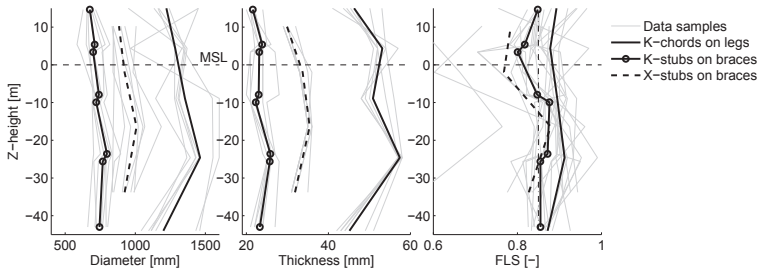

Figure 9: Diameter, thickness and fatigue damage for several members over the tower height. Data samples are given for all optimized designs.

on braces have their largest dimensions at the intersection of bay 1 and 2, or in bay 2, respectively. K-stubs on braces show small variations over the tower height. Changes are within the bays, e.g. from lower to upper member, while neighboring bays are optimized more or less to the same value. The influence of wave loads in the splash zone is slightly visible for K-chords. Diameter and thickness are increased for most of the designs at the intersection of bay 3 to 4 directly above the mean sea level (MSL). Figure 9 also shows the range of parameters taken by different cross section categories. For diameters, a large variation can be found due to the parameter range provided for the initial design as well as large step sizes dependent on the FLS result. This large range can cause restrictions for the optimization progress when diameters of chords on legs and stubs on braces are getting close to each other. Due to the validity of SCF-parameters, chords cannot be smaller than stubs, both in diameter and thickness.

Results for the fatigue damage, as an indication of efficient member utilization, are given in Figure 9 (right). It can clearly be seen that most of the designs at most locations over the tower height are approaching the target value of FLS=0.85 (23.5 years lifetime). At the same time, the offset to the threshold value of FLS=1.00 (20.0 years lifetime) is reasonable, as some results are found close to this limitation. Especially K-chords on legs are optimized to a value between the target and threshold value, probably due to the non-conservative sizing process for the FLS calculation. In general, material utilization in terms of fatigue achieved by the local optimization approach is found to be very good over the tower height. In fact, about 87% of all members are optimized to a lifetime between 20 and 25 years (FLS=0.8..1.0).

3.3.2. Eigenfrequency analysis

Caused by the adjustment of structural dimensions, the eigenfrequency of the support structure is changing as well over the number of iterations. The common intention of a soft-stiff tower design for wind turbines requires that the 1st global eigenfrequency of the structure should lie between the potential resonance ranges

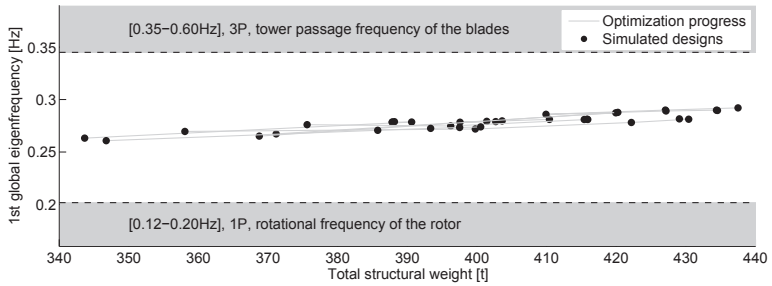

Figure 10: 1st global fore-aft eigenfrequency of all simulated designs, also showing the optimization progress for the change of structural weight.

of the rotational frequency of the rotor (1P) and the tower passage frequency of the blades (3P) (Hau, 2013). Figure 10 proves that all designs simulated during the optimization process are fulfilling this requirement. Critical excitation of the structure by lower rotational frequencies can be avoided. As expected, there seems to be a linear dependency of structural weight to 1st global eigenfrequency for the chosen designs.

4. Discussion

The two-staged local optimization approach presented here has its main objective in reducing computation time compared to a conventional full finite element analysis after each sizing step. A reduction of computational costs by about 70% could be achieved for a similar number of iteration and sizing steps. It has to be noted that a pure conventional optimization might need a smaller number of iterations as the sizing and directly following solver steps do not assess and utilize accuracy tolerances. However, a significant reduction in computation time is not expected in such a case.

For the two-staged approach, predicted results during the sizing process were in most cases found to be in the range of $\pm 20\%$ compared to a subsequent solver run. By this, large structural changes can be obtained with reasonable accuracy for low computational costs. Interestingly, the accuracy of the sizing process has different influences on several structural properties, such as ultimate and fatigue performance, as well as the BSF. The optimization process makes use of this information, focusing for example on critical values for FLS by setting the threshold value with an offset to the target value. As fatigue results are predicted non-conservatively in the sizing process, the offset increases the probability of approaching valid results after the solver run (ref. Fig. 9, right). The achieved accuracy of the sizing process can also be put into context to the simulation error caused by the variability of input loading. In the presented analysis, only one 10 minutes simulation with one wind seed and one wave seed was used. As shown by Zwick and Muskulus (2014a), a simulation error of the damage

equivalent load by up to 22% might occur for these conditions. In the worst case, this could cause a simulation error of the fatigue damage by up to 45% reduced lifetime. Compared to this observation, the achieved accuracy during the sizing process can be regarded as a reasonable approximation.

The level of optimization of a design can be evaluated by its used capacity under different load conditions. The local optimization is aiming for a full utilization of fatigue resistance, which was identified as a design driver in this study. Ultimate loading and BSFs could be maintained below and above the required constraints, respectively, and are not fully utilized. This is also the case for some locations where constraints prevent the optimization of proceeding towards a full utilization of the member. Results obtained by the optimization process after five iterations show that nearly full fatigue utilization can be achieved with various structural configurations. The principle of decomposition was applied successfully. In terms of fatigue utilization, the global solution is provided by several designs. In terms of weight, the lightest structure can be chosen among several optimized designs. The selection of diameter and thickness values for a new design in the internal sizing process was based on the general assumption that increased cross sectional properties reduce the fatigue damage of the member. However, in special cases, this might not be valid, e.g., when stress concentrations can be reduced by the use of less material. The success of the optimization depends also on the optimization pathway, e.g., the dimensional change scaled by the FLS-result in each sizing step. We adapted linear scaling in this analysis, while exponential or other scaling techniques were left out for further studies.

Selected member dimensions and the resulting topology with varying diameter and thickness values over the tower height show the adaptation of the structure to load conditions in the splash zone as well as under water. When comparing the shape of diameter and thickness curves over the tower height (ref. Fig. 9, left and middle) with results obtained during the iterative optimization approach by Zwick et al. (2012), a good agreement can be seen for corresponding tower heights, except for the lowest K-joint close to sea bottom. This deviation might result from different modeling approaches of soil pile model and clamped conditions at sea bottom, respectively. Variations from sea bottom to slightly above the water surface, where the transition piece is placed for the jacket design, are small in both studies. For the full-height lattice tower, larger variations are found close to the tower top and turbine nacelle, while the tubular tower for the jacket design in the present work was neither analyzed nor optimized. Comparing the two studies of local and iterative optimization in terms of material utilization, the implementation of chords and stubs in tubular joints solved restrictions on the simultaneous optimization of K- and X-joints, which were experienced under the analysis of the full-height lattice tower.

The proposed optimization method can in the same way be applied to other offshore wind turbine support structures, as for example tripods, tripiles or monopiles. These concepts represent a lower level of complexity, and by this reduced dependencies of one member to an other. It is expected that the local optimization of such structures will lead to an overall high level of material

utilization.

5. Conclusion

The further roll-out of offshore wind turbine installations in the future is closely related to the cost development. Large offshore wind parks can only be realized by the application of economic structures, among others in terms of design, material use and costs for operation and maintenance. The presented work on a two-staged local optimization approach of support structures is an attempt to address challenges in the design phase of such steel structures. Due to the complexity of the whole offshore wind turbine system and the stochastic loads applied, efficient simulation techniques are needed to be able to perform detailed numerical structural analyses in time domain. The success of the applied optimization approach can be stated as following:

- **Decomposition:**
  The assumption made that other structural members are not affected by a change of dimensional properties of a neighboring, or remote member was shown to lead to reasonable results. For a representative set of load cases, material utilization in terms of fatigue damage could be optimized to a large extent over the whole structure in all types of tubular joints.
- **Two-staged strategy:**
  The main goal of the separation of evaluation (by the external finite element solver) and optimization (by the internal sizing) was the reduction of total computation time. Roughly, a saving of about 70% could be achieved, by maintaining an accuracy of the sizing process of $\pm 20\%$.

As an interesting fact of the internal sizing process, it was found that the sizing by the local optimization approach influences structural results differently. While ultimate loads were predicted with both positive and negative deviation, a clear observation was made for the accuracy of fatigue damage prediction. FLS results were found to be estimated non-conservatively by the internal sizing process. The implementation of this result in the optimization approach by for example using a target value with an offset to the threshold value is favorable.

It was also indicated that the adjustment of several optimization parameters and constraints gives further opportunities for the development of this approach. Further studies are of interest for the investigation of several pathway directions, scaling techniques for the step size of diameter and thickness selection, or the extended analysis of optimization stability for varying starting points.

Acknowledgments

Support by NOWITECH, the Norwegian Research Centre for Offshore Wind Technology, is gratefully acknowledged (Research council of Norway, contract no. 193823). We thank in particular Fedem Technology AS for providing software licenses and quick and helpful feedback.

References

Amzallag, C., Gerey, J., Robert, J., Bahuaud, J., 1994. Standardization of the Rainflow Counting Method for Fatigue Analysis. International Journal of Fatigue 16, 287–293.

Ashuri, T., 2012. Beyond Classical Upscaling: Integrated Aeroservoelastic Design and Optimization of Large Offshore Wind Turbines. PhD thesis, TU Delft, The Netherlands.

Bleich, F., 1952. Buckling Strength of Metal Structures. McGraw-Hill Inc.: Columbus, USA.

Chandrasekaran, B., 1990. Design Problem Solving: A Task Analysis. AI Magazine 11, 59–71.

Davey, H.E., Nimmo, A., 2012. Offshore Wind Cost Reduction Pathways Study. Cost reduction study, The Crown Estate: London, United Kingdom.

Det Norske Veritas AS, 2012. Fatigue Design of Offshore Steel Structures. Recommended Practice, DNV-RP-C203, Det Norske Veritas AS: Høvik, Norway.

Domokos, G., Holmes, P., 1993. Euler's problem, Euler's method, and the standard map; or, the discrete charm of buckling. Journal of Nonlinear Science 3, 109–151.

Fischer, T., de Vries, W., Schmidt, B., 2011. Upwind Design Basis. WP4: Offshore Foundations and Support Structures, Endowed Chair of Wind Energy (SWE) at the Institute of Aircraft Design Universität Stuttgart: Stuttgart, Germany.

Freeman, P., Newell, A., 1971. A Model for Functional Reasoning in Design, in: Proceedings of the 2nd International Joint Conference on Artificial Intelligence, pp. 621–633.

Haftka, R.T., Gürdal, Z., 1991. Elements of Structural Optimization. Kluwer Academic Publishers: Dordrecht, The Netherlands.

Hau, E., 2013. Wind Turbines Fundamentals, Technologies, Application, Economics. Springer-Verlag: Heidelberg, Germany.

International Electrotechnical Commission, 2009. Wind Turbines - Part 3: Design Requirements for Offshore Wind Turbines. International Standard, IEC 61400-3, IEC Central Office: Geneve, Switzerland.

Jonkman, J., Butterfield, S., Musial, W., Scott, G., 2009. Definition of a 5-MW Reference Wind Turbine for Offshore System Development. NREL/TP-500-38060, National Renewable Energy Laboratory.

Miner, M.A., 1945. Cumulative Damage in Fatigue. Journal of Applied Mechanics 12, A159–A164.

Molde, H., Zwick, D., Muskulus, M., 2014. Simulation-based Optimization of Lattice Support Structures for Offshore Energy Converters with the Simultaneous Perturbation Algorithm. Journal of Physics: Conference Series in press.

Muskulus, M., Christensen, E., Zwick, D., Merz, K., 2013. Improved Tower Design for the NOWITECH 10MW Reference Turbine, in: Proceedings of EWEA Offshore 2013, Frankfurt, Germany, pp. PO127: 1–8.

Muskulus, M., Schafhirt, S., 2014. Design Optimization of Wind Turbine Support Structures - A Review. Journal of Ocean and Wind Energy 1, 12–22.

Naess, A., Moan, T., 2013. Stochastic Dynamics of Marine Structures. Cambridge University Press: New York, USA.

Palmgren, A.Z., 1924. Die Lebensdauer von Kugellagern. Zeitschrift des Vereins Deutscher Ingenieure 68, 339–341.

Pasamontes, L.B., Torres, F.G., Zwick, D., Schafhirt, S., Muskulus, M., 2014. Support Structure Optimization for Offshore Wind Turbines with a Genetic Algorithm, in: Proceedings of the 33rd International Conference on Ocean, Offshore and Arctic Engineering OMEA2014, San Francisco, USA, pp. 1–7.

Popko, W., Vorpahl, F., Zuga, A., Kohlmeier, M., Jonkman, J., Robertson, A., Larsen, T.J., Yde, A., Sætertrø, K., Okstad, K.M., Nichols, J., Nygaard, T.A., Gao, Z., Manolas, D., Kim, K., Yu, Q., Shi, W., Park, H., Vasquez-Rojas, A., Dubois, J., Kaufer, D., Thomassen, P., de Ruiter, M.J., Peeringa, J.M., Zhiwen, H., von Waaden, H., 2014. Offshore Code Comparison Collaboration Continuation (OC4), Phase I - Results of Coupled Simulations of an Offshore Wind Turbine with Jacket Support Structure. Journal of Ocean and Wind Energy 1, 1–11.

Standards Norway, 2004. Design of Steel Structures. Norsok Standard N-004, Standards Norway: Lysaker, Norway.

Vorpahl, F., Popko, W., Kaufer, D., 2011. Description of a Basic Model of the 'UpWind Reference Jacket' for Code Comparison in the OC4 Project under IEA Wind Annex XXX. IEA Wind Annex XXX, Fraunhofer Institute for Wind Energy and Energy System Technology (IWES): Bremerhaven, Germany.

Vorpahl, F., Schwarze, H., Fischer, T., Seidel, M., Jonkman, J., 2013. Offshore Wind Turbine Environment, Loads, Simulation, and Design. Energy and Environment 2, 548–570.

Zwick, D., Muskulus, M., 2014a. The Simulation Error caused by Input Loading Variability in Offshore Wind Turbine Structural Analysis. Wind Energy DOI: 10.1002/we.1767.

Zwick, D., Muskulus, M., 2014b. Simplified Fatigue Load Assessment in Offshore Wind Turbine Structural Analysis. Submitted for publication .

Zwick, D., Muskulus, M., Moe, G., 2012. Iterative Optimization Approach for the Design of Full-height Lattice Towers for Offshore Wind Turbines. Energy Procedia 24, 297–304.

Paper 6

Simulation-based optimization of lattice support structures for offshore wind energy converters with the simultaneous perturbation algorithm

Molde H, Zwick D, Muskulus M
Journal of Physics: Conference Series 2014; **555**: 012075:1-8

The Science of Making Torque from Wind 2012 IOP Publishing
Journal of Physics: Conference Series **555** (2014) 012075 doi:10.1088/1742-6596/555/1/012075

Simulation-based optimization of lattice support structures for offshore wind energy converters with the simultaneous perturbation algorithm

H Molde, D Zwick and M Muskulus

Department of Civil and Transport Engineering, Norwegian University of Science and Technology, Høgskoleringen 7a, 7491 Trondheim, Norway

E-mail: michael.muskulus@ntnu.no

Abstract. Support structures for offshore wind turbines are contributing a large part to the total project cost, and a cost saving of a few percent would have considerable impact. At present support structures are designed with simplified methods, e.g., spreadsheet analysis, before more detailed load calculations are performed. Due to the large number of loadcases only a few semi-manual design iterations are typically executed. Computer-assisted optimization algorithms could help to further explore design limits and avoid unnecessary conservatism.

In this study the simultaneous perturbation stochastic approximation method developed by Spall in the 1990s was assessed with respect to its suitability for support structure optimization. The method depends on a few parameters and an objective function that need to be chosen carefully. In each iteration the structure is evaluated by time-domain analyses, and joint fatigue lifetimes and ultimate strength utilization are computed from stress concentration factors. A pseudo-gradient is determined from only two analysis runs and the design is adjusted in the direction that improves it the most.

The algorithm is able to generate considerably improved designs, compared to other methods, in a few hundred iterations, which is demonstrated for the NOWITECH 10 MW reference turbine.

1. Introduction

Today, the design of wind turbine support structures is to a large extent a manual process. It requires a lot of experience on the designer's part, and the design tools are often based on simplified methods, e.g., preliminary sizing with spreadsheets. As larger structures are being developed and installations move to larger water-depths, multi-member support structures (such as the OWEC Quattropod® jacket) become increasingly interesting, but present specific challenges, e.g., the possibility of local vibrations [2]. These structures consist of a large number of members, which increases the need for efficient and accurate design-tools. Simulation-based optimization [6] is a promising technique that can help to automate this process.

Support structures for offshore wind turbines are typically fatigue-dominated, but an accurate assessment of fatigue lifetimes is time consuming and computationally costly. Therefore only a few design iterations are typically performed, and current designs might contain a considerable amount of convervatism. On the other hand, optimization of such designs has to be performed in an extremely efficient way, since analyses are so costly.

Figure 1. The NOWITECH 10MW reference turbine. Preliminary drawing.

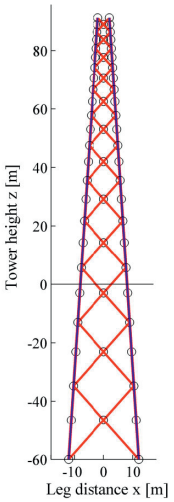

Figure 2. Geometry of the full-height lattice tower.

In this study Spall's simultaneous perturbation stochastic approximation (SPSA) algorithm [11, 12, 14] was used to automatically optimize thickness and diameter of the members in an offshore wind turbine support structure. The method utilizies a pseudo-gradient based on only two function evaluations per iteration, which allows for a computationally efficient process. Each evaluation of the design consisted of 2 min time-domain simulations of the complete wind turbine in Fedem Windpower (Fedem Technology AS, Trondheim), a flexible multibody solver that has recently been extended with functionality for aerodynamic and hydrodynamic loads.

Subsequently, rainflow counting was performed and joint lifetimes were calculated with stress concentration factors. The utilization of both ultimate and fatigue limit states is reported for each joint. Tower weight was chosen as an indicator of cost, and an objective function comprising variables for weight and joint lifetimes was defined. The method has shown promising results, and is able to find viable designs, even when starting from highly unacceptable starting points.

Some of the major challenges when using SPSA for multi-member support structures were the choice of the objective function and of the parameters governing the behavior of the algorithm. Existing guidelines [13] were followed when doing this calibration, but for an efficient search the parameters had to be modified. We report the results of a full calibration for the 10 MW NOWITECH reference turbine on a full-height lattice tower [10], which should provide a useful basis for application to other turbine sizes and water-depths.

2. Methods

All analyses were performed with Fedem Windpower software (pre-release version) and custom-written Matlab (The Mathworks, Inc.) functions.

2.1. Wind turbine model and environment

A preliminary version of the NOWITECH 10MW reference turbine was used (Fig. 1). The blades have been developed during the past two years [5] and the support structure is a novel concept that continues the typical jacket support structure up until the rotor-nacelle-assembly (Fig. 2), thereby avoiding the need for a complicated and costly transition piece [10]. Apart from

its intrinsic interest, this structure was chosen since it consists of a large number of members and thereby poses a challenge for optimization algorithms.

The target water depth is 60m, and the preliminary tower design features a total height of 151m achieved with 12 sections, 4 legs spaced with 24m bottom-distance and 4m top-distance, for a total of 240 members (beam elements) in the basic computer model. This results in a total of 48 design parameters for the sizing problem: all combinations of 12 sections, both legs and braces, and the sizing of both diameters and thicknesses.

Only one loadcase was considered for this study, corresponding to power production at a wind speed of $U = 13.5\,\mathrm{m/s}$ and turbulent fluctuations with a turbulent intensity of 0.16. The seastate was taken to be irregular linear waves from a JONSWAP spectrum, with significant wave height $H_s = 4\,\mathrm{m}$ and peak period $T_p = 9\,\mathrm{s}$. A simple PID controller was employed.

2.2. Analysis

The wind turbine was analysed by 2 min time-domain simulations with Fedem Windpower. Time series of stresses were saved, and hot spot stresses were obtained by rainflow counting and using stress concentration factors according to DNV guidelines [3]. The results were normalized to the design lifetime of 20 years, such that a joint utiliziation of 1.2, e.g., reflects an estimated joint lifetime of 24 years.

2.3. Stochastic simultaneous perturbation algorithm

Standard gradient-based search algorithms for design optimization [1] need to evalute changes in each parameter independently, resulting in $2n$ analyses for n design parameters, in order to obtain an estimate of the gradient (design sensitivity) by finite-differences.

If θ_k denotes the n-dimensional vector of design parameters at the k-th step of the iteration, such methods evaluate an objective function f to obtain the values $f(\theta_k + c_k e_i)$ and $f(\theta_k - c_k e_i)$, where e_i denotes the i-th unit vector and c_k the current *perturbation width*. The sensitivity $\frac{\partial f}{\partial x_i}$ is thereby approximated by the finite difference

$$\frac{\partial f}{\partial x_i} \approx \frac{f(\theta_k + c_k e_i) - f(\theta_k - c_k e_i)}{2c_k} \quad \text{for each} \quad i = 1, \ldots, n. \tag{1}$$

In contrast to this, the SPSA algorithm calculates a pseudo-gradient from only two function evaluations at $\theta_k^+ = \theta_k + c_k\Delta_k$ and $\theta_k^- = \theta_k - c_k\Delta_k$. The perturbation vector Δ_k consists of a random sample generated independently for each component from a zero-mean probability law with finite variance. Typically a Bernoulli distribution (with values $+1$ or -1 with equal probability) is chosen, and this example was followed here as well. The perturbation vector is chosen anew at each iteration of the algorithm.

Next the pseudo-gradient is calculated as

$$\hat{g}_k(\theta_k) = \frac{f(\theta_k^+) - f(\theta_k^-)}{2c_k} \begin{bmatrix} \Delta_{k,1}^{-1} \\ \Delta_{k,2}^{-1} \\ \vdots \\ \Delta_{k,n}^{-1} \end{bmatrix} \tag{2}$$

Finally, the design parameters are updated using a *gain sequence* a_k, according to

$$\theta_{k+1} := \theta_k - a_k \hat{g}_k \tag{3}$$

The gain sequence a_k and perturbation width c_k are typically given in terms of a few additional parameters a, c, A, α and γ:

$$a_k = \frac{a}{(1 + A + k)^\alpha}, \qquad c_k = \frac{c}{k^\gamma} \tag{4}$$

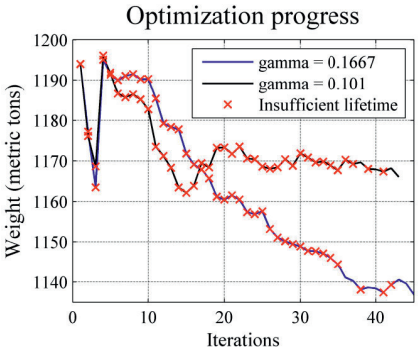

Figure 3. Dependence of optimization on perturbation width parameter γ.

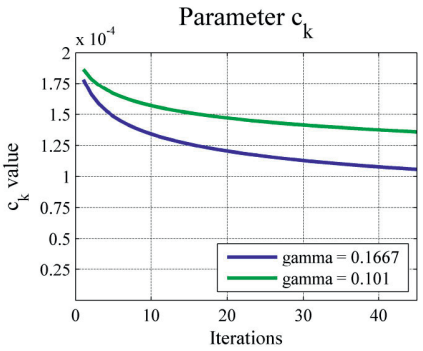

Figure 4. Perturbation width during optimization.

Default values are $\alpha = 0.602, \gamma = 0.101$. The parameter A is useful to reduce very large initial stepsizes and needs to be individually chosen. The following results were obtained with values of $a = 0.000025$, $c = 0.0005$ and $A = 15$, unless noted otherwise.

3. Results

3.1. Choice of objective function and algorithm parameters

The objective function controls the behavior of the algorithm and needs to be carefully chosen. Lower values represent a "better" design. Here we simply used structural steel weight as an indicator of cost, which shall be minimized. However, the design has to conform to the constraints given by the ultimate limit state (ULS) and the fatigue limit state (FLS). Designs that underperform have to be avoided. Various techniques exist for such constrained optimization problems, typically involving mirroring of parameters back into design space when a lifetime or strength constraint is violated.

We pursued a different and much simpler approach here: the objective function was extended by an additive term that quantifies how strongly a design violates the given design constraints, balancing the gain due to weight reduction. After some experimentation the following objective function was chosen:

$$\left(\frac{\text{weight} - 1200\,\text{t}}{50\,\text{t}}\right) + \sum_{L_i<1} \left((L_i - 1.25)^2 + (L_i - 1.10)^{20}\right), \tag{5}$$

where the sum on the right side runs over all joints whose normalized lifetime L_i does not fulfill the design limits.

This objective function leads to a substantial number of infeasible designs, but due to the stochastic nature of the algorithm (with only two directions to choose from at each iteration), the algorithm does intermittently find suitable designs (confer Fig. 3).

During testing, additional constraints were implemented: the minimum allowed member diameters were set to 5mm. If thicknesses became equal or larger than half the element diameters the diameters were slightly increased to avoid unphysical situations. Braces were also constrained to remain thicker than the corresponding sections of the legs.

Algorithm parameters were varied, within certain limits. The γ parameter controls the decrease of the perturbation width during the progress of the optimization. Too small a value slows the optimization process down, and an acceptable choice was obtained with $\gamma = 0.1667$

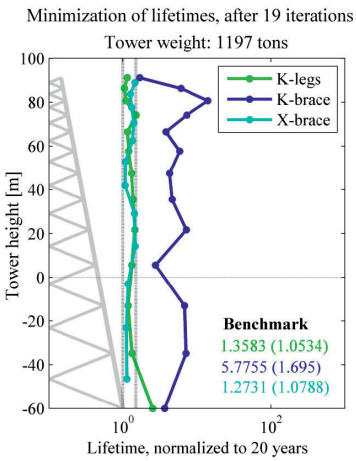

Figure 5. Performance of optimum design achieved by minimization-of-lifetimes method. Benchmark numbers refer to worst and average (in brackets) utilization of joints.

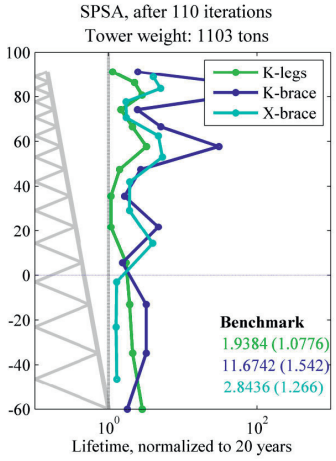

Figure 6. Performance of optimum design achieved by SPSA. Benchmark numbers refer to worst and average (in brackets) utilization of joints.

(Fig. 3). This leads to a relatively strong initial decrease of the perturbation width that then slowly levels out (Fig. 4).

Since in general the step size had a tendency to drop quicker than desired, the step size parameter α was taken at the lowest value recommended by Spall, $\alpha = 0.602$. Also the parameter A controlling the initial decrease in gain was set to 15, speeding up the optimization considerably.

In order to deal with variables with large differences in magnitude (e.g., diameters versus thicknesses) each component of the a_k and c_k values was scaled with a factor of 20 if it corresponded to a thickness parameter. Thereby all design variables showed approximately the same *relative* changes during an iteration.

3.2. Comparison with optimization-of-lifetimes method

The *optimization-of-lifetimes* method was introduced recently [15] to quickly perform an "optimal" sizing of a wind turbine support structure. It consists of a number of iterations where the present design utilization is evaluted. Then each member is sized independently of all the other members, weakening or strengthening the member until the utilization (assuming the exact same member forces as before) lies within 1.0–1.1. The analysis in the next iteration then typically leads to further redistribution of member dimensions, and the process is stopped if all joints perform within 1.0–1.5 utilization. The method converges quickly (Fig. 5). In contrast, the SPSA algorithm needs at least a factor of 10 more iterations (Fig. 6). However, although SPSA results in fewer feasible designs and takes significantly longer, it potentially results in better designs (Fig. 7).

This was confirmed by a restart simulation in which the best design obtained with the optimization-of-lifetimes method was used as starting point for the SPSA algorithm. A further reduction in weight of more than 90 tons was achieved (Fig. 8). Interestingly, the geometry of the final design was highly nontrivial, with alternating variations in leg diameters between sections that a human designer would not consider so quickly (Fig. 9).

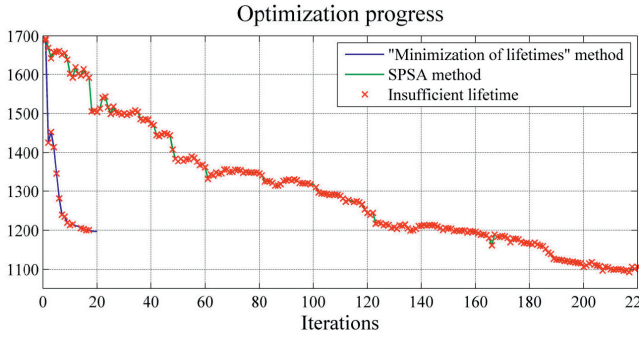

Figure 7. Comparison of minimization-of-lifetimes method and SPSA.

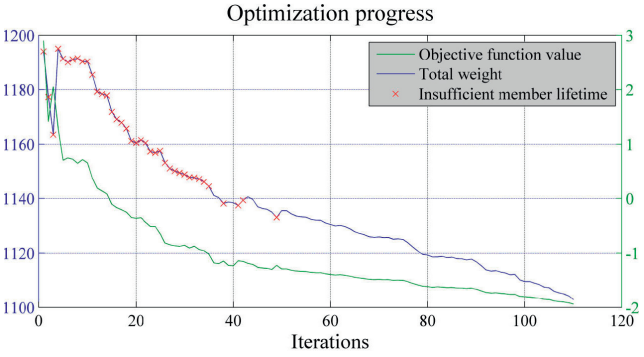

Figure 8. Optimization with SPSA from the best design obtained by the minimization-of-lifetimes method.

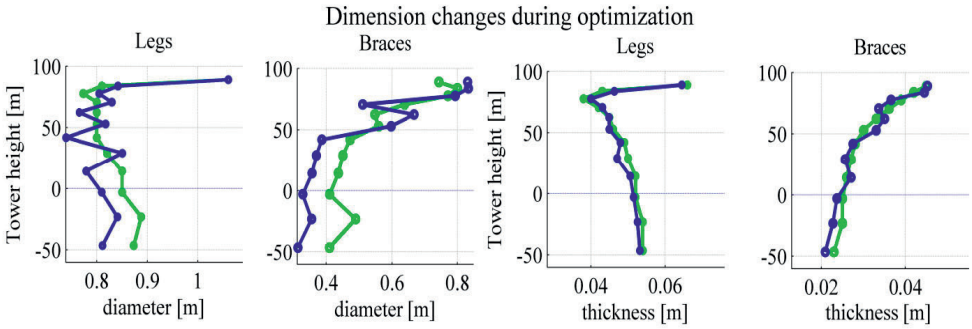

Figure 9. Geometry of the design optimized by SPSA. Green: original design (minimization-of-lifetimes method). Blue: optimized design after another 110 iterations.

3.3. A full optimization example

Starting from a design with constant member diameters and thicknesses, SPSA was run unsupervised for more than 300 iterations. During the process a number of interesting, feasible designs were obtained (Fig. 10) with weights similar to the above. The geometry of the design with 1132t mass (Fig. 11) differs markedly from the one previously obtained (Fig. 9). This illustrates the property that gradient-based algorithms (and therefore also pseudo-gradient based algorithms such as SPSA) will only lead to local optima. Different starting points and, for a

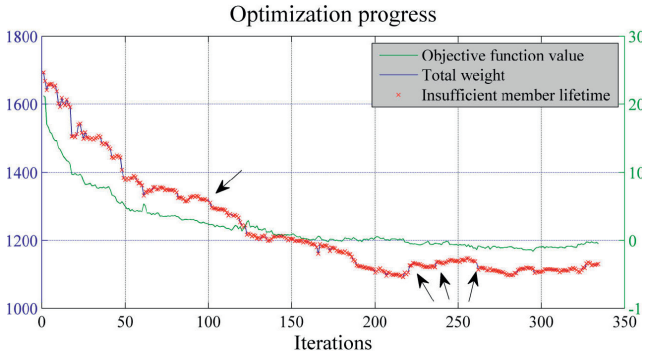

Figure 10. Full optimization example, using SPSA for an initial design with constant member dimensions.

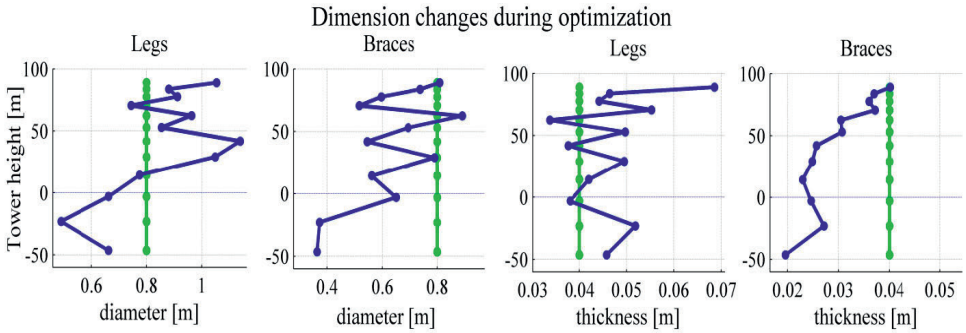

Figure 11. Geometry of the 1132t design optimized by SPSA. Green: original design (constant member dimensions). Blue: optimized design after 250+ iterations.

stochastic method such as SPSA, different perturbation vectors (random numbers) will generally lead to different results. Under certain conditions SPSA is actually provably able to find global optimal solutions [9], but these conditions are difficult to realize in practice.

4. Discussion

Optimization of offshore wind turbine support structures is a difficult problem, since fatigue lifetimes need to be estimated accurately. This typically necessitates a large number of loadcases (confer the loadcase tables in the relevant standards, e.g., [7]) with time-consuming time-domain simulations. SPSA has been designed for simulation-based optimization, where the evaluation of the objective function is computationally very expensive and should be attempted as few as possible.

The method was studied only with a single loadcase here. Moreover, no frequency (servicability) constraints were imposed and evalued for the designs, and the lifetime constraints were handled in a very simple manner. Nevertheless, the results demonstrate the potential of SPSA for automatic optimization of support structures. Further studies should focus on its application when multiple loadcases contribute to the value of the objective function. Also the effect of topology changes (e.g., differing the heights of sections) could be explored. Of course a better cost model taking into account manufacturing (welding) costs should be considered [4], as well as manufacturing constraints (e.g., discrete diameters and thicknesses for all tubular members).

Combined with a further approximation of fatigue lifetimes (e.g., using response-surface modeling [8]) that reduces the loadcases needed for fatigue estimation, the SPSA method seems a promising candidate for an automatic optimization algorithm.

Acknowledgements
We thank the Norwegian Research Centre for Offshore Wind Technology (NOWITECH FME, Research Council of Norway, contract no. 193823) for support, in particular the helpful staff of Fedem Technology AS.

References

[1] Belegundu A D and Chandrupatha T R 2011 *Optimization concepts and applications in engineering* (New York: Cambridge University Press)
[2] Böker C 2009 *Load simulation and local dynamics of support structures for offshore wind turbines* (Hannover: Institut für Stahlbau, Gottfried Wilhelm Leibniz Universität Hannover)
[3] Det Norske Veritas 2010 *Fatigue design of offshore steel structures* Recommended practice DNV-RP-C203 (Høvik: DNV)
[4] Farkas J and Jármai K 2008 Cost comparison of a ring-stiffened shell and a tubular truss structure for a wind turbine tower *Design and optmization of metal structures* (Westergate: Horwood Publishing) 225–43
[5] Frøyd L and Dahlhaug O G 2011 Rotor design for a 10 MW offshore wind turbine *Proc. 21st Int. Offshore Polar Engng. Conf. (Maui, Hawaii)* 327-34
[6] Gosavi A 2003 *Simulation-based optimization* (New York: Springer)
[7] International Electrotechnical Commission 2009 *Wind turbines. Part 3: Design requirements for offshore wind turbines* International standard IEC 61400–3 (Geneva: IEC)
[8] Khuri A I and Cornell J A 1996 *Response surfaces: designs and analyses* (New York: Marcel Dekker)
[9] Maryak J L and Chin D C 2008 Global random optimization by simultaneous perturbation stochastic approximation *IEEE Trans. Automatic Control* **53** 780–3
[10] Muskulus M 2012 The full-height lattice tower concept *Energy Procedia* **23** 371–7
[11] Spall J C 1992 Multivariate stochastic approximation using a simultaneous perturbation gradient approximation *IEEE Trans. Automatic Control* **37** 332–41
[12] Spall J C 1998 An overview of the simultaneous perturbation method for efficient optimization *John Hopkins APL Technical Digest* **19** 482–92
[13] Spall J C 1998 Implementation of the simultaneous perturbation algorithm for stochastic optimization *IEEE Trans. Aerospace Electr. Systems* **34** 817–23
[14] Spall J C 2003 *Introduction to stochastic search and optimization* (Hoboken: John Wiley & Sons)
[15] Zwick D, Muskulus M and Moe G 2012 Iterative optimization approach for the design of full-height lattice towers for offshore wind turbines *Energy Procedia* **24** 297–304

Paper 7

Support structure optimization for offshore wind turbines with a genetic algorithm

Pasamontes LB, Torres FG, Zwick D, Schafhirt S, Muskulus M
Proceedings of the 33rd International Conference on Ocean, Offshore and Arctic Engineering 2014, San Francisco, USA, OMAE; **9B**: V09BT09A033:1-7

Is not included due to copyright

Appendix B

Abstracts of additional publications

Offshore Wind Turbine Jacket Substructure: A Comparison Study Between Four-Legged and Three-Legged Designs

Kok Hon Chew[1], E.Y.K. Ng[1], Kang Tai[1], Michael Muskulus[2] and Daniel Zwick[2]

[1]School of Mechanical and Aerospace Engineering, Nanyang Technological University, Singapore
[2]Department of Civil and Transport Engineering, Norwegian University of Science and Technology (NTNU), Trondheim, Norway

Published in *Journal of Ocean and Wind Energy*, vol. 1, pp. 74-81, 2014.

Abstract

A comparison study was conducted between a conventional four-legged and a newly-developed three-legged bottom fixed jacket substructure for offshore wind applications. Fatigue (FLS) and ultimate limit state (ULS) analyses were performed, and results show that the three-legged concept is feasible as an interesting alternative to the four-legged design, while potentially more cost-efficient, with a 17-percent reduction of structural mass and a 25-percent reduction in the number of welded joints. Further analyses were carried out to evaluate the sensitivity of the dynamic performance with respect to different load cases, loading directionality, and wind-wave misalignment effects. Results show that both designs are highly susceptible to the change-of-load direction, therefore recommending a finer incident angle resolution (a gap of 15 degrees or less) to be used in the analysis. The overall wind-wave misalignment effect is comparably smaller, but could contribute to a significant impact if the joints are close to being critical.

Reanalysis of Jacket Support Structure for Computer-Aided Optimization of Offshore Wind Turbines with a Genetic Algorithm

Sebastian Schafhirt[1], Daniel Zwick[1] and Michael Muskulus[1]

[1]Department of Civil and Transport Engineering, Norwegian University of Science and Technology (NTNU), Trondheim, Norway

Published in *Journal of Ocean and Wind Energy*, vol. 1, pp. 209-216, 2014.

Abstract

The optimization of jacket support structures for offshore wind turbines is a nontrivial task. Due to nonlinear and time history-dependent effects, the analysis is simulation-based. Structural optimization using time-domain simulations is computationally demanding and difficult and typically requires a gradient-free approach. A genetic algorithm can be used for this purpose, but is limited by the computational resources available. This paper presents an approach to modifying the standard genetic algorithm for the automatic optimization of offshore wind turbines with jacket support structures under fatigue constraints. It is shown that performing a reanalysis of the jacket structures, by using performance data from earlier analyses in parallel with the simulation-based analysis process, requires a smaller number of iterations to obtain improved designs. Thus, the use of reanalysis within the genetic algorithm speeds up the algorithm significantly.

Specification of the NOWITECH 10MW Reference Wind Turbine

Ole Gunnar Dahlhaug[1], Petter Andreas Berthelsen[2], Trond Kvamsdal[3], Lars Frøyd[1], Sverre Skalleberg Gjerde[4], Zhaoqiang Zhang[4], Kevin Cox[5], Eric Van Buren[6] and Daniel Zwick[6]

[1]Department of Energy and Process Engineering, Norwegian University of Science and Technology (NTNU), Trondheim, Norway
[2]Offshore Hydrodynamics, Marintek, Trondheim, Norway
[3]Department of Mathematical Sciences, Norwegian University of Science and Technology (NTNU), Trondheim, Norway
[4]Department of Electric Power Engineering, Norwegian University of Science and Technology (NTNU), Trondheim, Norway
[5]Department of Engineering Design and Materials, Norwegian University of Science and Technology (NTNU), Trondheim, Norway
[6]Department of Civil and Transport Engineering, Norwegian University of Science and Technology (NTNU), Trondheim, Norway

Published as NOWITECH report, pp. 1-39, 2012.

Abstract

The NOWITECHs reference turbine is a horizontal axis three bladed offshore wind turbine that has a bottom fixed foundation at 60 meter water depth. The rated power is 10 MW and the diameter of the turbine is 141 meters. The turbine blades are upstream of the tower and are made out of a combination of glass fiber and carbon fiber. The turbine will operate with variable speed below rated power, constant speed above rated power and with maximum speed of 13.5 rpm. Above rated power, the blades will be pitched in such a way that it can keep constant power output.

It has a direct driven permanent magnet synchronous generator which has a nominal-voltage of 4 kV. The grid will have a voltage of 35 kV. The power electronic converter is in the case of an AC-grid consisting of two 3-level neutral point clamped converters in a back-to-back configuration. To achieve the DC voltage of 35 kV, a step-up (boost) converter is needed.

The support structure is a full-height lattice tower that is in total 151 meters high. The foundation of the lattice tower will consist of a single driven steel pile at each corner of the tower.

The tower will be equipped with a landing platform at sea level and a smaller platform below the nacelle. A lift will be attached to one of the legs of the lattice tower. The nacelle will have a helicopter platform on the roof.

The reference site is chosen as the Dutch K13-Alpha weather station which is relevant for the wind farms that will be installed at Doggerbank. Here, the average wind speed at 90 meter height is 10 m/s, turbulence intensity of 15% and the extreme wave height is chosen to be 30 meters. The turbine will be designed for a 20 year lifetime.

Improved Tower Design for the NOWITECH 10MW Reference Turbine

Michael Muskulus[1], Eirik Christensen[1], Daniel Zwick[1] and Karl Merz[1]

[1]Department of Civil and Transport Engineering, Norwegian University of Science and Technology (NTNU), Trondheim, Norway

Published in *Proceedings of the European Wind Energy Association Conference Offshore 2013*, Frankfurt, Germany, EWEA; pp. PO127:1-8, 2013.

Abstract

The Norwegian Research Centre for Offshore Wind Technology (NOWITECH) has developed a conceptual design and load model for a future 10 MW wind turbine as a common testcase and platform for open simulation studies. This so-called 10MW Reference Turbine represents the current state-of-art in offshore wind turbines. One novel feature is the support structure, which is a full-height lattice tower that goes all the way up from the seafloor to the nacelle, thereby removing the need for an expensive transition piece. In order to design this tower efficiently, an automatic optimization method was previously developed that iteratively improves the weight of the structure, while observing the structural limits. The algorithm is based on locality assumptions, and structural members are sized independently of each other, assuming that the loads will stay the same. This is only approximately true, but works well enough in practice, and only around 20-30 iterations are needed for convergence. In this study the method was used to optimize the tower individually for a number of different loadcases and variations in basic design variables, in order to identify their relative importance. Not surprisingly, higher structural strength is needed for higher wind speeds, but this is not only related to thrust loading. Interestingly, by reducing the weight in the middle sections the members at the bottom need to be strengthened, but the total weight can be reduced. Results also indicate that larger bottom-distance and fewer sections are advantageous. The latter is interesting since the manufacturing costs are less.

Appendix C

Simple beam model

The accuracy of sequential analyses related to results from integrated analyses is directly related to the simulation setup of these two analyses. The here presented example of a simple beam model shows that sequential analyses can provide the same detail of results as integrated analyses, provided that the following conditions are fulfilled:

- The same simulation code is used.
- Identical environmental conditions are applied.
- The simulation model of the analyzed component is represented in same detail.

The intention of this small analysis of a simple beam model was the investigation if wave forces have to be applied separately in sequential analysis, or if these forces are already covered by the applied displacement time series from the integrated analysis.

Simulation model of the simple beam

General specifications of the simulation model for the simple beam are: diameter 5m, thickness 50mm, material steel, water depth 30m. The height above MSL is 60m for beam (1) and 20m for beam (2), as shown in Figure C.1. Both beams are fixed to the GRD in all degrees of freedom in their lowest node. Each beam is divided into beam elements of 5m length, e.g., nodes are defined along the height of the beam in steps of 5m.

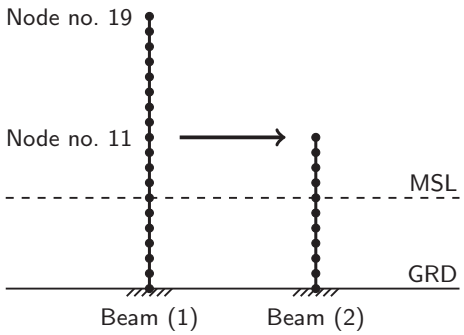

Figure C.1: Beam (1) to the left is a representation of the integrated model with a bottom fixed beam with in total 19 nodes. Beam (2) to the right is a representation of the sequential model. Time series displacements in all degrees of freedom were extracted at the interface node no. 11 of beam (1) and were applied to the top node no. 11 of beam (2).

Investigations

Several simulation cases were investigated to identify the importance of applied wind and wave loading in both integrated and sequential analysis. Wind and wave forces were modeled to be aligned and acting in positive x-direction. The following integrated simulations were performed with beam model (1):

Sim 1: Regular wave force only.

Sim 2: Regular wave force and a constant wind force, applied at node no. 19.

Sim 3: Regular wave force and a periodic wind force, applied at node no. 19.

Sim 4: Irregular wave force and a periodic wind force, applied at node no. 19.

After the simulation runs were fulfilled for beam model (1), displacement time series in all degrees of freedom at node no. 11 were extracted. Subsequently, these time series were applied to beam model (2) to prescribe the displacements of node no. 11 of the sequential model. For the identification of the importance of applied wave forces in the sequential model, simulation runs of beam (2) were performed with applied displacement time series only, as well as with both applied wave forces and displacements acting on node no. 11. Results of the response time series were extracted in node no. 8 at MSL in terms of displacements in x-direction for both beam (1) and (2).

Results

As an example of the four investigated simulation cases, displacement time series for Sim 1 are presented in Figure C.2 for a time period of 20 seconds. Absolute displacements are given for beam (1) as a reference in the upper figure. The deviation of the displacement in node no. 8 is shown in the lower figure, identifying the influence of applied wave forces in the sequential analysis. Only the comparison of a simulation run for beam (2) with both applied wave forces and displacements results in zero deviation to the reference simulation of beam (1).

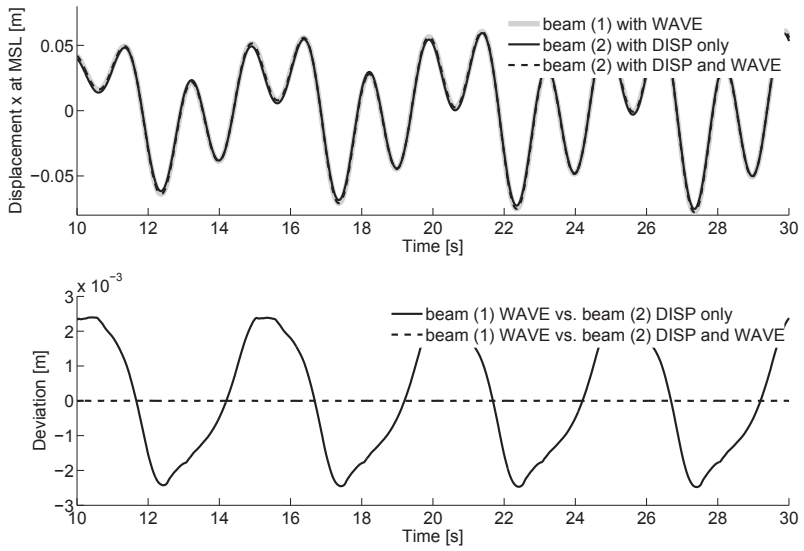

Figure C.2: Sim 1: regular wave forces with T=5s and H=8m. WAVE = wave forces applied in the simulation; DISP only = only displacement time series were applied at node no. 11; DISP and WAVE = both wave forces and displacement time series were applied.

Analyses for Sim 2 and 3 look very similar to the results shown in Figure C.2. First when irregular wave forces are applied (Sim 4), the displacement deviation for approaches without wave force was reduced. Figure C.3 (left) shows displacement ranges for all four investigated simulation cases in node no. 8 of beam (1). To the right, the range of displacement deviation without applied wave forces shows that this error is more or less independent from the type of wind loading applied in the

top node of beam (1), as these forces are correctly represented in the displacement time series. This behavior is changed for the application of irregular wave forces, resulting in a reduced deviation of the sequential approach without applied wave forces.

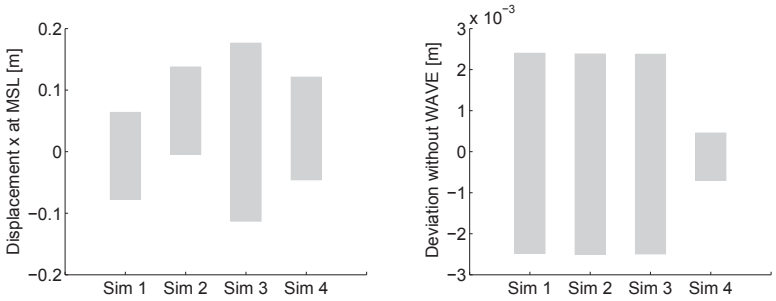

Figure C.3: Ranges of absolute displacement (beam (1) with WAVE) and deviation without wave forces (beam (2) DISP only) for all four simulation cases.

Conclusion

Results show that a correct implementation of the sequential analysis requires the simultaneously application of both wave forces and displacement time series at the interface node. Only by following this approach, integrated analyses are correctly represented by sequential analyses. It was also shown that wind loading at the tower top of the integrated model is represented in the displacement time series, while wave loads need to be accounted for separately in the sequential model.

Appendix D

Matlab code examples

D.1 Run time-domain simulation in Fedem Windpower from Matlab

The given code executed in Matlab defines a system command which starts Fedem Windpower from command line. The dynamic solver (*fedem_solver.exe*) will so be executed in the background, while Matlab is waiting for the simulation to finish. After Fedem Windpower terminates, Matlab continues in the code execution.

Note: to be able to run the command below, *fedem.exe* must be defined with its absolute path as Windows PATH-variable in the control panel of the operating system.

```
% Fedem modelfile name and location
  mf = '"D:\simulations\modelfile.fmm"';

% Choose Fedem solver option:
% - 'dynamics' for single run
% - 'events'   for parallel processing
  opt = 'dynamics';

% Define system command
  PSrun = ['powershell -inputformat none fedem ' ...
           sprintf('-f %s -solve %s',mf,opt)];

% Run Fedem from Matlab
  system(PSrun);
```

D.2 Move result files from RAM to HDD

As indicated in Figure 2.3 on Page 16, result files of finished simulations have to be moved to the HDD if they were performed on the limited RAM drive. The example below shows the principle of RAM drive survey by a while loop, which checks once a minute the time stamp of the simulation log file. If this file is not changed during the last minute, the simulation is assumed to be finished and the result folder can be moved to the storage location on the HDD.

Note: for simulations with turbulent wind files or the application of other time series data which has to be loaded by Fedem Windpower, the *delta_t* criteria may need some adjustment. This is caused by the fact that the *fedem_solver.res* file is not updated during the time Fedem Windpower needs to read external time series data.

```
% Define file locations
  % RAM drive and location of modelfile
    RAM = 'R:\';
  % HDD storage
    HDD = 'D:\simulations\';

% Start while loop
  loop = 1;
  while (loop == 1)
  % Check time stamp of fedem_solver.res file
    res = [RAM 'modelfile_RDB\response_0001\fedem_solver.res'];
    if (exist(res,'file') == 2)
      resinfo = dir(res);
      % Compare time stamp with actual time
        delta_t = now - resinfo.datenum;
      % Continue with file moving if log file is older
      % than 1 minute (1/24/60 = 0.000694)
        if (delta_t > 0.000694)
          movefile([RAM 'modelfile_RDB\'], HDD);
          loop = 0;
        end
    end
  % Wait 1 minute for next check
    pause(60);
  end
```

D.3 Generate parameterized jacket model by Fedem COM-API

The support of the COM functionality for programmatic/scripting automation of Fedem Windpower was used to implement a fully parameterized jacket model. As

Fedem Windpower is not supporting COM-commands directly from Matlab, which was the preferred programming language in this thesis, an alternative way was chosen by creating a Python-script from Matlab, which so was executed in Python.

Note: to be able to run the command below, *python.exe* must be defined with its absolute path as Windows PATH-variable in the control panel of the operating system. In addition to Python itself, Python extensions for Windows (pywin32) have to be installed on the system.

Main script

```
%% 1) Parameter definitions

% General jacket parameters
  % number of legs
    JAC( 1,1) = 4;
  % top distance between legs [m]
    JAC( 2,1) = 8;
  % bottom distance between legs [m]
    JAC( 3,1) = 12;
  % base Z-height of jacket bottom [m]
    JAC( 4,1) = -45;
  % rotation angle around Z-axis [deg]
    JAC( 5,1) = 0;
  % vertical offset of K-joints along legs from bay division [m]
    JAC( 6,1) = 0.2;
  % stub length leg close to K-joints [m]
    JAC( 7,1) = 2;
  % stub length brace close to K-joints [m]
    JAC( 8,1) = 2;
  % stub length brace close to X-joints [m]
    JAC( 9,1) = 1;
  % number of elements between stubs on legs
    JAC(10,1) = 4;
  % number of elements between stubs on braces
    JAC(11,1) = 3;

% Bay specific jacket parameters, from bottom (1) to top (..)
  % bay height definition [m]
    DIM{1,1} = [20; 15; 13; 11];
  % horizontal offset of K-joints along main leg line [m]
    DIM{2,1} = [0; 0; 0; 0; 0];


%% 2) Define jacket nodes and beams by calling function Jdef
  [Jnod, Jbea] = Jdef(JAC,DIM);
```

```
%% 3) Write PYTHON script with COM-API commands

  % open file
    pyfile = sprintf('jacketCOMAPI.py');
    fid    = fopen(pyfile,'w');

  % write header
    fprintf(fid,'# CREATE FMM by FEDEM COM-API via PYTHON\n');
    fprintf(fid,'#\n');

  % assign COM-API
    fprintf(fid,'#\n');
    fprintf(fid,'# Assign COM-API\n');
    fprintf(fid,'#\n');
    fprintf(fid,'import win32com.client\n');
    fprintf(fid,'F = win32com.client.Dispatch("FEDEM.Application")\n');

  % create triads
    fprintf(fid,'#\n');
    fprintf(fid,'# Triads\n');
    fprintf(fid,'#\n');
    for n=1:length(Jnod(:,1))
      if (all(Jnod(n,:)==0) == 0)
        clear Jc Jn
        Jc = sprintf('%7.3f,%7.3f,%7.3f',Jnod(n,1),Jnod(n,2),Jnod(n,3));
        Jn = sprintf('"JT-ID: %d"',n);
        fprintf(fid,'triad%d = F.CreateTriad(%s,0,0,0,%s)\n',n,Jc,Jn);
      end
    end

  % create material
    fprintf(fid,'#\n');
    fprintf(fid,'# Materials\n');
    fprintf(fid,'#\n');
    fprintf(fid,'mat1 = F.CreateMaterial(7850,2.1e11,0.29,"JM: Steel")\n');

  % create cross sections
    fprintf(fid,'#\n');
    fprintf(fid,'# Cross sections\n');
    fprintf(fid,'#\n');
    % identify unique cross sections
      Mpro(1,1) = 1;
      for n=1:length(Jbea(:,1))
        if (all(Jbea(n,:)==0) == 0)
          if (any(Jbea(n,3)==Mpro) == 0)
```

```
            Mpro(end+1,1) = Jbea(n,3);
          end
        end
      end
    % extract beam properties and create cross section
      % jacket parameters
        Jleg = JAC( 1,1);
        Jshe = DIM{1,1};
        Do   = 0.8;
        Di   = 0.75;
      for n=1:length(Mpro(:,1))
        clear Jn
        Jn = sprintf('"JC-ID: %d"',Mpro(n,1));
        fprintf(fid,'cs%d = F.CreateCrossSection(0,mat1,%s)\n',Mpro(n,1),Jn);
        fprintf(fid,'cs%d.SetPipeDiameters(%d,%d)\n',Mpro(n,1),Do,Di);
        fprintf(fid,'cs%d.SetHydroBuoyancyAndDragDiameters(%d,%d)\n', ...
                Mpro(n,1),Do,Do);
      end

  % create beams
    fprintf(fid,'#\n');
    fprintf(fid,'# Beams\n');
    fprintf(fid,'#\n');
    for n=1:length(Jbea(:,1))
      if (all(Jbea(n,:)==0) == 0)
        % description
          if (n < 2000)
            desc = 'K-joint central beam';
          elseif ((n > 2000) && (n < 4000))
            desc = 'K-joint leg stub';
          elseif ((n > 4000) && (n < 6000))
            desc = 'K-joint brace stub';
          elseif ((n > 6000) && (n < 8000))
            desc = 'X-joint brace stub';
          elseif ((n > 8000) && (n < 10000))
            desc = 'Legs';
          else
            desc = 'Braces';
          end
        clear Jc Jn
        Jc = sprintf('triad%d,triad%d,cs%d',Jbea(n,1),Jbea(n,2),Jbea(n,3));
        Jn = sprintf('"JB-ID: %d (%s)"',n,desc);
        fprintf(fid,'beam%d = F.CreateBeam(%s,%s)\n',n,Jc,Jn);
        fprintf(fid,'beam%d.SetStructuralDamping(0,0.01)\n',n);
      end
    end
```

```
  % close file
    fprintf(fid,'#\n');
    fprintf(fid,'# End of file\n');
    fclose(fid);


%% 4) Run PYTHON script and create new .fmm-file
  system(['python ' pyfile]);
```

Function Jdef

```
function [Jnod, Jbea] = Jdef(JAC,DIM)

% INPUT parameters
% ------------------------------------------------------------
%  JAC  - general jacket parameters
%  DIM  - bay specific jacket parameters

% OUTPUT parameters
% ------------------------------------------------------------
%  Jnod - jacket node coordinates [m]
%  Jbea - jacket beam and cross section identification


%% 1) Calculate NODE coordinates

% numbering convention
  % 1..    - A) bay division joints
  % 1000.. - B) K-joints
  % 2000.. - C) X-joints
  % 3000.. - D) stub joints
  % 7000.. - E) discretization joints

% definitions
  % X / Y / Z
    Jnod = zeros(7000,3);

% A) - bay division joints
  % definitions
    NAind = 0;
  % scale factor for distance from tower center
    Ftc = 2 * sin(180/JAC(1,1)*pi/180);
  % for all bays and legs
    for i=1:length(DIM{1,1})+1
      for j=1:JAC(1,1)
        % distance from tower center
```

```
          Dtc = JAC(2,1)/Ftc + DIM{2,1}(i) ...
                + ((JAC(3,1)/Ftc-JAC(2,1)/Ftc)/sum(DIM{1,1}) ...
                * (sum(DIM{1,1})-sum(DIM{1,1}(1:i-1))));
        % angle factor for rotation of elements
          Fro = 360/(2*JAC(1,1)) + (j-1)*360/JAC(1,1) + JAC(5,1);
        % X/Y/Z-coordinates
          NAind         = NAind + 1;
          Jnod(NAind,1) = cos(Fro*pi/180) * Dtc;
          Jnod(NAind,2) = sin(Fro*pi/180) * Dtc;
          Jnod(NAind,3) = sum(DIM{1,1}(1:i-1)) + JAC(4,1);
      end
    end

% B) - K-joints
  % definitions
    NAind =    0;
    NBind = 1000;
  % for all bays and legs
    for i=1:length(DIM{1,1})
      for j=1:JAC(1,1)
        % lower and upper bay division joints
          NAind = NAind + 1;
          P1    = Jnod(NAind,:);
          P2    = Jnod(NAind+JAC(1,1),:);
        % vector length and scale factor
          V = P2-P1;
          L = sqrt(V(1,1)^2 + V(1,2)^2 + V(1,3)^2);
          S = JAC(6,1) / L;
        % lower K-joint
          NBind         = NBind + 1;
          Jnod(NBind,:) = P1 + S * V;
        % upper K-joint
          NBind         = NBind + 1;
          Jnod(NBind,:) = P2 - S * V;
      end
    end
  % store K-joints of each side plane in P-matrix
    NBind = 1000;
    P     = cell(length(DIM{1,1}),JAC(1,1));
    for i=1:length(DIM{1,1})
      for j=1:JAC(1,1)
        NBind       = NBind + 1;
        P{i,j}(1,:) = Jnod(NBind                                ,:);
        P{i,j}(2,:) = Jnod(NBind + 2-fix(j/JAC(1,1))*2*JAC(1,1),:);
        NBind       = NBind + 1;
        P{i,j}(3,:) = Jnod(NBind                                ,:);
        P{i,j}(4,:) = Jnod(NBind + 2-fix(j/JAC(1,1))*2*JAC(1,1),:);
```

```
      end
    end

% C) - X-joints
  % definitions
    NCind = 2000;
  % for all bays and side planes
    for i=1:length(DIM{1,1})
      for j=1:JAC(1,1)
        % intersection
          t  = (P{i,j}(1,:)-P{i,j}(2,:)) / ...
               (P{i,j}(3,:)-P{i,j}(2,:)-P{i,j}(4,:)+P{i,j}(1,:));
          PS = P{i,j}(1,:) + t*(P{i,j}(4,:)-P{i,j}(1,:));
        % calculate coordinates
          NCind         = NCind + 1;
          Jnod(NCind,:) = PS(1,:);
      end
    end

% D) - stub joints
  % definitions
    NBind = 1000;
    NCind = 2000;
    NDind = 3000;
  % along legs
    % for all bays and legs
      for i=1:length(DIM{1,1})
        for j=1:JAC(1,1)
          % lower and upper K-joint
            NBind = NBind + 1;
            P1    = Jnod(NBind,:);
            NBind = NBind + 1;
            P2    = Jnod(NBind,:);
          % vector and scale factor
            V = P2 - P1;
            L = sqrt(V(1,1)^2 + V(1,2)^2 + V(1,3)^2);
            S = JAC(7,1) / L;
          % lower stub joint
            NDind         = NDind + 1;
            Jnod(NDind,:) = P1 + S * V;
          % upper stub joint
            NDind         = NDind + 1;
            Jnod(NDind,:) = P2 - S * V;
        end
      end
  % along braces close to K-joints
    % for all bays and legs
```

```
      for i=1:length(DIM{1,1})
        for j=1:JAC(1,1)
          % vector from K-joint to K-joint and scale factor
            V = P{i,j}(4,:)-P{i,j}(1,:);
            L = sqrt(V(1,1)^2 + V(1,2)^2 + V(1,3)^2);
            S = JAC(8,1) / L;
          % calculate coordinates
            for k=1:4
              NDind         = NDind + 1;
              Jnod(NDind,:) = P{i,j}(k,:) + S * ...
                              (P{i,j}(5-k,:)-P{i,j}(k,:));
            end
        end
      end
  % along braces close to X-joints
    % for all bays and legs
      for i=1:length(DIM{1,1})
        for j=1:JAC(1,1)
          % X-joint
            NCind = NCind + 1;
            PX    = Jnod(NCind,:);
          % stub-joints
            for k=1:4
              % vector from X-joint to K-joint and scale factor
                V = P{i,j}(k,:) - PX;
                L = sqrt(V(1,1)^2 + V(1,2)^2 + V(1,3)^2);
                S = JAC(9,1) / L;
              % calculate coordinates
                NDind         = NDind + 1;
                Jnod(NDind,:) = PX + S * V;
            end
        end
      end

% E) discretization joints
  % definitions
    NDind = 3000;
    NEind = 7000;
  % on legs
    if (JAC(10,1) > 1)
      % for all bays and legs
        for i=1:length(DIM{1,1})
          for j=1:JAC(1,1)
            % lower stub-joint
              NDind = NDind + 1;
              P1    = Jnod(NDind,:);
            % upper stub-joint
```

```
              NDind = NDind + 1;
              P2    = Jnod(NDind,:);
            % discretization
              for d=1:JAC(10,1)-1
                NEind         = NEind + 1;
                Jnod(NEind,:) = P1 + d/JAC(10,1) * (P2-P1);
              end
          end
        end
    end
  % on braces
    if (JAC(11,1) > 1)
      % definitions
        NDindK = 3000 + length(DIM{1,1})*JAC(1,1)*2;
        NDindX = 3000 + length(DIM{1,1})*JAC(1,1)*6;
      % for all bays and side planes
        for i=1:length(DIM{1,1})
          for j=1:JAC(1,1)
            for k=1:4
              % stub-joint close to K-joint
                NDindK = NDindK + 1;
                P1     = Jnod(NDindK,:);
              % stub-joint close to X-joint
                NDindX = NDindX + 1;
                P2     = Jnod(NDindX,:);
              % discretization
                for d=1:JAC(11,1)-1
                  NEind         = NEind + 1;
                  Jnod(NEind,:) = P1 + d/JAC(11,1) * (P2-P1);
                end
            end
          end
        end
    end


%% 2) Extract BEAM and CROSS SECTION numbering

% BEAMS - numbering convention
  % 1..     - A) leg beam from bay division to K-joints
  % 2000..  - B) K-joint leg stubs
  % 4000..  - C) K-joint brace stubs
  % 6000..  - D) X-joint stubs
  % 8000..  - E) legs
  % 10000.. - F) braces

% CROSS SECTION - numbering convention
```

```
  % 1..    - A) K-joint leg stubs and bay division beams
  % 100..  - C) K-joint brace stubs
  % 200..  - D) X-joint brace stubs
  % 300..  - E) discretization legs
  % 400..  - F) discretization beams

% definitions
  % Node no.1 / Node no.2 / Cross section property
    Jbea = zeros(10000,3);

% A) leg beam from bay division to K-joints
  % definitions
    NAind = 0;
    BAind = 0;
    NBind = 1000;
    CAind = 0;
  % for all bays and legs
    for i=1:length(DIM{1,1})
      CAind = CAind + 1;
      for j=1:JAC(1,1)
        % lower beam
          NAind         = NAind + 1;
          BAind         = BAind + 1;
          NBind         = NBind + 1;
          Jbea(BAind,1) = NAind;
          Jbea(BAind,2) = NBind;
          Jbea(BAind,3) = CAind;
        % upper beam
          BAind         = BAind + 1;
          NBind         = NBind + 1;
          Jbea(BAind,1) = NAind + JAC(1,1);
          Jbea(BAind,2) = NBind;
          Jbea(BAind,3) = CAind + 1;
      end
    end

% B) K-joint leg stubs
  % definitions
    NBind = 1000;
    BBind = 2000;
    NDind = 3000;
    CAind = 0;
  % for all bays and legs
    for i=1:length(DIM{1,1})
      CAind = CAind + 1;
      for j=1:JAC(1,1)
        % lower and upper beam
```

```
          for k=1:2
            NBind         = NBind + 1;
            BBind         = BBind + 1;
            NDind         = NDind + 1;
            Jbea(BBind,1) = NBind;
            Jbea(BBind,2) = NDind;
            Jbea(BBind,3) = CAind + (k-1);
          end
      end
    end

% C) K-joint brace stubs
  % definitions
    NBind = 1000;
    BCind = 4000;
    NDind = 3000 + length(DIM{1,1})*JAC(1,1)*2;
    CCind = 100;
  % for all bays and side planes
    for i=1:length(DIM{1,1})
      CCind = CCind + 1;
      for j=1:JAC(1,1)
        % K-joints
          clear P
          NBind  = NBind + 1;
          P(1,1) = NBind;
          P(2,1) = NBind + 2 - 2*fix(j/JAC(1,1))*JAC(1,1);
          NBind  = NBind + 1;
          P(3,1) = NBind;
          P(4,1) = NBind + 2 - 2*fix(j/JAC(1,1))*JAC(1,1);
        % assign beam numbering
          for k=1:4
            BCind         = BCind + 1;
            NDind         = NDind + 1;
            Jbea(BCind,1) = P(k,1);
            Jbea(BCind,2) = NDind;
            Jbea(BCind,3) = CCind + fix(k/3);
          end
      end
      CCind = CCind + 1;
    end

% D) X-joint stubs
  % definitions
    NCind = 2000;
    BDind = 6000;
    NDind = 3000 + length(DIM{1,1})*JAC(1,1)*6;
    CDind = 200;
```

```
  % for all bays and side planes
    for i=1:length(DIM{1,1})
      CDind = CDind + 1;
      for j=1:JAC(1,1)
        % X-joint
          NCind = NCind + 1;
        % assign beam numbering
          for k=1:4
            BDind         = BDind + 1;
            NDind         = NDind + 1;
            Jbea(BDind,1) = NCind;
            Jbea(BDind,2) = NDind;
            Jbea(BDind,3) = CDind + rem(k+2,3);
          end
      end
      CDind = CDind + 2;
    end

% E) discretization legs
  % definitions
    NDind = 3000;
    BEind = 8000;
    NEind = 7000;
    CEind = 300;
  % for all bays and legs
    for i=1:length(DIM{1,1})
      CEind = CEind + 1;
      for j=1:JAC(1,1)
        % lower and upper stub-joint
          NDind = NDind + 1;
          P1    = NDind;
          NDind = NDind + 1;
          P2    = NDind;
        % check level of discretization
          if (JAC(10,1) == 1)
            BEind         = BEind + 1;
            Jbea(BEind,1) = P1;
            Jbea(BEind,2) = P2;
            Jbea(BEind,3) = CEind;
          else
            % first beam
              NEind         = NEind + 1;
              BEind         = BEind + 1;
              Jbea(BEind,1) = P1;
              Jbea(BEind,2) = NEind;
              Jbea(BEind,3) = CEind;
            % intermediate beams
```

```
              for d=2:JAC(10,1)-1
                NEind         = NEind + 1;
                BEind         = BEind + 1;
                Jbea(BEind,1) = NEind-1;
                Jbea(BEind,2) = NEind;
                Jbea(BEind,3) = CEind;
              end
            % last beam
              BEind         = BEind + 1;
              Jbea(BEind,1) = NEind;
              Jbea(BEind,2) = P2;
              Jbea(BEind,3) = CEind;
          end
      end
    end

% F) discretization braces
  % definitions
    BFind = 10000;
    NDindK = 3000 + length(DIM{1,1})*JAC(1,1)*2;
    NDindX = 3000 + length(DIM{1,1})*JAC(1,1)*6;
    NEind  = 7000 + length(DIM{1,1})*JAC(1,1)*(JAC(10,1)-1);
    CFind  = 400;
  % for all bays and side planes
    for i=1:length(DIM{1,1})
      CFind = CFind + 1;
      for j=1:JAC(1,1)
        for k=1:4
          % stub joint close to K-joint
            NDindK = NDindK + 1;
            P1     = NDindK;
          % stub joint close to X-joint
            NDindX = NDindX + 1;
            P2     = NDindX;
          % check level of discretization
            if (JAC(11,1) == 1)
              BFind         = BFind + 1;
              Jbea(BFind,1) = P1;
              Jbea(BFind,2) = P2;
              Jbea(BFind,3) = CFind + fix(k/3);
            else
              % first beam
                NEind         = NEind + 1;
                BFind         = BFind + 1;
                Jbea(BFind,1) = P1;
                Jbea(BFind,2) = NEind;
                Jbea(BFind,3) = CFind + fix(k/3);
```

```
              % intermediate beams
                for d=2:JAC(11,1)-1
                  NEind         = NEind + 1;
                  BFind         = BFind + 1;
                  Jbea(BFind,1) = NEind-1;
                  Jbea(BFind,2) = NEind;
                  Jbea(BFind,3) = CFind + fix(k/3);
                end
              % last beam
                BFind         = BFind + 1;
                Jbea(BFind,1) = NEind;
                Jbea(BFind,2) = P2;
                Jbea(BFind,3) = CFind + fix(k/3);
            end
          end
        end
        CFind = CFind + 1;
      end

end   % of function
```

Bibliography

[1] International Energy Agency, *2013 Key World Energy Statistics*. International Energy Agency (IEA): Paris, France, 2013.

[2] I. Dincer, "Renewable Energy and Sustainable Development: a Crucial Review," *Renewable and Sustainable Energy Reviews*, vol. 4, pp. 157–175, 2000.

[3] P. A. Lynn, *Onshore and Offshore Wind Energy, an Introduction*. John Wiley & Sons Inc.: Chichester, United Kingdom, 2012.

[4] M. D. Esteban, J. J. Diez, J. S. López, and V. Negro, "Why Offshore Wind Energy?," *Renewable Energy*, vol. 36, pp. 444–450, 2011.

[5] J. Twidell and G. Gaudiosi, *Offshore Wind Power*. Multi-Science Publishing Co. Ltd: Brentwood, United Kingdom, 2009.

[6] D. Matha, M. Schlipf, A. Cordle, R. Pereira, and J. Jonkman, "Challenges in Simulation of Aerodynamics, Hydrodynamics and Mooring Line Dynamics of Floating Offshore Wind Turbines," in *Proceedings of the Twenty-first (2011) International Offshore and Polar Engineering Conference: Maui, USA*, pp. 421–428, 2011.

[7] International Electrotechnical Commission, *Wind Turbines - Part 3: Design Requirements for Offshore Wind Turbines*. International Standard, IEC 61400-3, IEC Central Office: Geneve, Switzerland, 2009.

[8] Det Norske Veritas AS, *Design of Offshore Wind Turbine Structures*. Offshore Standard, DNV-OS-J101, Det Norske Veritas AS: Høvik, Norway, 2013.

[9] S.-P. Breton and G. Moe, "Status, Plans and Technologies for Offshore Wind Turbines in Europe and North America," *Renewable Energy*, vol. 34, pp. 646–654, 2009.

[10] D. Toke, "The UK Offshore Wind Power Programme: a Sea-change in UK Energy Policy?," *Energy Policy*, vol. 39, pp. 526–534, 2011.

[11] P. Higgins and A. M. Foley, "Review of Offshore Wind Power Development in the United Kingdom," in *Proceedings of the 12th International Conference on Environment and Electrical Engineering (EEEIC): Wroclaw, Poland*, pp. 589–593, 2013.

[12] A. Naess and T. Moan, *Stochastic Dynamics of Marine Structures*. Cambridge University Press: New York, USA, 2013.

[13] K. E. Thomsen, *Offshore Wind, a Comprehensive Guide to Successful Offshore Wind Farm Installation*. Academic Press: Waltham, USA, 2012.

[14] D. J. MacKay, *Sustainable Energy - Without the Hot Air*. UIT Cambridge Ltd.: Cambridge, United Kingdom, 2008.

[15] H. E. Davey and A. Nimmo, *Offshore Wind Cost Reduction Pathways Study*. Cost reduction study, The Crown Estate: London, United Kingdom, 2012.

[16] E. Hau, *Wind Turbines Fundamentals, Technologies, Application, Economics*. Springer-Verlag: Heidelberg, Germany, 2013.

[17] J. D. Sørensen, "Framework for Risk-based Planning of Operation and Maintenance for Offshore Wind Turbines," *Wind Energy*, vol. 12, pp. 493–506, 2009.

[18] F. Vorpahl, H. Schwarze, T. Fischer, M. Seidel, and J. Jonkman, "Offshore Wind Turbine Environment, Loads, Simulation, and Design," *Energy and Environment*, vol. 2, pp. 548–570, 2013.

[19] P. Ragan and L. Manuel, "Comparing Estimates of Wind Turbine Fatigue Loads using Time-domain and Spectral Methods," *Wind Engineering*, vol. 31, pp. 83–99, 2007.

[20] J. van der Tempel, *Design of Support Structures for Offshore Wind Turbines*. PhD thesis, Delft University of Technology: Delft, the Netherlands, 2006.

[21] M. Seidel, "Wave Induced Fatigue Loads, Insights from Frequency Domain Calculations," *Stahlbau*, vol. 83, pp. 535–541, 2014.

[22] M. I. Kvittem and T. Moan, "Time Domain Analysis Procedures for Fatigue Assessment of a Semi-Submersible Wind Turbine," *Marine Structures*, vol. 40, pp. 38–59, 2014.

[23] L. Manuel, P. S. Veers, and S. R. Winterstein, "Parametric Models for Estimating Wind Turbine Fatigue Loads for Design," *Journal of Solar Energy Engineering*, vol. 123, pp. 346–355, 2001.

[24] L. M. Fitzwater, *Estimation of Fatigue and Extreme Load Distributions from Limited Data with Application to Wind Energy Systems*. Sandia Report SAND 2004-0001, Sandia National Laboratories: Albuquerque, USA, 2004.

[25] W. Dong, T. Moan, and Z. Gao, "Long-term Fatigue Analysis of Multi-planar Tubular Joints for Jacket-type Offshore Wind Turbine in Time Domain," *Engineering Structures*, vol. 33, pp. 2002–2014, 2011.

[26] C. Böker, *Load Simulation and Local Dynamics of Support Structures for Offshore Wind Turbines*. PhD thesis, Gottfried Wilhelm Leibniz Universität Hannover: Hannover, Germany, 2009.

[27] T. Ashuri, *Beyond Classical Upscaling: Integrated Aeroservoelastic Design and Optimization of Large Offshore Wind Turbines*. PhD thesis, Delft University of Technology: Delft, the Netherlands, 2012.

[28] R. Damiani and H. Song, *A Jacket Sizing Tool for Offshore Wind Turbines Within the Systems Engineering Initiative*. OTC-24140-MS, Offshore Technology Conference: Houston, USA, 2013.

[29] M. Muskulus and S. Schafhirt, "Design Optimization of Wind Turbine Support Structures - a Review," *Journal of Ocean and Wind Energy*, vol. 1, pp. 12–22, 2014.

[30] T. Ashuri, M. Zaaijer, J. Martins, G. van Bussel, and G. van Kuik, "Multidisciplinary Design Optimization of Offshore Wind Turbines for Minimum Levelized Cost of Energy," *Renewable Energy*, vol. 68, pp. 893–905, 2014.

[31] S. Yoshida, "Wind Turbine Tower Optimization Method Using a Genetic Algorithm," *Wind Engineering*, vol. 30, pp. 453–470, 2006.

[32] H. Long, G. Moe, and T. Fischer, "Lattice Towers for Bottom-fixed Offshore Wind Turbines in the Ultimate Limit State: Variation of some Geometric Parameters," *Journal of Offshore Mechanics and Arctic Engineering*, vol. 134, pp. 021202:1–13, 2012.

[33] H. Long and G. Moe, "Preliminary Design of Bottom-fixed Lattice Offshore Wind Turbine Towers in the Fatigue Limit State by the Frequency Domain

Method," *Journal of Offshore Mechanics and Arctic Engineering*, vol. 134, pp. 031902:1–10, 2012.

[34] W. Musial, S. Butterfield, and B. Ram, *Energy from Offshore Wind*. NREL/CP-500-39450, National Renewable Energy Laboratory: Golden, USA, 2006.

[35] W. de Vries, N. K. Vemula, P. Passon, T. Fischer, D. Kaufer, D. Matha, B. Schmidt, and F. Vorpahl, *Support Structure Concepts for Deep Water Sites*. WP4: Offshore Foundations and Support Structures, Delft University of Technology: Delft, the Netherlands, 2011.

[36] M. Seidel and D. Gosch, "Technical Challenges and their Solution for the Beatrice Windfarm Demonstrator Project in 45m Water Depth," in *Conference Proceedings DEWEK 2006: Wilhelmshaven, Germany*, 2006.

[37] M. Seidel, "Jacket Substructures for the REpower 5M Wind Turbine," in *Proceedings of European Offshore Wind Conference and Exhibition (EOW 2007): Berlin, Germany*, 2007.

[38] F. Vorpahl, W. Popko, and D. Kaufer, *Description of a Basic Model of the 'UpWind Reference Jacket' for Code Comparison in the OC4 Project under IEA Wind Annex XXX*. IEA Wind Annex XXX, Fraunhofer Institute for Wind Energy and Energy System Technology (IWES): Bremerhaven, Germany, 2011.

[39] H. Long and G. Moe, "Truss Type Support Structures for Offshore Wind Turbines," in *Proceedings of European Offshore Wind Conference and Exhibition (EOW 2007): Berlin, Germany*, 2007.

[40] M. Muskulus, "The Full-height Lattice Tower Concept," *Energy Procedia*, vol. 24, pp. 371–377, 2012.

[41] K. H. Chew, E. Y. K. Ng, K. Tai, M. Muskulus, and D. Zwick, "Offshore Wind Turbine Jacket Substructure: a Comparison Study Between Four-legged and Three-legged Designs," *Journal of Ocean and Wind Energy*, vol. 1, pp. 74–81, 2014.

[42] S. Schafhirt, D. Kaufer, and P. W. Cheng, "Optimisation and Evaluation of Pre-design Models for Offshore Wind Turbines with Jacket Support Structures and their Influence on Integrated Load Simulations," *Journal of Physics: Conference Series*, vol. 555, pp. 012088:1–10, 2014.

[43] J. Jonkman, S. Butterfield, W. Musial, and G. Scott, *Definition of a 5-MW Reference Wind Turbine for Offshore System Development*. NREL/TP-500-38060, National Renewable Energy Laboratory: Golden, USA, 2009.

[44] O. G. Dalhaug, P. A. Berthelsen, T. Kvamsdal, L. Frøyd, S. S. Gjerde, Z. Zang, K. Cox, E. Van Buren, and D. Zwick, *Specification of the NOWITECH 10 MW Reference Wind Turbine*. NOWITECH Report, Norwegian Research Centre for Offshore Wind Technology: Trondheim, Norway, 2012.

[45] C. Bak, F. Zahle, R. Bitsche, T. Kim, A. Yde, L. Henriksen, A. Natarajan, and M. Hansen, *Description of the DTU 10 MW Reference Wind Turbine*. DTU Wind Energy Report-I-0092, Technical University Denmark: Roskilde, Denmark, 2013.

[46] M. O. L. Hansen, *Aerodynamics of Wind Turbines*. Earthscan: Abingdon, United Kingdom, 2008.

[47] K. Lesny, *Foundations for Offshore Wind Turbines, Tools for Planning and Design*. VGE Verlag GmbH: Essen, Germany, 2010.

[48] A. Barker, G. Timco, H. Gravesen, and P. Vølund, "Ice Loading on Danish Wind Turbines, Part 1: Dynamic Model Tests," *Cold Regions Science and Technology*, vol. 41, pp. 1–23, 2005.

[49] I. Jusoh and J. Wolfram, "Effects of Marine Growth and Hydrodynamic Loading on Offshore Structures," *Jurnal Mekanikal*, vol. 1, pp. 77–96, 1996.

[50] H. M. Page, J. E. Dugan, and F. Piltz, *Biofouling, Chapter 18: Fouling and Antifouling in Oil and other Offshore Industries*. Blackwell Publishing Ltd.: Chichester, United Kingdom, 2010.

[51] E. Norton, *Wind and Wave Misalignment Effects on Fatigue Loading*. IEC Working Group 3 (Wind Turbine Offshore Standard), Document 10084, Garrad Hassan: Bristol, United Kingdom, 2003.

[52] P. Fuglsang, C. Bak, J. G. Schepers, B. Bulder, T. T. Cockerill, P. Claiden, A. Olesen, and R. van Rossen, "Site-specific Design Optimization of Wind Turbines," *Wind Energy*, vol. 5, pp. 261–279, 2002.

[53] T. Fischer, W. de Vries, and B. Schmidt, *Upwind Design Basis*. WP4: Offshore Foundations and Support Structures, Endowed Chair of Wind Energy (SWE) at the Institute of Aircraft Design Universität Stuttgart: Stuttgart, Germany, 2011.

[54] J. M. Jonkman and M. L. Buhl Jr., *FAST Users Guide*. NREL/EL-500-38230, National Renewable Energy Laboratory: Golden, USA, 2005.

[55] T. J. Larsen and A. M. Hansen, *How 2 HAWC2, the User's Manual*. Risø-R-1597(ver. 3-1)(EN), Risø National Laboratory: Risø, Denmark, 2007.

[56] A. Myhr, K. J. Maus, and T. A. Nygaard, "Experimental and Computational Comparisons of the OC3-HYWIND and Tension-leg-buoy (TLB) Floating Wind Turbine Conceptual Designs," in *Proceedings of the Twenty-first (2011) International Offshore and Polar Engineering Conference: Maui, USA*, pp. 353–360, 2011.

[57] DNV GL - Energy, *Bladed User Manual*. Verion 4.6, Garrad Hassan & Partners Ltd.: Bristol, United Kingdom, 2014.

[58] Fedem Technology AS, *Fedem User's Guide*. Release 7.1, Fedem Technology AS: Trondheim, Norway, 2014.

[59] P. E. Thomassen, P. I. Bruheim, L. Suja, and L. Frøyd, "A Novel Tool for FEM Analysis of Offshore Wind Turbines with Innovative Visualization Techniques," in *Proceedings of the Twenty-second (2012) International Offshore and Polar Engineering Conference: Rhodes, Greece*, pp. 374–379, 2012.

[60] W. Popko, F. Vorpahl, A. Zuga, M. Kohlmeier, J. Jonkman, A. Robertson, T. J. Larsen, A. Yde, K. Sætertrø, K. M. Okstad, J. Nichols, T. A. Nygaard, Z. Gao, D. Manolas, K. Kim, Q. Yu, W. Shi, H. Park, A. Vasquez-Rojas, J. Dubois, D. Kaufer, P. Thomassen, M. J. de Ruiter, J. M. Peeringa, H. Zhiwen, and H. von Waaden, "Offshore Code Comparison Collaboration Continuation (OC4), Phase I - Results of Coupled Simulations of an Offshore Wind Turbine with Jacket Support Structure," *Journal of Ocean and Wind Energy*, vol. 1, pp. 1–11, 2014.

[61] Fedem Technology AS, *Fedem Theory Guide*. Release 7.1, Fedem Technology AS: Trondheim, Norway, 2014.

[62] O. A. Bauchau and J. I. Craig, *Structural Analysis*. Springer-Verlag: Heidelberg, Germany, 2009.

[63] S. K. Chakrabarti, *Hydrodynamics of Offshore Structures*. WIT Press: Southampton, United Kingdom, 1987.

[64] M. K. McKusick, M. J. Karels, and K. Bostic, "A Pageable Memory Based Filesystem," in *Proceedings of the Usenix Summer 1990 Technical Conference: Anaheim, USA*, pp. 137–144, 1990.

[65] Fedem Technology AS, *Fedem COM-API Documentation*. Release 7.1, Fedem Technology AS: Trondheim, Norway, 2014.

[66] Det Norske Veritas AS, *Fatigue Design of Offshore Steel Structures*. Recommended Practice, DNV-RP-C203, Det Norske Veritas AS: Høvik, Norway, 2012.

[67] International Electrotechnical Commission, *Wind Turbines - Part 1: Design Requirements*. International Standard, IEC 61400-1, IEC Central Office: Geneve, Switzerland, 2014.

[68] C. Amzallag, J. Gerey, J. Robert, and J. Bahuaud, "Standardization of the Rainflow Counting Method for Fatigue Analysis," *International Journal of Fatigue*, vol. 16, pp. 287–293, 1994.

[69] A. Z. Palmgren, "Die Lebensdauer von Kugellagern," *Zeitschrift des Vereins Deutscher Ingenieure*, vol. 68, pp. 339–341, 1924.

[70] M. A. Miner, "Cumulative Damage in Fatigue," *Journal of Applied Mechanics*, vol. 12, pp. A159–A164, 1945.

[71] G. Freebury and W. Musial, *Determining Equivalent Damage Loading for Full-Scale Wind Turbine Blade Fatigue Tests*. NREL/CP-500-27510, National Renewable Energy Laboratory: Golden, USA, 2000.

[72] The Carbon Trust, *Offshore Wind Power: Big Challenge, Big Opportunity - Maximising the Environmental, Economic and Security Benefits*. Report CTC743, The Carbon Trust: London, United Kingdom, 2008.

[73] P. W. Christensen and A. Klarbring, *An Introduction to Structural Optimization*. Springer-Verlag: Heidelberg, Germany, 2009.

[74] P. Freeman and A. Newell, "A Model for Functional Reasoning in Design," in *Proceedings of the 2nd International Joint Conference on Artificial Intelligence: London, United Kingdom*, pp. 621–633, 1971.

[75] B. Chandrasekaran, "Design Problem Solving: a Task Analysis," *AI Magazine*, vol. 11, pp. 59–71, 1990.

[76] R. T. Haftka and Z. Gürdal, *Elements of Structural Optimization*. Kluwer Academic Publishers: Dordrecht, The Netherlands, 1991.

[77] J. C. Spall, "Multivariate Stochastic Approximation Using a Simultaneous Perturbation Gradient Approximation," *IEEE Transactions on Automatic Control*, vol. 37, pp. 332–341, 1992.

[78] J. C. Spall, "An Overview of the Simultaneous Perturbation Method for Efficient Optimization," *Johns Hopkins APL Technical Digest*, vol. 19, pp. 482–492, 1998.

[79] J. C. Spall, *Introduction to Stochastic Search and Optimization*. John Wiley & Sons Inc.: Hoboken, USA, 2003.

[80] A. D. Belegundu and T. R. Chandrupatla, *Optimization Concepts and Applications in Engineering*. Cambridge University Press: New York, USA, 2011.

[81] D. E. Goldberg, *Genetic Algorithms in Search, Optimization and Machine Learning*. Addison-Wesley Longman Publishing Co., Inc.: Boston, USA, 1989.

[82] D. Whitely, "A Genetic Algorithm Tutorial," *Statistics and Computing*, vol. 4, pp. 65–85, 1994.

[83] W. M. Jenkins, "Towards Structural Optimization via the Genetic Algorithm," *Computers & Structures*, vol. 40, pp. 1321–1327, 1991.

[84] M. Seidel, "Design of Support Structures for Offshore Wind Turbines Interfaces between Project Owner, Turbine Manufacturer, Authorities and Designer," *Stahlbau*, vol. 79, pp. 631–636, 2010.